University of Stavanger

Faculty of Science and Technology

MASTER'S THESIS

Study program/Specialization: Master i Konstruksjoner og Materialer	Spring semester, 2021 Open / Restricted access
Writer: Greta Kullashi -239085	……Greta Kullashi…… (Writer's signature)
Faculty supervisor: Sudath C. Siriwardane External supervisor(s):	
Thesis title: Time dependent degradation of buckling capacity of steel beams	
Credits (ECTS): 30	
Key Words: LTB FEM Corrosion	Pages: ……157…… + enclosure: …… Stavanger, 15/06/2021 Date/year

Universitetet
i Stavanger

Master Thesis

Study Program: *Bygg – Konstruksjoner og Materialer*

Author: *Greta Kullashi - 2239085*

Course Leader: *Sudath C. Siriwardane*

Supervisor: *Sudath C. Siriwardane*

Tittle: *Time dependent degradation of buckling capacity of steel beams/plate*

Institutt for maskin, bygg og materialteknologi

Universitetet i Stavanger

15/06/2020

Abstract

Thickness reduction and material degradation due to uniform corrosion increase the tendency of lateral torsion buckling (LTB) of open cross sections and it reduces the moment capacity of the beam. There are lack of studies and analytical formulas to detirmine the LTB moment capacity under different corrosion states. In this thesis, the LTB moment capacity of corroded I-beams is studied in detail, where five different cases are considered. One of the cases is without corrosion, while the rest of the considered cases consist of corrosion on various locations of the I beam cross-section. The considered corrosion cases are,

I. **Case non-corrosion:** The non-corrosion case doesn't contain any form or type of corrosion.
II. **Case corrosion 1:** Case corrosion 1 represents the situation that everywhere of the I beam is subjected to uniform corrison and therefore uniform thickness reduction is applied throughout the I-beam cross section.
III. **Case corrosion 2**: Case corrosion 2 represents the situation that bottom flange and the lower half of the web are subjected to uniform corrosion and therefore uniform thickness reduction is applied throughout the bottom flange and the lower half of the web of the I-beam cross section.
IV. **Case corrosion 3 -model 1:** Case corrosion 3-Model 1 represents the situation that 1/3 of mid-span length of the I-beam at the top flange, bottom flange, and web are subjected to uniform corrosion and therefore uniform thickness reduction is applied over 1/3 of the length of the I-beam at the top flange, bottom flange, and web.
V. **Case corrosion 3 -model 2:** Case corrosion 3-Model 2 represents the situation that 1/3 of mid-span length of the I-beam at the at the bottom flange and the lower half of the web are subjected to uniform corrosion and therefore uniform thickness reduction is is applied over 1/3 of the length of the I-beam at the bottom flange and the lower half of the web.

The main objectives of this thesis is to analyse the effect of the various corrosion cases on the LTB moment capacity ($M_{b,Rd}$) of the I-beam. Thesis proposes an analytical framework for patch corroded I-beams and provide a guideline to simulate the nonlinear lateral torsional buckling behaviour of patch corroded simple beams. Hence investigate the degree of effect of different corrsion scenarios to reduce the buckling reduction factor (χ_{LT}) versus the non-dimentional slenderness ratio (λ_{LT}) by conducting a parametric study. Tweleve different beam lengths were considered with the previously explained corrosion cases in this parametric study.

The linear buckling analysis and the nonlinear buckling analysis were performed on the finite element models for each of the considered corrosion cases which, additionally, included each of the defined beam lengths, creating 5x12 finite element models. In order to analyse the various results obtained from the 60 finite element models, 12 plots were created for each of the defined beam lengths which included the results for each of the five considered corrosion cases.

In order to obtained a comparison between the LTB moment capacities obtained from the finite element models and the LTB moment capacity ($M_{b,Rd}$) obtained from Eurocode 3, the observed LTB moment capacities for the corrosion case "Case non-corrosion", were plotted for the "non-dimensional slenderness" parameter (λ_{LT}) against the "reduction factor" (χ_{LT}) parameter and for the "non-dimensional slenderness" parameter (λ_{LT}) against the "LTB moment capacity" ($M_{b,Rd}$). Furthermore, in order to obtained a comparison between the LTB moment capacities obtained from the finite element models and the LTB moment capacity ($M_{b,Rd}$) obtained from the analytical approach, the observed LTB moment capacities Mbrd 2 and Mbrd 3 for the corrosion cases "Case corrosion 1" and "Case corrosion 2", were plotted for the "non-dimensional slenderness" parameter (λ_{LT}) against the "reduction factor" (χ_{LT}) parameter and for the "non-dimensional slenderness" parameter (λ_{LT}) against the "LTB moment capacity" (Mbrd).

Hence the following conclusions are made,

- The reduced LTB moment capacity for the chosen corrosion cases which are mentioned above are illustrated on the figures presented in section *"4.4.8 Plots - Applied Moment vs Lateral deflection, five different cases for 12 lengths"*.
- Additionally, case corrosion 1 has the lowest moment buckling capacity ($M_{b,Rd}$) due to the fact that the cross-sectional area of the I beam does get reduced the most due to corrosion.
- Furthermore, the curve for the case corrosion 3- model 2 observed from the figures mentioned in section 4.4.8 "Plots – Applied Moment vs Lateral deflection, five different cases for 12 lengths" illustrate that the LTB moment capacity (Mbrd) reduces approximately up to 48.8% due to corrosion when the length of the I-beam increases.
- Finally, the LTB stiffness of the curve for the case corrosion 3 -model 2 decreases drastically after the lateral deflection is approximately equal to 7 mm, especially for beam lengths 3.4 m and 4m, due to local stress concentration and its effect to the nonlinear behaviour. The local stress concentration arises due to the transition of the geometry, such as the transition from the non-corroded part to the corroded part.

The conclusions are discussed more in detail at the conclusion section.

Acknowledgement

This master\s thesis was written during spring 2021 at the faculty of science and technology, University of Stavanger. This is in partial fulfilment for a Master of science degree in Mechanical and Structural engineering and material science. I wish to express my gratitude to alle those that assisted me one way or the other towards making the journey a success.

I would like to express my deep thanks to the professor Sudath C. Siriwardane who supported and guided me during my specialization and master's project. I would also like to thank the co-supervisor Mostafa Atteya for the support and guidance, as well as academic competence.

Table of Contents

List of Tables

List of Figures

Symbols and Abbreviations

The alphabetical list of the most significant symbols and abbreviations used in this thesis are mentioned below. Those symbols which are not mentioned here are specified in the text/chapter in which they are used.

A, A_{eff}	Cross-sectional area, effective cross-sectional area
E	Young's modulus
υ	Poisson’s ratio in elastic stage
FEA	Finite element analysis
fy	Yield stress
γ_m	General partial factor
h	Height of corrosion patch
i	Radius of gyration
L	Length of structural member
Lcr	Critical buckling length
H	Hight
B	Width
hw	Web high
tf	Flange Thickness
tw	Web thickness
Hc	Corroded Hight
Bc	Corroded Width
tfc	Corroded Flange thickness
twc	Corroded Web thickness
Hwc	Corroded Web high
Iyy	Moment of Inertia in y-y axis
Izz	Moment of Inertia in z-z axis
Iw	Warping constant
It	Torsional constant
Iyyc	Corroded Moment of Inertia in y-y axis
Izzc	Corroded Moment of Inertia in z-z axis
Iwc	Corroded Warping constant
Itc	Corroded torsional constant

1 Introduction

1.1 Background

Outdoor structures, bridges and offshore structures are exposed to corrosion. In general, five of the most common types of corrosion affect railway bridges.[1,2] The most common type of corrosion is general (uniform) corrosion, which occurs in a uniform pattern across the surface. In the bridges, general corrosion frequently occurs where water accumulates, such as on the upper side of the bottom flange of broad flange beams, I beam stringers, cross-girders, plate girders, built up sections, and both flanges of built-up sections consisting of riveted angles.[1,3]

Pitting corrosion is a form of corrosion that is restricted to a small area and typically starts with a surface irregularity and which is called local corrosion. This form or type of corrosion is dangerous because it has the potential to trigger localized stress concentrations. Crevice corrosion is a form of localized corrosion that occurs when different structural components are close together, resulting in narrow spaces. When two separate metals are placed in an electrolyte and electrically linked, as is possible at bolt or welded connections, galvanic corrosion occurs. Corrosion fatigue is the mechanical degradation of a material caused by the combined action of localized corrosion and cycle loading, which is the last and most common form of corrosion. [4]

In general, bridge structures exposed to aggressive environmental conditions suffer from time-dependent loss of both coating and material due to corrosion. As a results, the thickness of structural steel is steadily decreasing. [5,6,7,8,1]

A reduction in thickness is accompanied by a reduction in a few other geometric/cross sectional properties that govern structural behaviour, such as effective cross-sectional area, moment of inertia about the y-axis and the z-axis, torsional constant and warping constant. [5,6,7,8,1]One of the main structural behaviours of flexural members with open cross sections, which governs the capacity, is the lateral torsional buckling (LTB) and due to the patch corrosion, the buckling capacity may reduce. Finally, the overall stiffness of the structure and the structural behaviour may change due to patch corrosion.

1.2 Problem statement/ Research gaps

The lack of studies are found in the literature for simulating the effect of corrosion for reduction of lateral torsional buckling moment capacity of open cross sections. Several experimental works have been performed in order to get a better understanding about the lateral torsional buckling moment capacity of structural members, which are affected by corrosion. However there is no genarlized analytical formula/framework to calculate remaining elastic critical moment (M_{cr}) and the lateral torsional buckling moment ($M_{b,rd}$) which applicable to different uniform/general corrosion cases/scenarios. Altenatively, the design capacity can be determined based on simulations from finite element methods (FEM), but there is no general guideline or procedure for the different corrosion cases. Eventhough the FEM is a smart method to simulate non-lnear structural behaviour, the accurate simulation of nonlinear lateral torsional buckling behaviour is quite challenging due to the interaction effect of local buckling behaviour with both geometrical and material non-linear behaviours and numerical descripencies at the supports. The feasibility and the accuracy of the results is also depend of the features/options available in the particular FEM tools and ANSYS workbench is one of the example for it.

1.3 Objectives

In order to overcome above mentioned research gaps to some extent, the main objectives of this thesis is to,

I. Provide an analytical framework for patch corroded I-beams. The framework consists of the the time dependent degradation formulas of effective second moment of areas (I_{eff}), effective torsional constant (I_T) and effective warping constant of the corroded member cross sections which are required to determine the time-dependent degradation of elestic critical bending moment (M_{cr}) and buckling moment capacity ($M_{b,rd}$).
II. Provide a guideline to simulate the nonlinear lateral torsional buckling behaviour of patch corroded simple beams.
III. Investigate the degree of effect of different corrsion scenarios to reduce the buckling reduction factor (χ) versus the non-dimentional slenderness ratio ($\bar{\lambda}$).

A parametric study is conducted for four different corrosion scenarios by changing the length of the beam which leads to a change in the imperfection scale factor L/1000. This change sets the initial imperfection for the different beam lengths and, additionally, the support boundary conditions and loading type and value are changed for each case in the parametric study.

1.4 Outline of the thesis

Chapter 2 consists of the the Lateral torsional buckling theory (LTB) in detail including the LTB design codes and the discussion about the capacity of LTB of corroded beams. The the proposed analytical approach is discussed in the Chapter 3 and corrsepnding details relevant to perfomed analytical parametric study is includeded. In this Chapter 4, the finite element simulations are discussed and details are shown. Chapter 5 contains the comparison of the obtained results and discussions. The concluding remarks and recomendtaion of future studies are presented in the Chapter 6.

2 Lateral torsional buckling (LTB)

2.1 LTB-Review

LTB-Lateral Torsional Buckling:

If the beam doesn't have sufficient lateral support or lateral stiffness, then the beam which is loaded in its stiffer principal plane may buckle out of plane and the buckling load may be substantially lower. There are no out-of-plane deformations for an idealised perfectly straight elastic beam until the applied Moment M approaches the elastic buckling moment Mcr, at which point the beam buckles by deflecting laterally and twisting. Deflecting laterally and twisting are interdependent: as the beam deflects laterally, the applied Moment has a component that causes the beam to twist by exerting a torque about the deflected longitudinal axis, as shown in Figures 2.1-1 and 2.1-3. This behaviour is called as elastic flexural-torsional buckling, also known as elastic lateral-torsional buckling in EC which is important and most common for long unrestrained I-beams with low resistance to lateral bending and torsion. Lateral torsional buckling of a cantilever I-beam is shown in figure 2.1-2. [9]

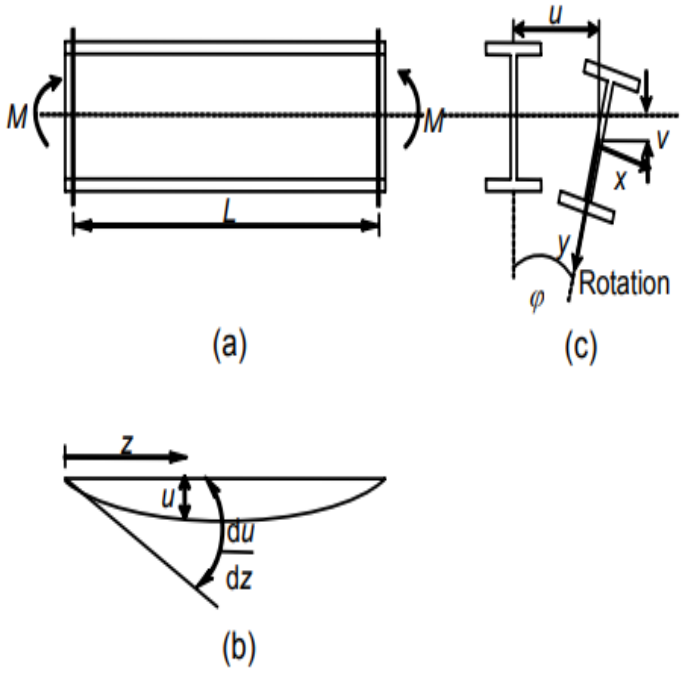

Figure 2.1-1: Lateral Torsional Buckling of a simply supported I-beam. (a) Elevation; (b) Plan on the longitudinal axis; (c) Section [10]

Figure 2.1-2: Lateral Buckling of a cantilever [9]

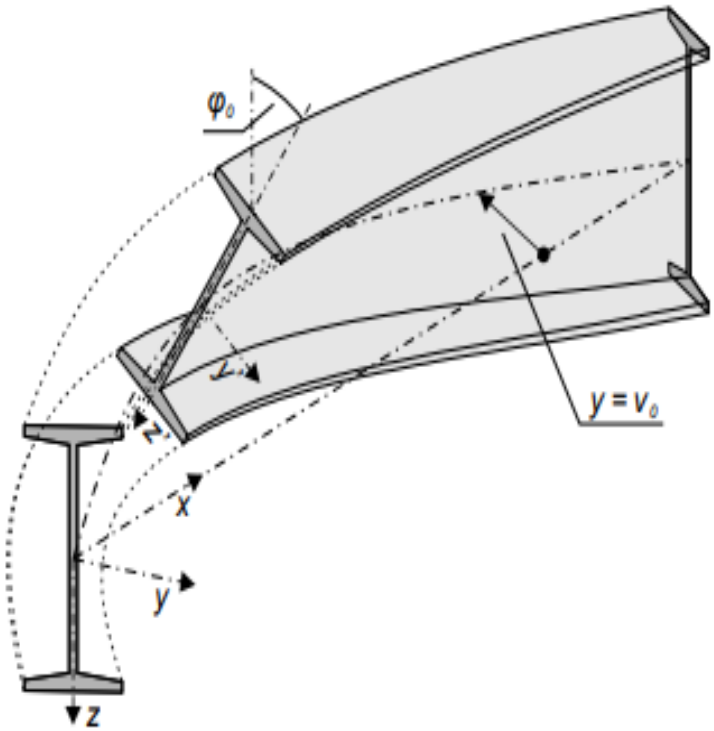

Figure 2.1-3: A 3D view of I-beam deflecting [11]

The load at which Lateral torsional buckling may occur depends on the classification of the I-beam. For very stocky beams, such as class 2, the inelastic Moment may or can be higher than the in-plane plastic collapse Mp, in which case lateral buckling has very little effect on the beam's moment resistance. For semi-compact beam sections, such as class 3, the inelastic Moment may or can reach after the yielding Moment My and before the in-plane plastic collapse Mp. For slender beam sections, such as class 4, the elastic buckling moment may or can reach before the yielding Moment My. All the given information for the behaviour of the different cross section types above is shown in the figure below.

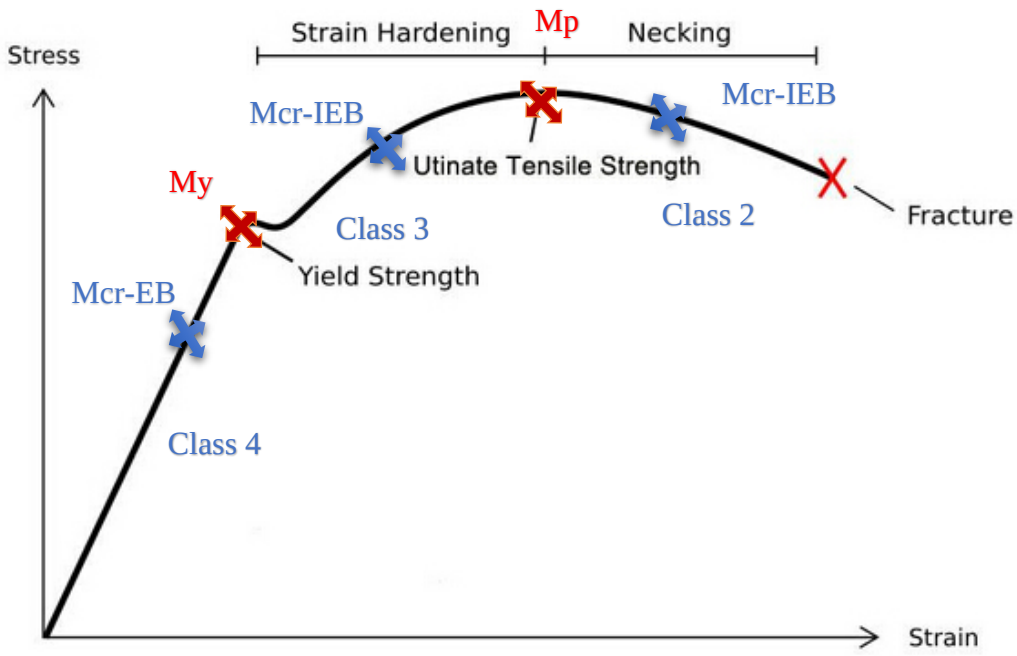

Figure 2.1-4: Representing the elastic/inelastic critical moment for different class cross section in stress strain curve.

Where:

Mcr-EB =Elastic buckling critical moment

Mcr-IEB=Inelastic buckling critical moment

2.2 LTB Design Codes

LTB equations, such as the elastic critical moment (Mcr), Non-dimensional slenderness LT (λ_{LT}) and buckling resistance moment (Mb, Rd) are dependent on the parameters moment of inertia about z-z (Izz), moment of inertia about y-y (Iyy), torsional constant (It) and warping constant (Iw) which are shown below and have to be calculated first. Those important parameters which are mentioned above are dependent on the given or chosen steel cross section.

The main parameters which affect LTB behavior are shown below from equation Nr. 1.1 to 4.

Classification without corrosion:

Flange-compression:

$$\frac{cf}{tf\varepsilon} = \frac{\frac{(b - tw)}{2}}{tf\varepsilon} < 9 \qquad \text{Eq. 1a}$$

[12]

Class 1 < 9
Class 2 <10
Class 3 < 14
Class 4 > 14

Web-Bending:

$$\frac{cw}{tw\varepsilon} = \frac{(h - 2tf)}{tw\varepsilon} < 72 \qquad \text{Eq. 1b}$$

[12]

Class 1 < 72
Class 2 < 83
Class 3 < 124
Class 4 > 124

Classification with corrosion:

Flange-compression:

$$\frac{cfc}{tfc\varepsilon} = \frac{\frac{(bc - twc)}{2}}{tfc\varepsilon} < 9 \qquad \text{Eq.1c}$$

Web-Bending

$$\frac{cwc}{twc\varepsilon} = \frac{(hc - 2tfc)}{twc\varepsilon} < 72 \qquad \text{Eq. 1d}$$

$$\varepsilon = \sqrt{\frac{235}{fy}} \qquad \text{Eq. 1e [12]}$$

Where;

cw= is the depth of the web

cf= is the with of the flange

cwc= is the depth of the corroded web

cfc= is the with of the corroded flange

ε =coefficient depending on fy

Moment of inertia about z-z axis:

For a rectangular cross-section:

$$Izz = \frac{tf * B^3}{12} \qquad \text{Eq. 1.1}$$

For an I-beam (2 flanges + 1 web):

$$Izz = 2 * \left(\frac{tf * B^3}{12}\right) + \frac{Bw * \ tw^3}{12} \qquad \text{Eq. 1.2}$$

Moment of inertia about y-y axis:

For a rectangular cross-section:

$$Iyy = \frac{B * tf^3}{12} \qquad \text{Eq. 2.1}$$

For an I-beam (2 flanges + 1 web):

$$Iyy = 2 * \left(\frac{B * tf^3}{12}\right) + 2 * \left(B * tf * \left(\frac{H}{2} - \frac{tf}{2}\right)^2\right) + \frac{tw * \ Bw^3}{12} \qquad \text{Eq. 2.2}$$

Torsion Rigidity:

For an I-beam (2 flanges + 1 web):

$$It = 2 * \left(\frac{B * tf^3}{3}\right) + \left(\frac{Bw * tw^3}{3}\right) \qquad \text{Eq. 3}$$

Torsion Warping:

For an I-beam (2 flanges + 1 web):

$$Iw = \frac{B^3 * (H - tf)^2 * tf}{24} \qquad \text{Eq. 4}$$

Critical elastic Moment (Mcr):

$$Mcr = \sqrt{\left(\frac{\pi^2 EIzz}{L^2}\right) * \left(GIt + \left(\frac{\pi^2 EIw}{L^2}\right)\right)} \qquad \text{Eq. 5 [9]}$$

Non dimensional slenderness ratio:

$$\lambda_{LT} = \sqrt{\frac{Wy * fy}{Mcr}} \qquad \text{Eq. 6 [12]}$$

$Wy = Wply$ For Class 1 or 2 Cross Section

$Wy = Wel, y$ For Class 3 Cross Section

$Wy = Wel, y$ For Class 4 Cross Section

The plastic section modulus (Wply):

$$Wply = \left(B * tf * \left(\frac{H - tf}{2}\right)\right) * 2 + \left(\left(\frac{H}{2} - tf\right) * tw * \frac{\left(\frac{H}{2} - tf\right)}{2}\right) * 2 \qquad \text{Eq. 7}$$

2.2.1 Most conservative method stepwise:

Table 1: Table 6.4: Recommended values for lateral torsional buckling curves for cross-section using equation (8) [12]

Cross-section	Limits	Buckling curve
Rolled I-sections	$h/b \leq 2$ $h/b > 2$	**a** **b**
Welded I-sections	$h/b \leq 2$ $h/b > 2$	**c** **d**
Other cross-sections	-	**d**

I. Select the chosen Cross Section.

II. By selecting the Limits which are depended on the chosen parameters, such as the Hight (h), width (b), we can get the buckling curve.

Table 2: Table 6.3: Recommended values for imperfection factors for lateral torsional buckling [12]

Buckling curve	a	b	c	d
Imperfection factor α_{LT}	0,21	0,34	0,49	0,76

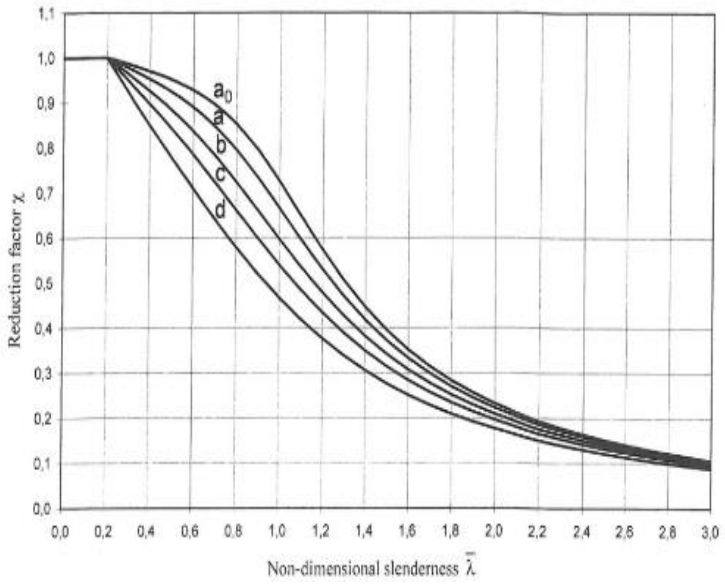

Figure 2.2-1: Figure 6.4: Buckling curves [12]

Reduction factor (χ_{LT}):

$$\chi_{LT}=\frac{1}{(\phi_{LT}+\sqrt{\phi_{LT}^{2}-\lambda_{LT}^{2}})} \quad \text{but } \chi_{LT}\leq 1.0 \qquad \text{Eq. 8 [12]}$$

Where

$$\phi_{LT} = 0.5\left[(1 + \alpha_{LT}(\lambda_{LT} - 0.2) + \lambda_{LT}^{2}\right]$$

α_{LT} is an imperfection factor

The buckling moment capacity Mbrd:

$$Mb, Rd = \chi_{LT} * Wy * \frac{fy}{\Upsilon m1} \qquad \text{Eq. 9 [12]}$$

Since case corrosion 1 is a uniformly corrosion we can use the equations which are shown above by changing the initial dimensions with the corroded dimensions. Especially for equations 1.1 to equation 9, which are shown above.

Corroded- Moment of inertia about z-z axis:

For a corroded I-beam (2 flanges + 1 web):

$$Izzc = 2 * \left(\frac{tfc * Bc^{3}}{12}\right) + \frac{Bwc * \ twc^{3}}{12} \qquad \text{Eq. 10}$$

Corroded- Moment of inertia about y-y axis:

For a corroded I-beam (2 flanges + 1 web):

$$Iyyc = 2 * \left(\frac{Bc * tfc^{3}}{12}\right) + 2 * \left(Bc * tfc * \left(\frac{Hc}{2} - \frac{tfc}{2}\right)^{2}\right) + \frac{twc * \ Bwc^{3}}{12} \qquad \text{Eq. 11}$$

Corroded- Torsion Rigidity:

For a corroded I-beam (2 flanges + 1 web):

$$Itc = 2 * \left(\frac{Bc * tfc^3}{3}\right) + \left(\frac{Bwc * twc^3}{3}\right) \quad \text{Eq.12}$$

Torsion Warping:

For an I-beam (2 flanges + 1 web):

$$Iw = \frac{Bc^3 * (Hc - tfc)^2 * tfc}{24} \quad \text{Eq. 13}$$

Corroded- The plastic section modulus (Wplyc):

$$Wplyc = \left(Bc * tfc * \left(\frac{Hc - tfc}{2}\right)\right) * 2 + \left(\left(\frac{Hc}{2} - tfc\right) * twc * \frac{\left(\frac{Hc}{2} - tfc\right)}{2}\right) * 2 \quad \text{Eq. 14}$$

Corroded- Critical elastic Moment (Mcr):

$$Mcrc = \sqrt{\left(\frac{\pi^2 EIzzc}{L^2}\right) * \left(GItc + \left(\frac{\pi^2 EIwc}{L^2}\right)\right)} \quad \text{Eq. 15}$$

Corroded- Non dimensional slenderness ratio:

$$\lambda_{LTC} = \sqrt{\frac{Wplyc * fy}{Mcrc}} \quad \text{Eq. 16}$$

Corroded- Reduction factor:

$$\chi_{LTc}=\frac{1}{(\phi_{LTc}+\sqrt{\phi_{LTc}{}^2-\lambda_{LTc}{}^2})} \quad \text{but } \chi_{LTc}\leq 1.0 \qquad \text{Eq. 17}$$

Where

$$\phi_{LTc} = 0.5\left[(1 + \alpha_{LT}(\lambda_{LTc} - 0.2) + \lambda_{LTc}{}^2\right]$$

α_{LT} is an imperfection factor

Corroded- The buckling Moment capacity Mbrd:

$$Mb, Rdc = \chi_{LTc} * Wplyc * \frac{fy}{\Upsilon m1} \qquad \text{Eq. 18}$$

2.2.2 Stepwise calculation- No corrosion:

I. One of the first steps is to calculate the main parameters which affect LTB, such as Eq. 1.a to Eq. 1b, Eq 1e, Eq. 1.2, Eq. 2.2, Eq.3 and Eq. 4.

II. The next step calculates the elastic critical Moment Mcr, such as (Eq.5), which depends on the parameters calculated first.

III. The third step is to calculate the plastic section modulus (Eq.7) and the non-dimensional slenderness ratio (Eq.6).

IV. The Buckling curve is necessary to get the imperfection factor α_{LT}, which is necessary to calculate the LTB equations above. From Table 1 we can get the buckling curve, which is explained in detail above, and from Table 2 we can get the imperfection factor α_{LT} if the buckling curve is known.

V. The last step is to calculate the corroded-reduction factor part 1 ϕ_{LTc} and part 2 χLt (Eq.8), and LTB moment capacity Mbrd (Eq.9).

2.2.3 Stepwise calculation- Case corrosion 1:

I. One of the first steps is to calculate the main corroded- parameters which affect LTB, such as Eq.1c to 1.d and Eq.1e, Eq.10, Eq.11, Eq.12, and Eq.13.

II. The next step calculates the corroded- elastic critical Moment Mcr, such as (Eq.15), which depends on the parameters calculated first.

III. The third step is to calculate the plastic section modulus (Eq. 14) and the non-dimensional slenderness ratio (Eq.16).

IV. The Buckling curve is necessary to get the imperfection factor α_{LT}, which is necessary to calculate the LTB equations above. From Table 1we can get the buckling curve, which is explained in detail above, and from Table 2 we can get the imperfection factor α_{LT} if the buckling curve is known.

V. The last step is to calculate the corroded-reduction factor part 1 ϕ_{LTc} and part 2 χLt (Eq.17), and the LTB moment capacity Mbrd (Eq.18).

2.3 The capacity of LTB of corroded beams

The most significant deterioration mechanism in determining the remaining life of steel structures appears to be corrosion. In various parts of the world, the infra-structures, particularly in Asia, are getting older. Many steel structures have been in operation for more than 50 years and are often in a seriously damaged condition. Steel is widely used in the petrochemical industry in most countries as the primary structural material for pipe bridges, vessel support frames, and process equipment. Corrosion is the most common issue with many of these steel structures and occurs more rapidly in the aggressive environments of chemical plants. Furthermore, chemical plants are often located in exposed coastal areas, which exacerbates the problem. [13]

Deterioration due to corrosion of a steel structure can alter its behaviour and stiffness. As a result, there may be a difference between the analyses of corrosion-damaged structures and the structure's analyses under design. Corrosion may cause a fracture, yielding, and buckling in steel structural members. Due to corrosion, the stress may increase. The geometric properties and the build-up products may change, and the member cross-section properties, such as the section modulus or the stiffness ratio, may be reduced. [14]

The thickness loss data was collected from four samples of corrosion-damaged I-beams, which were removed from a petro-chemical plant in the article “Evaluation of the remaining lateral torsional buckling capacity in corroded steel members”. The four corroded beams were visually examined and found to be uniformly corroded. For each beam, a large number of surface roughness measurements were taken in order to improve the accuracy of the results. A total of 770 values were taken into account to determine the average thickness of the flanges and the webs for each beam. The data which was collected was used to develop a corrosion decay model that calculated the percentage of lateral torsional buckling capacity of beams with long and short spans that are unrestrained laterally. Figure 2.3-1 illustrates the varying thickness loss model when the beam is exposed to corrosion. [10]

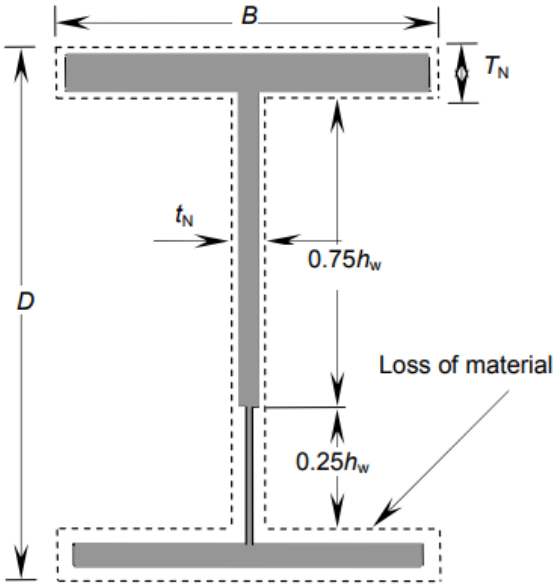

Figure 2.3-1: Varying thickness loss model [10]

$$T_{c=}T_N(1-\mu) \qquad (1a)$$

$$t_{c=}t_N(1-0.5\mu) \qquad (1b)\ [10]$$

Where

Tc = Average Thickness of the flange (after corrosion effect)

tc = Average Thickness of the (after corrosion effect)

TN= is the flange thickness of intact cross-sectional

t_N = The web thickness of intact cross-sectional

B = The width of intact cross section

D = The overall depth of intact cross section

hw = The hight of the web

Figure 2.3-2: Typical locations where Corrosion can occur on a steel girder bridge [10]

The class of sections, such as plastic, compact, semi-compact, or slender, may change due to corrosion-induced loss of thickness in compression flanges and webs. For example, due to loss of thickness, a plastic or compact section may become semi-compact, and due to local buckling, the development of a full plastic moment may be prevented in such cases. [15] In addition, depending on the relative thickness loss in its various parts, the modes of failure of a member may vary from one mechanism to another. It was shown in the article "Structural Assessment of Corrosion Damaged Steel Work" that the shear failure mechanism becomes critical after several years, while the bending failure mode governs a member in its early stage. When holes created by corrosion are present in the web, the shear mode becomes critical. [16]

Figure 2.3-2 illustrates the typical locations where corrosion can occur on a steel girder bridge [10]. According to the article "Mechanical Properties of Samples of Structural Steel Affected by Corrosion", the most fundamental consequence of corrosion is a reduction in the material strength and in section size due to material loss. This, in turn, causes a reduction in the structure's carrying capacity and member's stiffness, resulting in excessive member distortion. [17] Article "Remaining capacity assessment of corrosion damaged beams using minimum curves" investigated the effects of corrosion on the remaining shear and moment capacities of steel beams using minimal curves. [18] Rahgozar suggested a series of universal I-beam minimum curves combined with the information on percentage thickness loss to estimate the percentage of the remaining capacity of corrosion-damaged beams. [19,10]

In the "Limit States Design of Structural Steelwork (3rd Ed.)" book, it is mentioned that local buckling strength and lateral distortional buckling are important factors when the strength of a corrosion-damaged beam is taken into account. [20]

The main objective of the article "Evaluation of the remaining lateral torsional buckling capacity in corroded steel members" is to calculate the percentage of remaining lateral torsional buckling capacity of long span and short span beams that are not laterally restrained using the measurement data and the corrosion model decay which was developed. [10]

2.4 Ansys simulations

The analysis of the limit states of steel I-beams using nonlinear FEM is a challenging problem that requires the processing of a large amount of data. Geometrical and material nonlinear solutions can be used to analyse stability problems with imperfections, such as geometrical and material imperfections. More numerical data must be entered as software inputs as the FEM advances. The objective of the article "FE nonlinear analysis of lateral-torsional buckling resistance" is to investigate or study the inelastic lateral-torsional buckling's ultimate limit condition. The advanced FE modelling elements as shells or solids are required for inelastic analysis. [11]

The study of the effect of the stability phenomena on the ultimate limit state of a steel beam subjected to uniform bending moment along its length is the topic of the article which is mentioned above. Imperfection and slenderness are two important factors that affect the load carrying capacity. The article mentioned above compares the elastic and inelastic resistance obtained using the nonlinear finite element method with analytical and standardised approaches. The computational FE models were created with the Ansys Mechanical APDL software with the initial imperfections as shown in the figure below. The inelastic resistance was calculated using the Ansys software's geometric and material nonlinear solutions. [11]

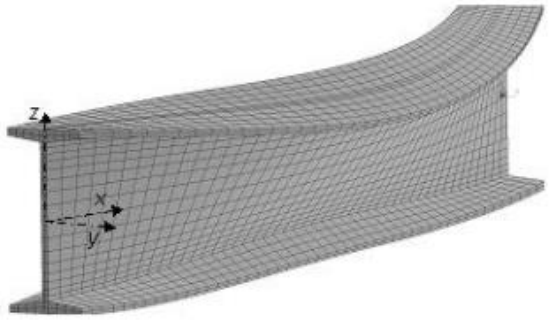

Figure 2.4-1: Fig. 5 computational model in Ansys- axonometry [11]

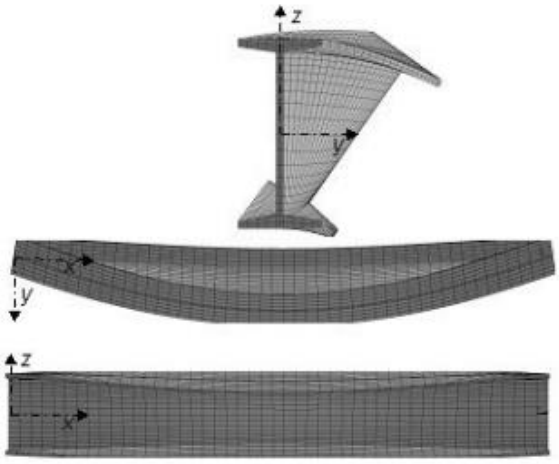

Figure 2.4-2: Fig 6 Computational model in Ansys- views [11]

With the software Ansys Workbench there are three ways to perform a nonlinear analysis:

1. Performing a static linear analysis and a linear buckling analysis in order to get an LTB buckling eigen mode, which will give a model with an LTB behaviour and then we can perform a nonlinear analysis with LTB behaviour.

2. Performing a nonlinear analysis with lateral load and uniformly line pressure load on top of the beam in order to include LTB behaviour.

3. Performing a nonlinear analysis where the computational model was created with the initial imperfections as shown in figure 2.4.1 and in figure 2.4.2.

With the software Ansys Mechanical APDL there are two ways to perform a nonlinear analysis:

I. Performing a nonlinear analysis with lateral load and uniformly line pressure load on top of the beam in order to include LTB behaviour.
II. Performing a nonlinear analysis where the computational model was created with the initial imperfections as shown in figure 2.4.1 and in figure 2.4.2.

Samanta et al. [2015] studied distortional buckling of simple supported monosymmetric I-beams, taking into account three different types of loads: a point load, a uniformly distributed load, and a uniform sagging moment. The software ABACUS was used for the entire investigation. The load was applied to the top flange and bottom flange position. The analysis was carried out by calculating moment modification factors that account for web distortion and then compared to those which are based on the SSRC guidelines, which are specifically focused on the study of lateral torsional buckling. [21]

Snijder et al. [2013] suggest a new design rule for determining the new reduction factor and slenderness ratio. The authors compiled a list of five design principles and used finite element analyses to verify their validity. Following that, the ultimate load generated by these five design rules were compared to material and geometrical nonlinear analyses of imperfect (GMNIA) beams with channel cross sections. The load was applied through the web of the channel while the cross-section dimensions, such as the beam length to section height ratio were varying. A new design rule has been proposed that can be used safely for any vertical load application that lies between the web's center and the shear center. [21]

Hamid et.al [2010] presented the theoretical and finite element results of lateral torsional buckling of an I-girder with corrugated webs and lateral bracing under uniform bending. They used ANSYS 10.0 to create a three-dimensional finite element model of an I-girder with corrugated webs for the study of lateral torsional buckling and the effects of lateral bracing stiffness on the critical moment of a simply supported I-girder with corrugated webs which is under pure bending. [21]

Hermann et al. [2007] calculated the elastic critical moment for eccentrically loaded beams with different softwares, such as SAP2000, LTBEAM, STAAD pro, COLBEAM and ADINA. The analyses were performed with varying types of loads, beam lengths, and eccentricities of the load, including the centric load. The results from the different softwares are compared to the results obtained using an empirical expression identified as the 3-factor formula, which was derived from the EURO code. [21,22]

The nonlinear lateral torsional buckling analysis of an unstiffened slender web plate girder (SWPGs) subjected to central loading is investigated by **Amin Mohebkhah et al [2004].** For the inelastic nonlinear flexural torsional analysis of SWPGs, a 3D finite element model is created using the software ABAQUS. The moment gradient factor of the unbraced length and load height effects are calculated. They came to the conclusion that the Cb factor used by AISC in steel building specifications is generally conservative for elastic and inelastic SWPGs under the point load cases considered. It's was observed that the height of the applied load has no effect on the relationship between moment resistance and unbraced length. [21]

The objective of the article "*A Review on Simulation Analysis in Lateral Torsional Buckling of Channel Section by using Ansys Software*" is to perform a software analysis with ANSYS WORKBENCH 14.0 on channel sections in designing bridges. The factors that will affect the lateral torsional buckling of channel beams where investigated. The eigen buckling load factor was determined using the simulation software ANSYS WORKBENCH 14.0. A comparison between the elastic critical moment using the formula given in clause 2.2.1 of the 800:2007 standard with the finite technique was performed for validation. The comparison is performed by calculating the reduction and slender factor using the general method which is given in the IS 800-2007 code and with "New Design Rule (Snijder)". Where the bending capacity is calculated by using the general method which is given the 800-2007 code and with the "New Design Rule (Snijder)". [21]

3 Proposed Analytical Approach

3.1 Corrosion wastage rate modelling

The formula for the time-dependent growth of corrosion wastage rate is obtained by taking into account the most common form of corrosion, such as general corrosion. The formula is a nonlinear function due to the fact that the studies illustrated that a nonlinear function can be used to predict corrosion propagation with reasonable accuracy. [23]

$$c(t) = A(t - t_0)^B \qquad ; t > t_0$$

Eq. 19 [23]

Where:

C(t) = The average corrosion penetration

t = is the age in years

t_0=is the time in years of first the appearance of the sign of general/uniform Corrosion

A= Model Parameter (The corrosion rate in the first year of exposure)

B=Model Parameter (The corrosion rate for representing the long-term decrease) [23]

Table 3: Model parameters of general corrosion rate model [1]

	Carbon steel		Weathering steel	
Environment	*A* (mm)	*B*	*A* (mm)	*B*
Rural	0.0340	0.650	0.0333	0.498
Urban	0.0802	0.593	0.0507	0.567
Marine	0.0706	0.789	0.0402	0.557

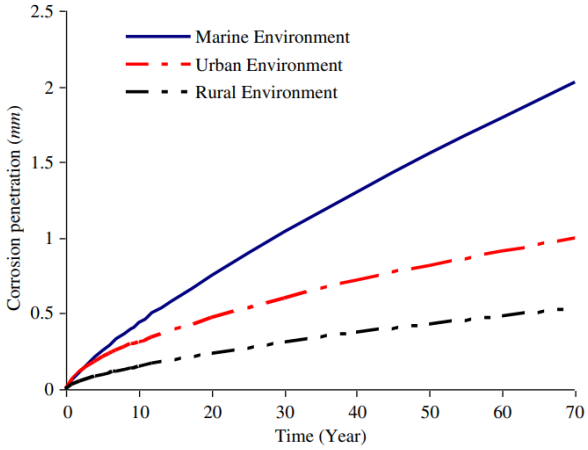

Figure 3.1-1: Corrosion penetration versus time for carbon steel in various environments [1]

3.2 Effective cross-sectional Area

The members time dependent effective cross-sectional area is obtained as follows, taking into account the reduction in plate thickness due to general corrosion: [23]

$$A_{eff}(t) = A_0 - \sum_{i=1}^{n} C_i(t) l_i \qquad \text{Eq. 20 [23]}$$

Where:

A_0= is the initial cross-sectional area

t = is the age in years

l_i=is the Length of general Corrosion spread over the cross-section at the i^{th} corroded surface as shown in figure below. [23]

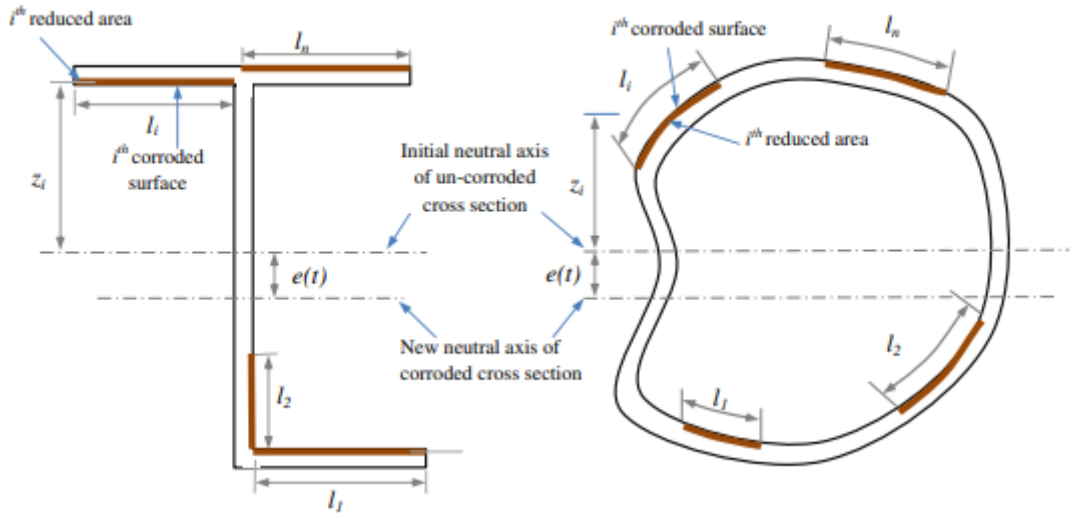

Figure 3.2-1: Schematic representations of effective cross-sectional parameters of corroded cross-sections: (a) open sections, (b) closed sections [23]

3.3 Effective second moment of area about the z-z axis

The new neutral axis about the z-axis of the effective cross-sectional area, which is derived by considering the reduction in plate thickness due to general corrosion wastage, is used to obtain the effective second moment of area about the z-axis of the corroded member cross-section. [23]

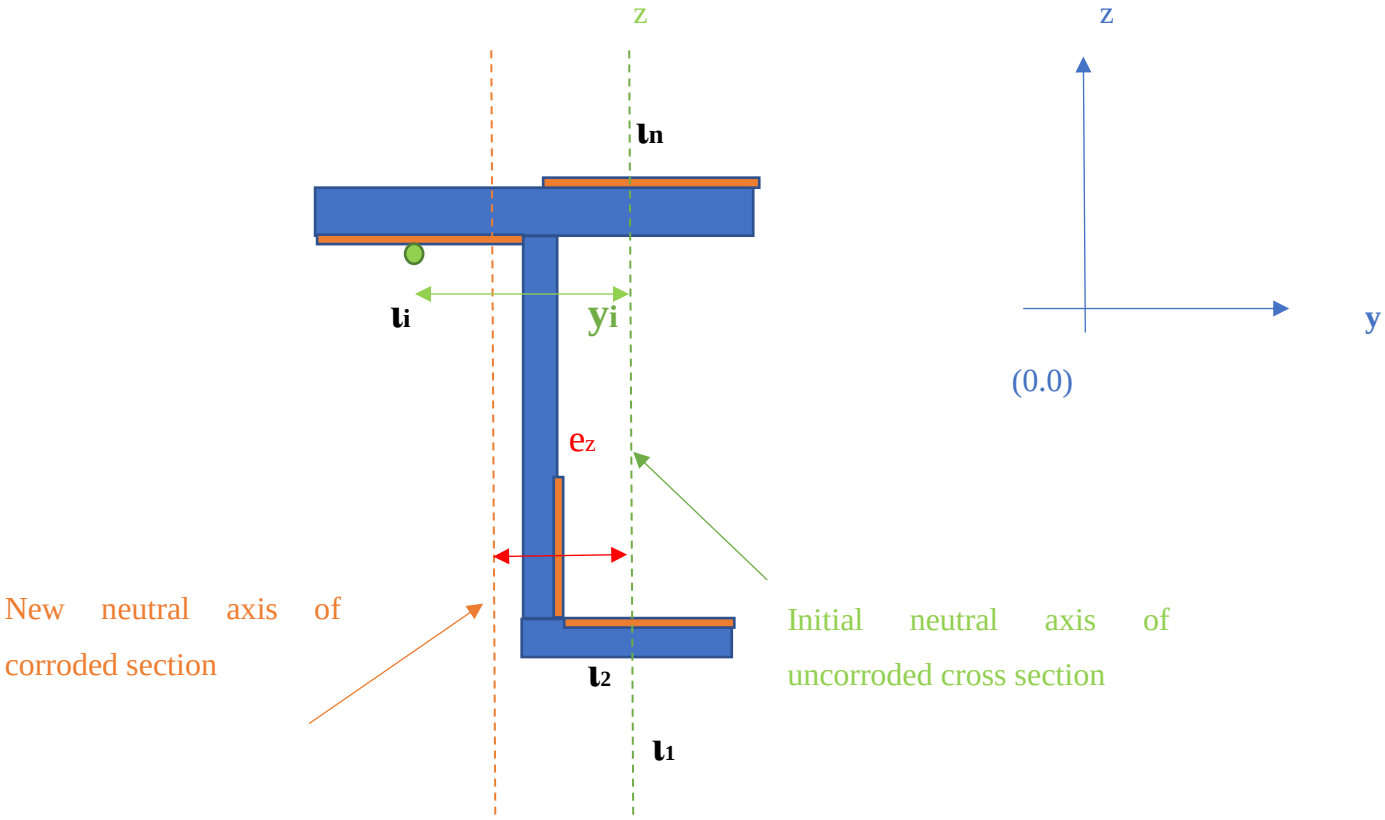

Figure 3.3-1: A demonstration of the corroded I-beam – Effective second moment in z-z axis

$$e_{z(t)=}\frac{\sum_{i=1}^{n} c_{i(t)} l_i \, y_i}{A_{eff(t)}} \qquad \text{Eq. 21 [23]}$$

Where:

y_i= is the height from initial neutral axis to the centroid of the i^{th} corroded axis to the y direction.

$$I_{z,eff=}I_{0,z}+A_0 e_{z(t)}{}^2-\sum_{i=1}^{n}\{AI_{i,z}+c_i(t)l_i[y_i+e_z(t)]^2\} \qquad \text{Eq. 22 [23]}$$

3.4 Effective torsional constant and Effective warping constant

Effective torsional constant

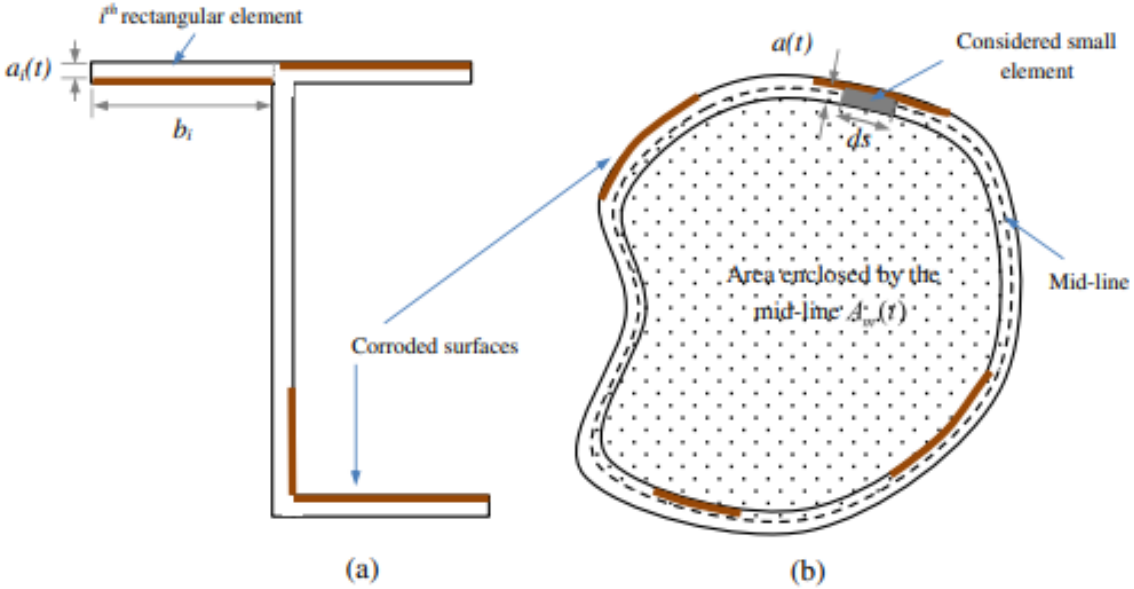

Figure 3.4-1: Schematic representations of torsional parameters of corroded cross-sections: (a) open sections, (b) closed section [23]

The effective torsional constant for a corroded member with a thin-walled open cross-section is as follows, taking into consideration the reduction in plate thickness due to general corrosion wastage. [23]

$$I_{T,eff}(t) = \frac{1}{3}\sum_{i=1}^{n} b_i\, a_i(t)^2 \qquad \text{Eq. 23 [23]}$$

Where:

b_i = is the developed Length of the mid-line

$a_i(t)$ = is the Thickness of the i^{th} rectangular element of the cross-section in Figure 3.4.1(a).

The effective torsional constant for a corroded member with a thin-walled closed cross-section is as follows, taking into consideration the reduction in plate thickness due to general corrosion wastage. [23]

$$I_{t,eff}(t) = \frac{4A_m(t)^2}{\int \frac{ds}{a(t)}} \qquad \text{Eq. 24 [23]}$$

Where

$$a(t) = a_0 - C(t), \qquad when\ t > t_0$$
$$a(t) = a_0, \qquad when\ t \leq t_0 \qquad \text{Eq. 25 [23]}$$

where:

$A_m(t)$ = is the area enclosed by the cross-mid-line, section's as shown in Figure 2b.

ds = is developed mid-line Length.

$a(t)$ = is the Thickness of the considered small element of the cross-section, as shown in Figure 2(b).

a_0 = is the initial Thickness of the considered small element of the cross-section.

$C(t)$ = is the average corrosion penetration on micrometers (10^{-3})

t = is the age in years

t_0=is the time in years of first the appearance of the sign of general/uniform Corrosion [23]

Effective Warping constant

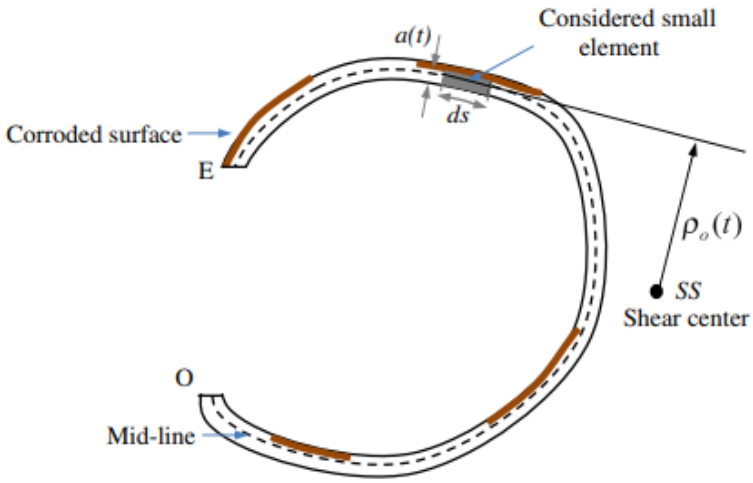

Figure 3.4-2: Schematic representations of warping parameters of thin-walled open cross-sections [23]

For a corroded member with a thin-walled open cross-section, the effective warping constant is approximately calculated by considering the plate thickness reduction due to general corrosion wastage. As shown in Figure 3.4.2, ρo(t) is the perpendicular distance between the shear centre SS and the tangent to the mid-line of the section wall of the considered small element. [23]

ρ_o= is the perpendicular distance from the shear center SS to the tangent to the mid-line of the section wall of the considered small element.

$$I_{w,eff}(t) = \int_0^E \{\alpha_n(t) - \alpha(t)\}^2 \, a(t) \, ds \qquad \text{Eq. 26 [23]}$$

$$\alpha(t) = \int_0^S \rho_o ds \qquad \text{Eq. 27 [23]}$$

And

$$\alpha_n(t) = \frac{1}{A_{eff}(t)} \int_0^E \alpha(t) a(t)\, ds \qquad \text{Eq. 28 [23]}$$

3.5 Corroded Critical Moment (Mcr, Cor), Corroded Landa LT (λLT, Cor) and

$$Mcr, cor = \sqrt{\left(\frac{\pi^2 EIzz, eff}{L^2}\right) * \left(GIt, eff + \left(\frac{\pi^2 EIw, eff}{L^2}\right)\right)} \qquad \text{Eq. 29 [23]}$$

Corroded dimensional slenderness ratio:

$$\lambda_{LT,cor} = \sqrt{\frac{Wplyeff * fy}{Mcr, cor}} \qquad \text{Eq. 30 [23]}$$

$Wy = Wply$ For Class 1 or 2 Cross Section

$Wy = Wel, y$ For Class 3 Cross Section

$Wy = Wel, y$ For Class 4 Cross Section

Corroded dimensional plastic neutral axis:

$$T = C$$

$$At * fy = Ac * fy$$

$$yp = \frac{((Hc * tw) - (tfc * tw) - (Hw/2 * tw) + (Hw/2 * twc) + (Bc * tfc) - (B * tf) + (tf * tw))}{2 * tw}$$ Eq. 31

Corroded Plastic modulus Wply:

Tension Part	Compression Part
At1=B*tf	Ac1=Bc*tfc
At2=(yp-tf)*tw	Ac2=(Hw/2)*twc
yt1=yp-(tf/2)	Ac3=(Hc-yp-tfc-(Hw/2))*tw
yt2=(yp-tf)/2	yc1=Hc-yp-(tfc/2)
	yc2=Hc-yp-tfc-(Hw/4)
	yc3=(Hc-yp-tfc-(Hw/2))/2

$$Wplyeff = (At1 * yt1) + (At2 * yt2) + (Ac1 * yc1) + (Ac2 * yc2) + (Ac3 * yc3)$$ Eq. 32

3.5 Corroded LTB moment capacity

In this section the formulas for the corroded LTB moment capacity are illustrated below:

$$\chi_{LT,cor} = \frac{1}{(\phi_{LT,cor} + \sqrt{\phi_{LT,cor}^{\ 2} - \lambda_{LT,cor}^{\ 2}})}$$ Eq. 33

Where:

$$\phi_{LT,cor} = 0.5\left[(1 + \alpha_{LT}(\lambda_{LT,cor} - 0.2) + \lambda_{LT,cor}^{\ 2}\right]$$

α_{LT} is an imperfection factor

$$MbRd, cor = \chi_{LT,cor} * Wy * \frac{fy}{\Upsilon m1}$$ Eq. 34

3.6.1 Stepwise calculation- Case corrosion 2

I. One of the first steps is to calculate the main effective parameters which affect LTB, such as from **Eq.19 to Eq.28.**

II. The next step calculates the Corroded elastic critical Moment Mcr, such as (**Eq.29),** which depends on the parameters calculated on the previous step.

III. The third step is to calculate the plastic neutral axis and the plastic section modulus with **(Eq.31) and (Eq.32),** and the non-dimensional slenderness ratio (**Eq.30)**.

IV. The Buckling curve is necessary to get the imperfection factor α_{LT}, which is necessary to calculate the LTB equations above. From Table 1 we can get the buckling curve, which is explained in detail above, and from Table 2 we can get the imperfection factor α_{LT} if the buckling curve is known.

V. The last step is to calculate the corroded-reduction factor part 1 ϕ_{LTc} and part 2 χLt **(Eq.33)**, and the buckling moment capacity Mbrd **(Eq.34).**

Appendix E includes the calculated /performed main corroded parameters in software; Sap2000 and Ansys Workbench.

4 Finite element simulation

4.1 Ansys workbench and modelling procedure

Ansys Workbench 2020 is the software which is used to generate the models and to obtain the necessary results for the LTB performance.

1. Engineering data
2. Geometry
3. Model
4. Setup
5. Solution
6. Results

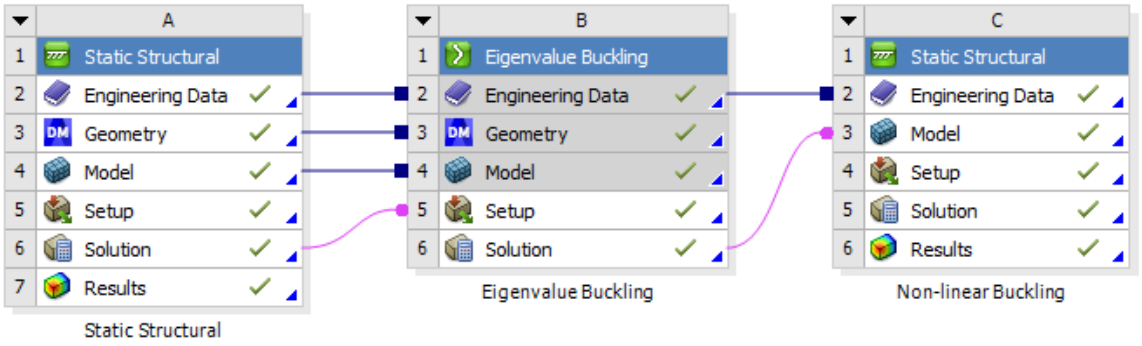

Figure 4.1-1: The flowchart model in Ansys workbench 2020. System A and C are static structural system, system B is an eigenvalue buckling system.

Modelling and performing any kind of analysis in Ansys include the three steps as follows:

I. Preprocessing
II. Solution
III. Post processing

i. Pre-processing

Preprocessing includes defining the engineering properties and creating the geometry of the wanted model.

Engineering properties

Outline of Schematic A2, B2, C2: Engineering Data

	A	B	C	D	E
1	Contents of Engineering Data			Source	Description
2	Material				
3	High strength low alloy steel, YS355			GRA	High strength low alloy steel, hot rolled, yield strength 355 MPa (EN 10149-2:1996 S355MC) Data compiled by the Granta Design team at ANSYS, incorporating various sources including JAHM and MagWeb. ANSYS Inc. provides no warranty for this data.
4	Structural Steel			Gen	Fatigue Data at zero mean stress comes from 1998 ASME BPV Code, Section 8, Div 2, Table 5-110.1
5	Structural Steel NL			Gen	Fatigue Data at zero mean stress comes from 1998 ASME BPV Code, Section 8, Div 2, Table 5-110.1
*	Click here to add a new material				

Properties of Outline Row 3: High strength low alloy steel, YS355

	A	B	C	D	E
1	Property	Value	Unit		
2	Material Field Variables	Table			
3	Density	7850	kg m^-3		
4	Isotropic Secant Coefficient of Thermal Expansion				
5	Coefficient of Thermal Expansion	1,196E-05	C^-1		
6	Isotropic Elasticity				
7	Derive from	Young's Modulus and Poisson's Ratio			
8	Young's Modulus	2,1E+11	Pa		
9	Poisson's Ratio	0,3			
10	Bulk Modulus	1,75E+11	Pa		
11	Shear Modulus	8,0769E+10	Pa		
12	Bilinear Isotropic Hardening				
13	Yield Strength	390,2	MPa		
14	Tangent Modulus	951	MPa		
15	S-N Curve	Tabular			
16	Interpolation	Semi-Log			
17	Scale	1			
18	Offset	0	Pa		
19	Tensile Yield Strength	Tabular			
20	Tensile Ultimate Strength	Tabular			

Figure 4.1-2: Engineering library in Ansys Workbench

Geometry

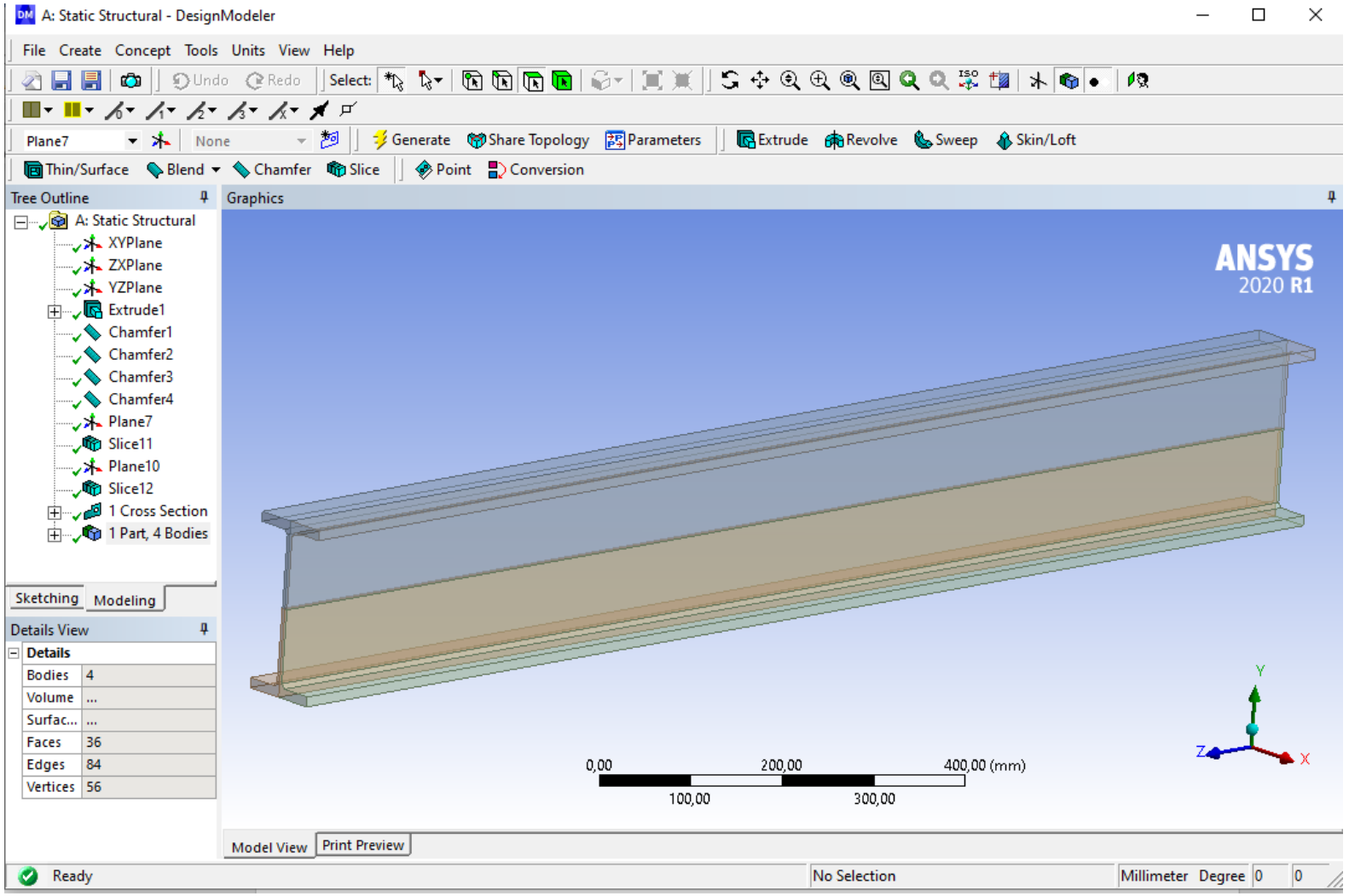

Figure: 4.1-3 A Sketch of an I-Beam model

ii. Solution

Boundary conditions, meshing, and loading are added to the model in this static structural multiple method.

Loading and boundary conditions

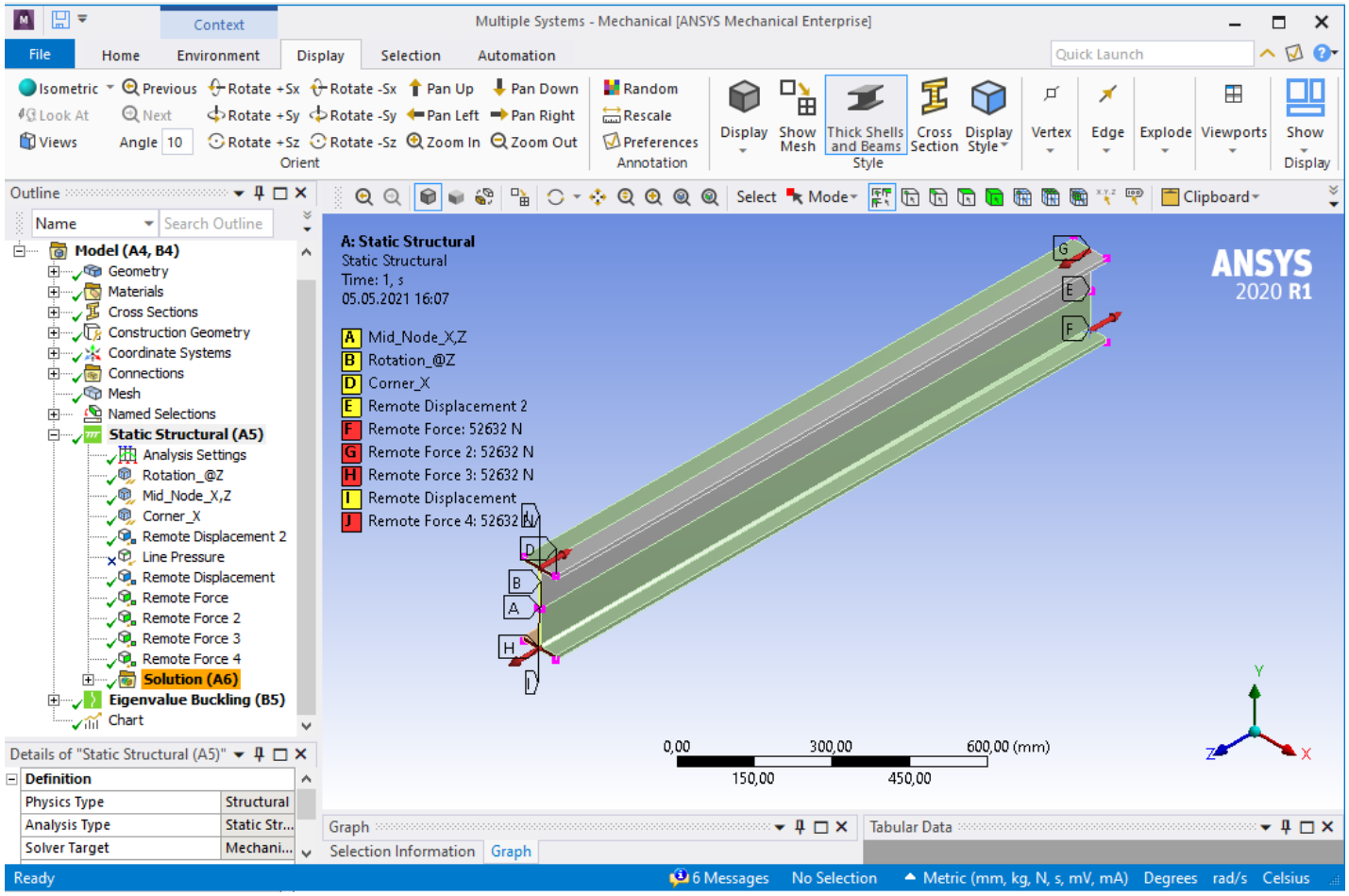

Figure: 4.1-4: The loading and boundary conditions

Meshing

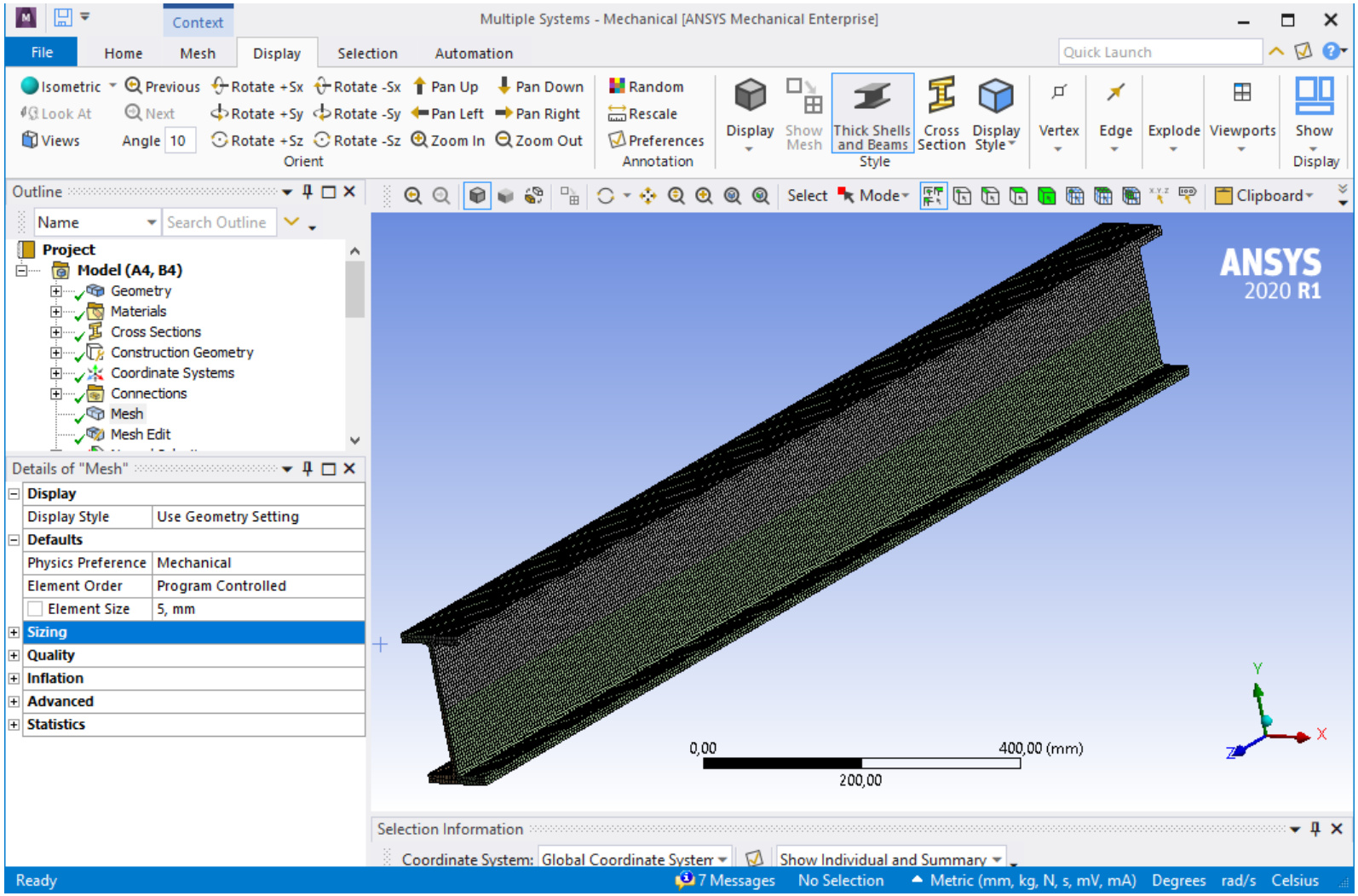

Figure: 4.1-5: The model with the Mesh

iii. Postprocessing

Eigenvalue buckling mode shape

Position 1

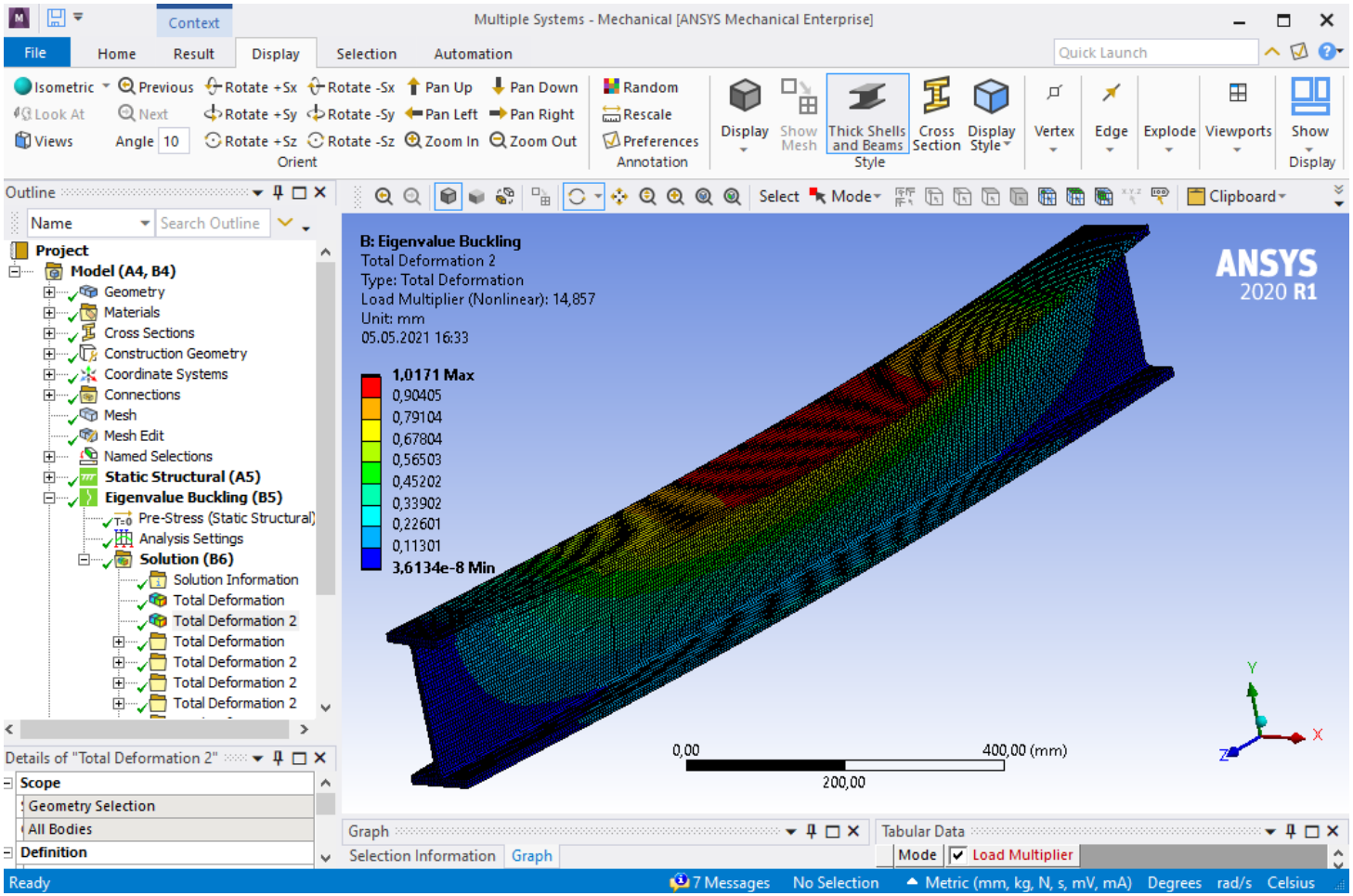

Figure 4.1-6: Eigen value buckling analysis-position 1

Eigenvalue buckling mode shape

Position 2

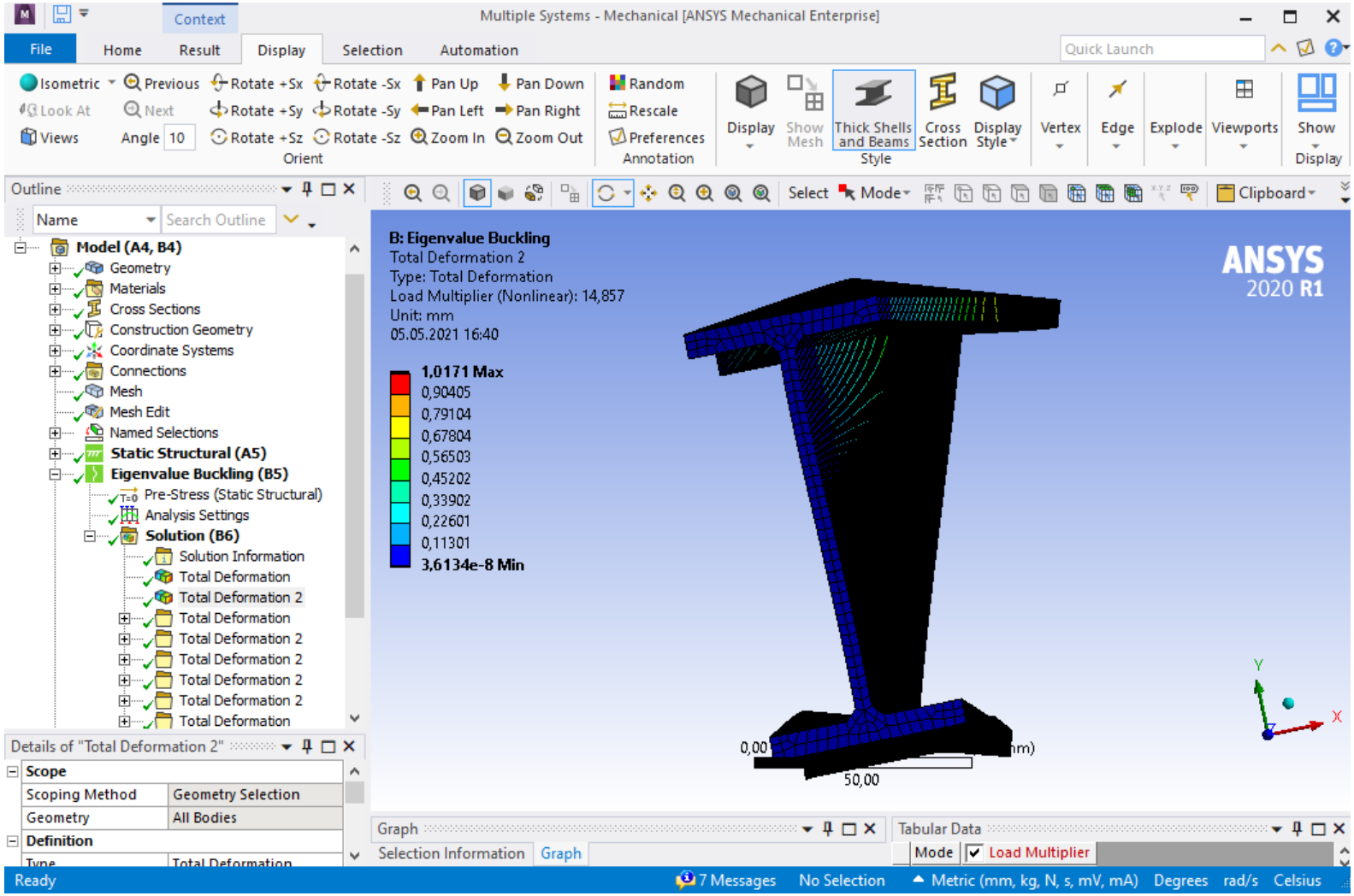

Figure 4.1-7: Eigen value buckling analysis-position

4.2 FEM Model (Computational model)

Boundary condition

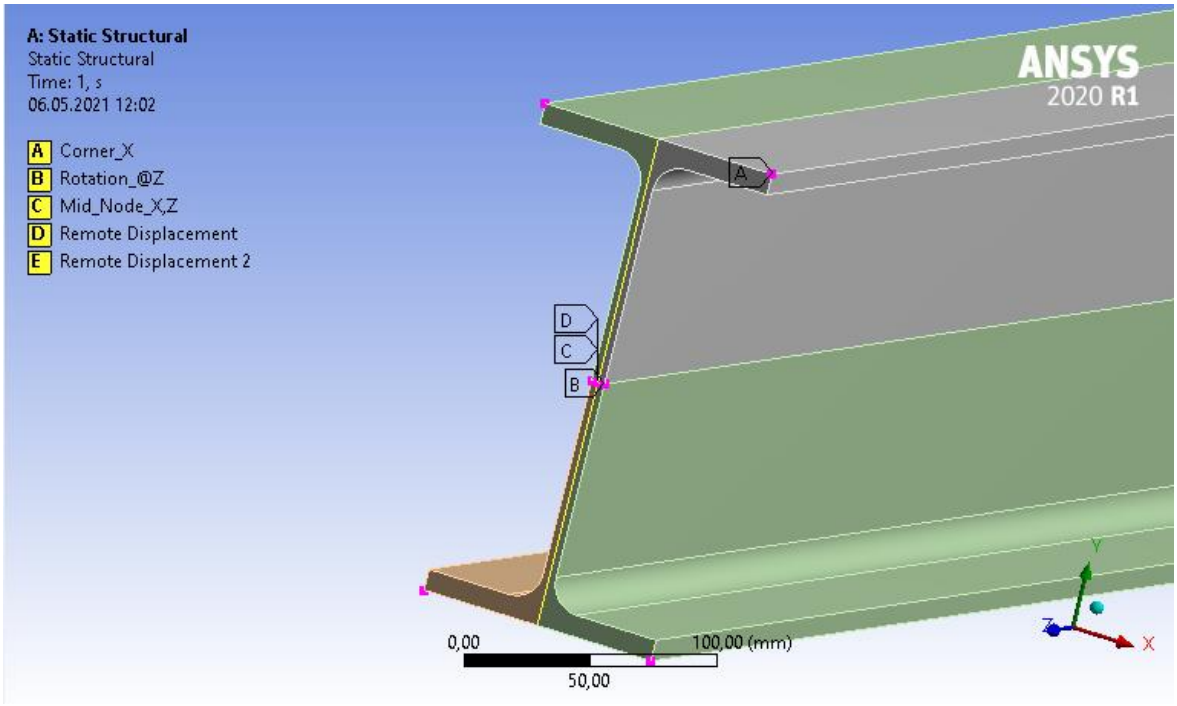

Figure 4.2-1: The chosen boundary condition

Table 4: The considered boundary condition assumption

	Ux	Uy	Uz	URx	URy	URz
Corner_X	0	0	-	-	-	-
Rotation_@Z	-	0	-	-	-	-
Mid_Node_X, Z	0	-	0	-	-	-
Remote Displacement 1	-	0	-	-	-	-
Remote Displacement 2	-	0	-	-	-	-

Ux=Displacement in x-axes

Uy=Displacement in y-axes

Uz=Displacement in z-axes

URx=Rotation in x-axes

URy=Rotation in y-axes

URz=Rotation in z-axe

Note:

- Boundary conditions: Corner_X, Rotation_ and Mid_Node_X,Z, include the nodes for both ends, while in the picture only one end is shown.
- In the picture only remote displacement 1 is visible, while remote displacement 2 is not because it is attached at the other end.
- At first it was not possible to prevent rotation in the z-axis in workbench, instead the displacement in the y-axis was prevented which gives the same behaviour as "No rotation in z the axis".

The first boundary condition was taken from the article *"FE nonlinear analysis of lateral-torsional buckling resistance*" and is illustrated on Figure 4.2-2.

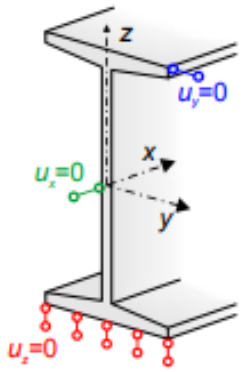

Figure 4.2-2: The first boundary condition assumption [11]

The second boundary condition was taken from the article *"The influence of structural imperfections on the LTB strength of I-beams"* and is illustrated on Figure 4.2-3.

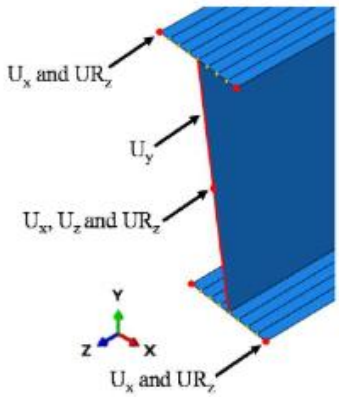

Figure 4.2-3: The second boundary condition assumption [25]

The Loading types

Table 5: The considered loading type

Loading type
Ends moment at the end of the beam
Uniform line pressure

Table 6: The considered Loading type and its elastic critical moment value given by workbench Ansys

Load Type	Mcr (KNm) (Eigen Value*Applied M)
Ends moment at the end of the beam	14.154*10=141.54
Uniform line pressure	11.139*10=111.39

End moment at the end of the beam

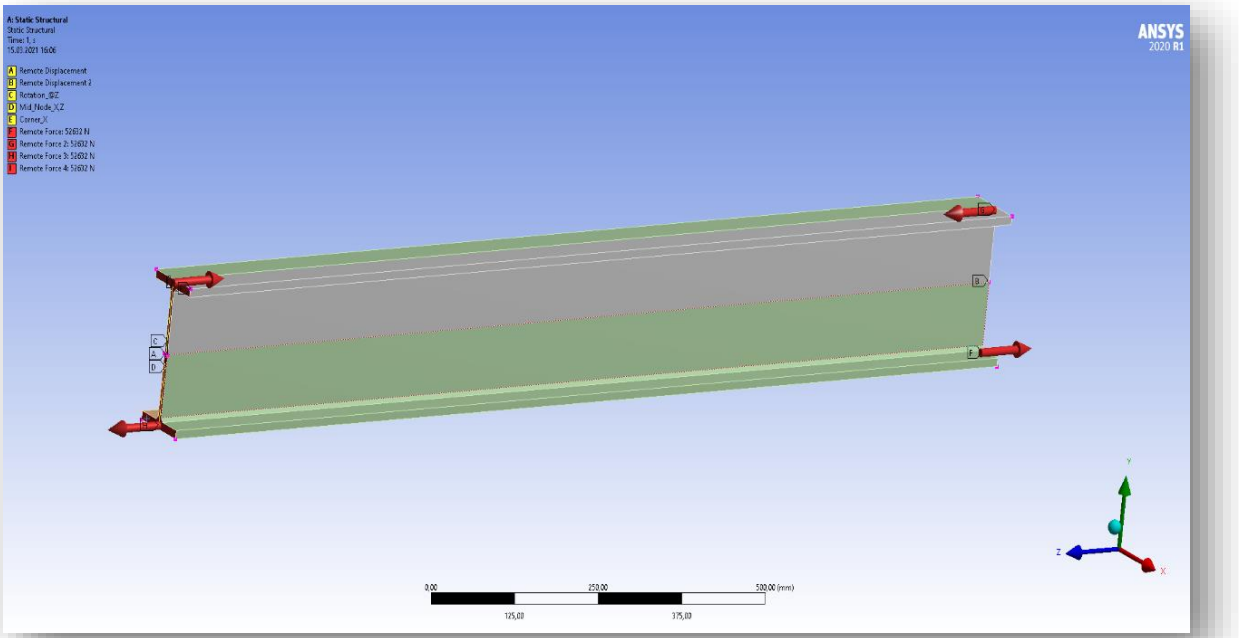

Figure 4.2-4: Ends moment at the end of the beam

Uniform line pressure

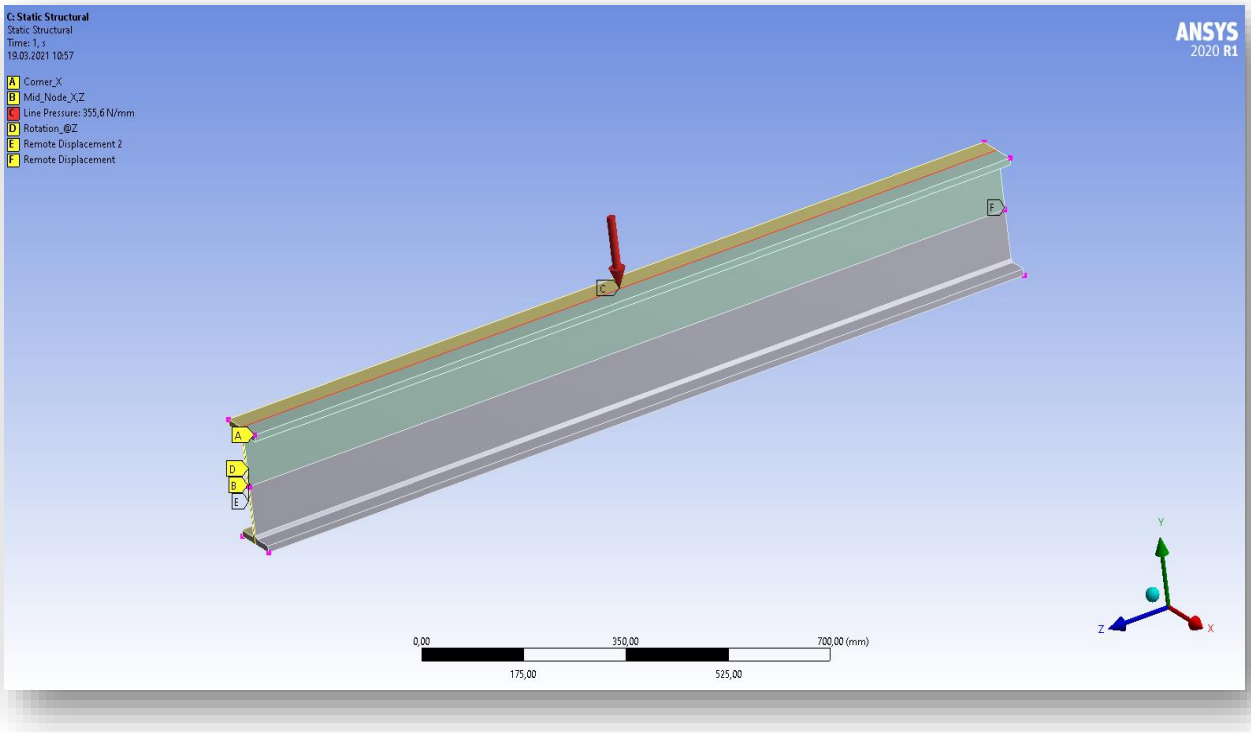

Figure 4.2-5: Uniform line pressure

Meshing

Experimenting with the mesh; (or maximum stress vs mesh density and maximum displacement vs mesh density)

The way to find the right mesh density for all the finite element model's cases is by redoing the linear analysis and buckling analysis with different mesh densities. By decreasing the mesh density the software uses less time to perform the analysis, but the results are less accurate. By increasing the mesh density the software uses more time to perform the analyses and the results are more accurate. The chosen mesh density for all the FEM Analyses is 5mm.

Different Length vs Imperfection scale factor for the Nonlinear Analyses

By using the formula which was given in the article "*FE nonlinear of Lateral-torsional buckling resistance"*

$$eo = \frac{L}{1000} \qquad \text{Eq. 35 [11]}$$

One example:

$$eo = \frac{1500}{1000} = 1.5$$

Table 7: Different Length vs Different Imperfection scale factor for the Nonlinear Analyses

Length (mm)	$\boldsymbol{eo = \frac{L}{1000}}$
550	**0.55**
1000	**1**
1500	**1.5**
2000	**2**
2300	**2.3**
2500	**2.5**
3000	**3**
3400	**3.4**
4000	**4**
5000	**5**
7000	**7**
10000	**10**

Applied Load for linear- and nonlinear Analyses

In order to continue with the nonlinear analysis after the linear- and eigenvalue buckling analyses, we have to press/select “solution” and chose the mode shape which gives the LTB performance and the scale factor which is dependent on the length of the beam.

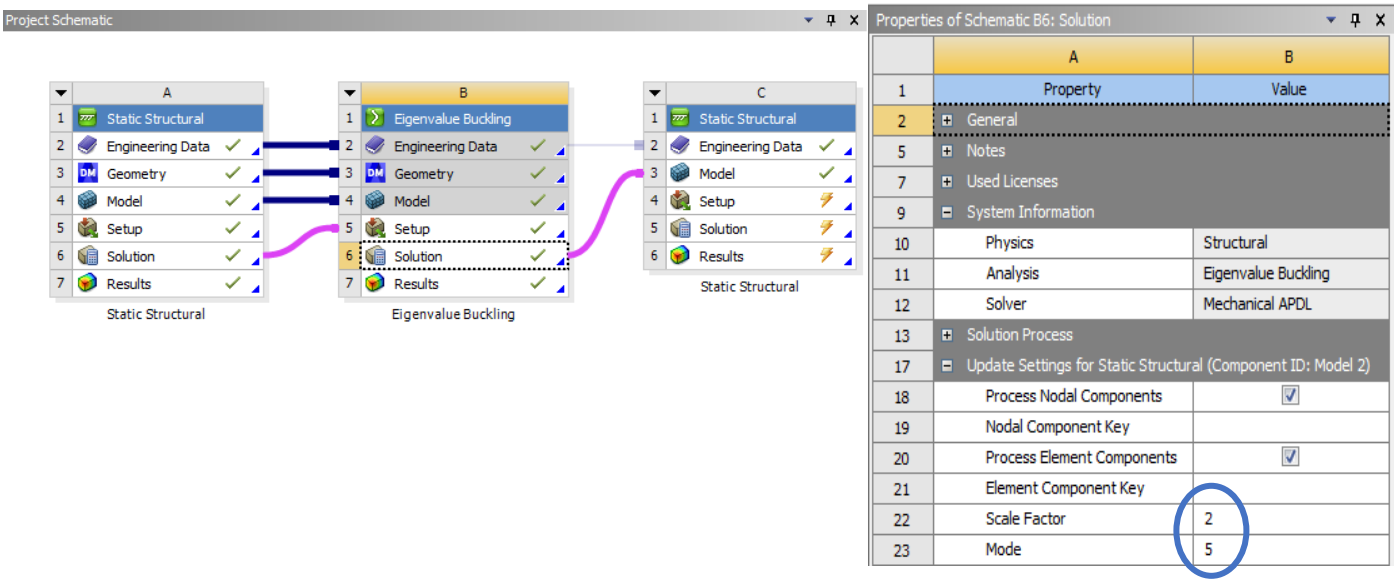

-

4.3 Considered Corrosive states/cases

The formulas which where use:

If we use uniform line pressure:

$$M = \frac{wL^2}{8}$$

Reshape the Formula

$$w = \frac{M * 8}{L^2}$$

If we use uniform pressure:

$$w' = \frac{w}{B}$$

Where the B is the width if the I-beam

Material properties of the I-beam

Table 8: The Material properties of the I-beam

Material	High strength low alloy steel, YS355
Modulus of elasticity	210000 Mpa
Shear modulus	80769 Mpa
Poisson's ratio	0.3
Tensile Yield Strength	390.2 Mpa
Tensile Ultimate Strength	486.3 Mpa

4.3.1 Case-No Corrosion

The non-corrosion case doesn't contain any form or type of corrosion and the dimensions implemented in the finite element model are given on *Table 9.*

Table 9: The Dimensions for No corrosion

Hight (mm)	200
Top Flange Width (mm)	90
Bottom Flange Width (mm)	90
Web Thickness (mm)	7.5
Web hight (mm)	177.4
Top Flange thickness (mm)	11.3
Bottom Flange thickness (mm)	11.3
Hypotenuse (mm)	$\sqrt{5^2 + 5^2} = 5\sqrt{2}$
Wply (mm^3)	$250.92 * 10^3$
Izz (mm^4)	$1.38 * 10^6$
Iyy (mm^4)	$2.16 * 10^7$
It (mm^4)	$1.11 * 10^5$
Iw (mm^6)	$1.22 * 10^{10}$

Meshing - Boundary condition- Loading part

Geometry-Modelling Part

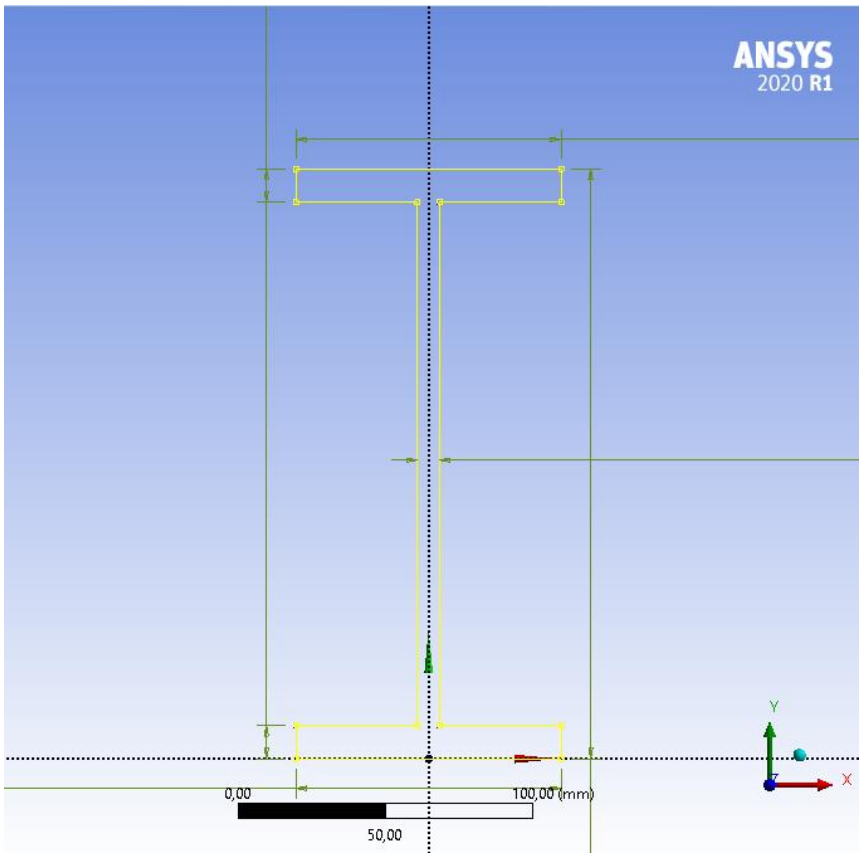

Figure 4.3.1-1: 2D View -Geometry- Modelling Part- No Corrosion

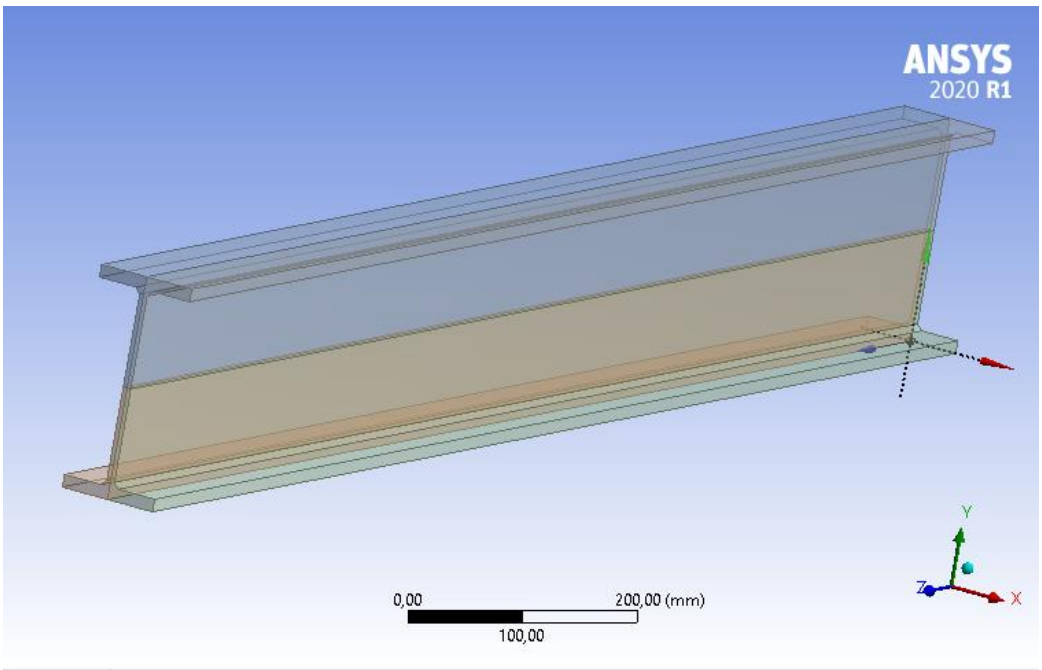

Figure 4.3.1-2: 3D-Geometry- Modelling Part- No Corrosion

Meshing

Table 10: Meshing performers-No corrosion

Mesh performers	**Program controlled**
Mesh density	5mm

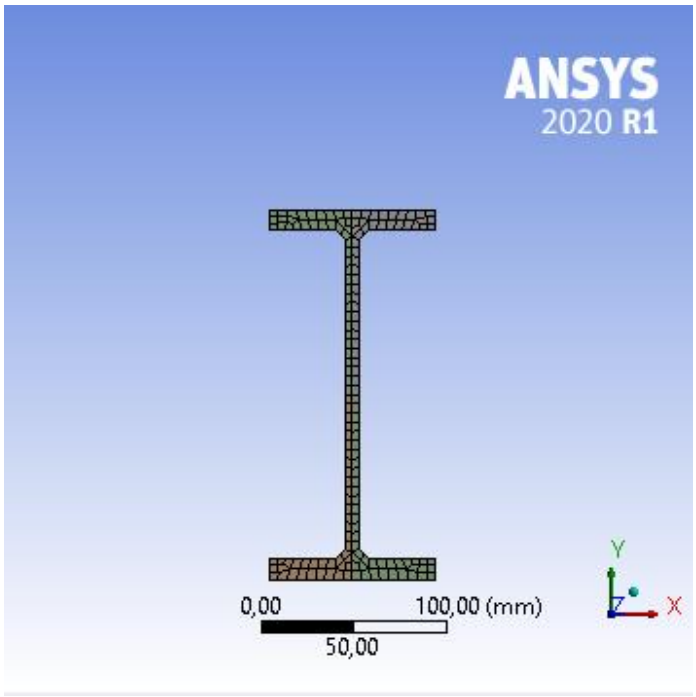

Figure 4.3.1-3: 2D Meshing View- No corrosion

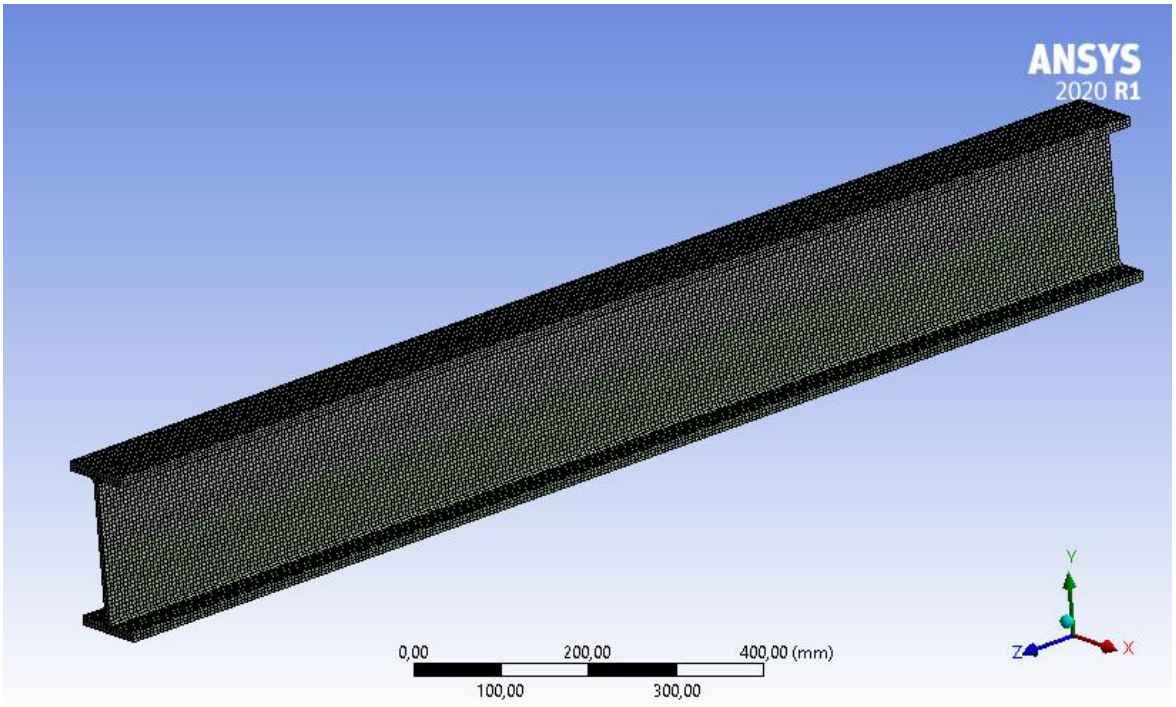

Figure 4.3.1-4: 3D Meshing View – No corrosion

Boundary condition and loading

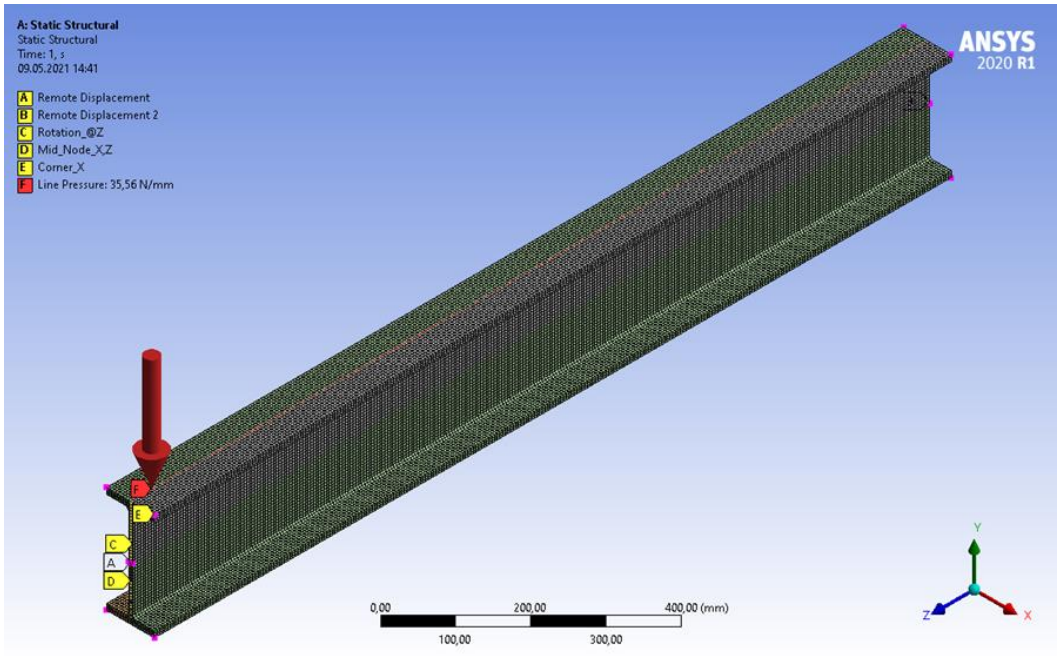

Figure 4.3.1-5: The 3D view -The boundary condition - No corrosion

Where:

L	Length
AM-SLA	Applied M - Static Analyses
AW-SL-LP	Applied W - Static Linear – Line Pressure
AM-NLA	Applied M – Non-Static Analyses
AW-NL-LP	Applied W – Nonlinear – Line Pressure

Table 11: No Corrosion- Applied Load for linear and nonlinear Analyses

L (m)	*AM-SLA (Knm)*	*AW-SLA (N/mm)*	AM-NLA *(Knm)*	*AW-NL-LP (N/mm)*
0.55	*10*	*264.5*	*120*	*3174*
1	*10*	*80*	*110*	*880*
1.5	*10*	*35.6*	*100*	*356*
2	*10*	*20*	*100*	*200*
2.3	*10*	*15.1*	*65*	*98.3*
2.5	*10*	*12.8*	*60*	*76.8*
3	*10*	*8.9*	*60*	*53.3*
3.4	*10*	*6.9*	*40*	*27.7*
4	*10*	*5*	*40*	*20*
5	*10*	*3.2*	*30*	*9.6*
7	*10*	*1.6*	*15*	*2.4*
10	*10*	*0.8*	*15*	*1.2*

4.3.2 Case Corrosion 1

Case corrosion 1 contains a corrosion case which is uniformly applied throughout the I-beam cross section and the dimensions implemented in the finite element model are given on *Table 12*.

The Dimension

Table 12: The Dimensions for Case Corrosion 1

Hight (mm)	**196.908**
Top Flange Width (mm)	**86.908**
Bottom Flange Width (mm)	**86.908**
Web Thickness (mm)	**4.408**
Web hight (mm)	**180.492**
Top Flange thickness (mm)	**8.208**
Bottom Flange thickness (mm)	**8.208**
Hypotenuse (mm)	$\sqrt{5^2 + 5^2} = 5\sqrt{2}$
Wply (mm^3)	$170.49 * 10^3$
Izz (mm^4)	$9.06 * 10^5$
Iyy (mm^4)	$1.49 * 10^7$
It (mm^4)	$3.72 * 10^4$
Iw (mm^6)	$7.99 * 10^9$

Meshing - Boundary condition- Loading part

Geometry-Modelling part

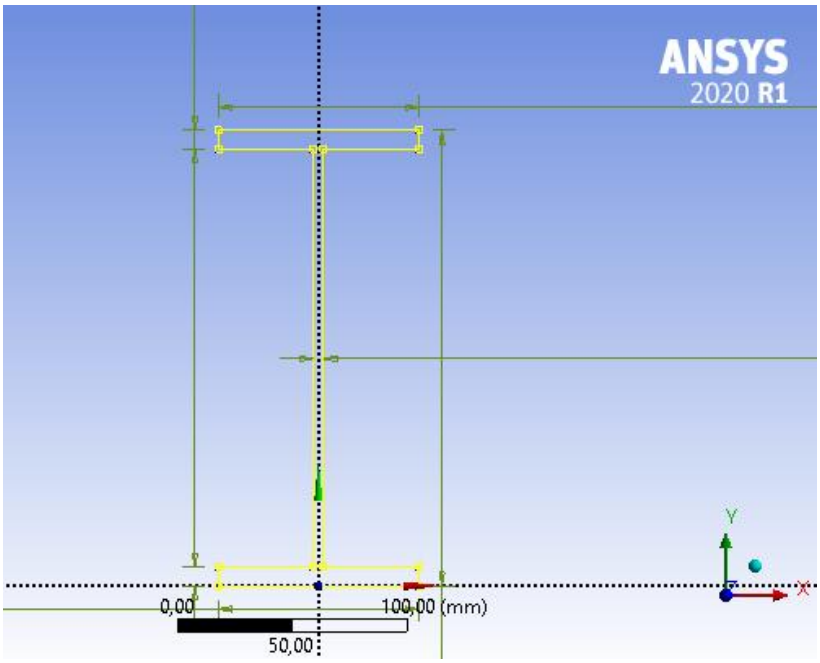

Figure 4.3.2-1: 2D View – Geometry – Modelling Part – Case Corrosion 1

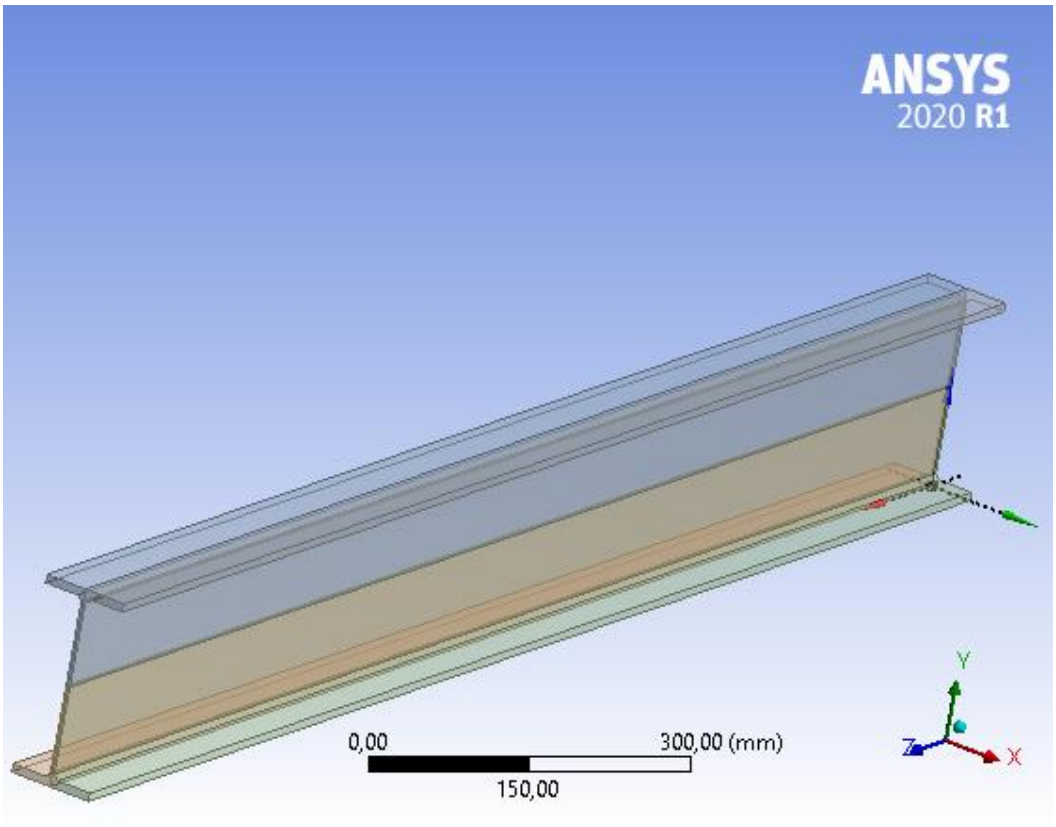

Figure 4.3.2-2: 3D-Geometry -Modelling Part – Case Corrosion 1

Meshing

Table 13: Meshing Performers-Case Corrosion 1

Mesh performers	**Program controlled**
Mesh density	5mm

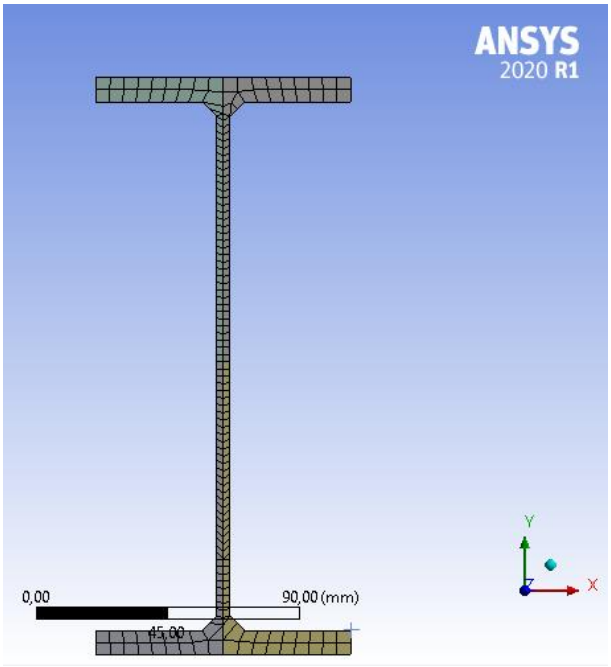

Figure 4.3.2-3: 2D Meshing View – Case Corrosion 1

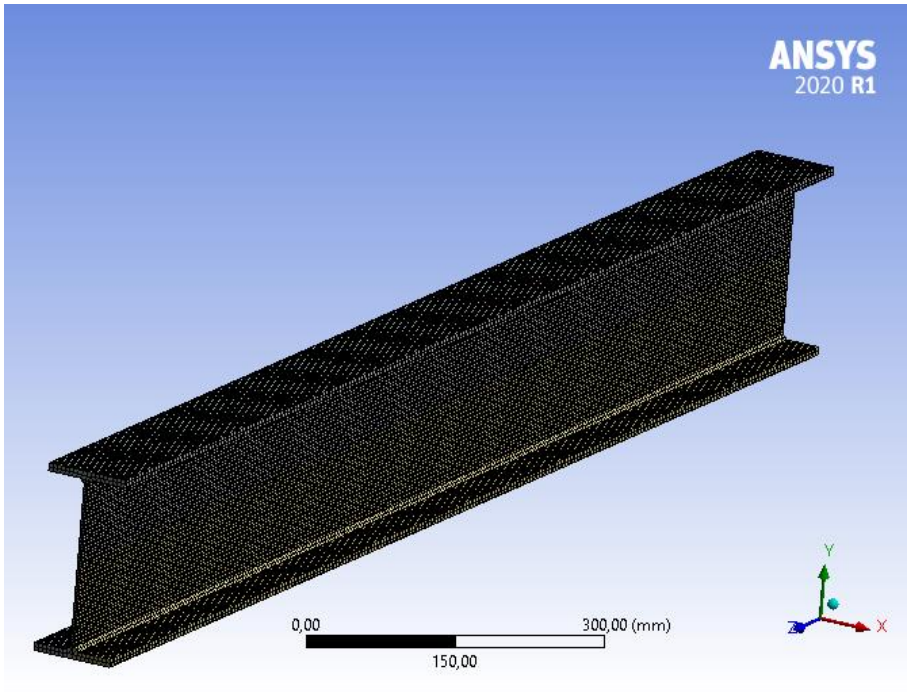

Figure 4.3.2-4: 3D Meshing View – Case Corrosion

Boundary conditions and loading

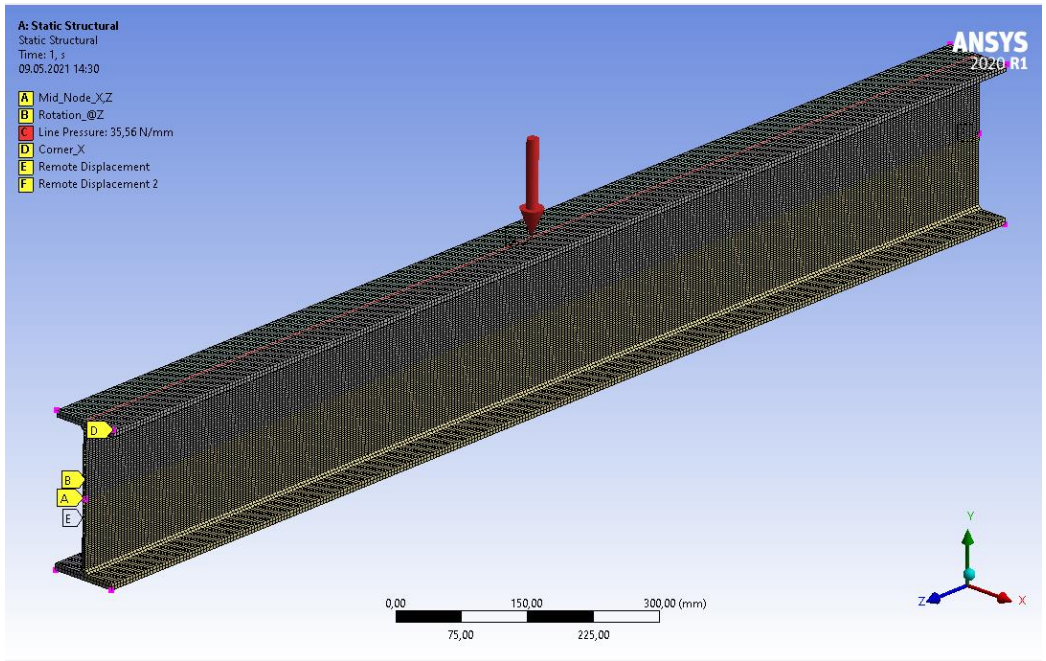

Figure 4.3.2-5: The 3D View – The Boundary Condition – Case Corrosion 1

Where:

L	Length
AM-SLA	Applied M - Static Analyses
AW-SL-LP	Applied W - Static Linear – Line Pressure
AM-NLA	Applied M – Non-Static Analyses
AW-NL-LP	Applied W – Nonlinear – Line Pressure

Table 14: Case Corrosion 1 - Applied load for linear and nonlinear Analyses

L ***(m)***	**AM-SLA** ***(Knm)***	***AW-SL-LP*** ***(N/mm)***	***AM-NLA*** ***(Knm)***	***AW-NL-LP*** ***(N/mm)***
0.55	*10*	*264.5*	*120*	*3174*
1	*10*	*80*	*110*	*880*
1.5	*10*	*35.6*	*100*	*356*
2	*10*	*20*	*70*	*140*
2.3	*10*	*15.1*	*65*	*98.3*
2.5	*10*	*12.8*	*100*	*128*
3	*10*	*8.9*	*40*	*35.6*
3.4	*10*	*6.9*	*40*	*27.7*
4	*10*	*5*	*40*	*20*
5	*10*	*3.2*	*30*	*9.6*
7	*10*	*1.6*	*15*	*2.4*
10	*10*	*0.8*	*15*	*1.2*

4.3.3 Case Corrosion 2

Case corrosion 2 contains a corrosion case which is uniformly applied throughout the bottom flange and the bottom section of the web of the I-beam cross section and the dimensions implemented in the finite element model are given on *Table 15*.

Table 15: The Dimensions for Case Corrosion 1

Hight (mm)	**198.454**
Top Flange Width (mm)	**90**
Bottom Flange Width (mm)	**86.908**
Top Web Thickness (mm)	**7.5**
Bottom Web Width (mm)	**4.408**
Web hight (mm)	**178.946**
Top Flange thickness (mm)	**11.3**
Bottom Flange thickness (mm)	**8.208**
Hypotenuse 1-NC (mm)	$\sqrt{5^2 + 5^2} = 5\sqrt{2}$
Hypotenuse 1-C (mm)	$\sqrt{2.81^2 + 2.81^2} = 3.974$
Wply (mm^3)	$199.931 * 10^3$
Izz (mm^4)	$1.139 * 10^6$
Iyy (mm^4)	$1.766 * 10^7$
It (mm^4)	$7.383 * 10^4$
Iw (mm^6)	$9.643 * 10^9$

NC-No Corrosion

C-Corrosion

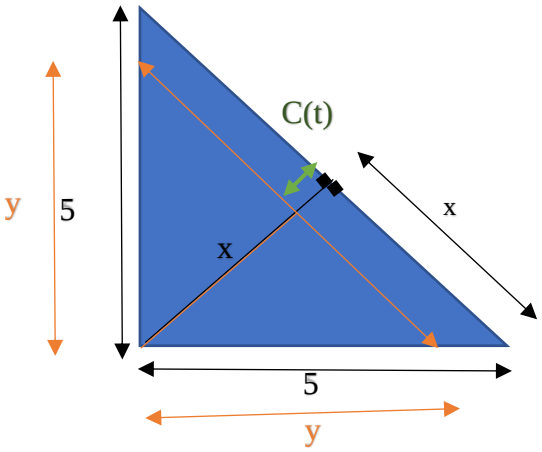

Figure 4.3.3-1: Illustration

$$\sqrt{x^2 + x^2} = 5^2$$

$$\sqrt{2x^2} = 5^2$$

$$\sqrt{2x^2} = 5^2$$

$$x = \sqrt{\frac{5^2}{2}}$$

$$x = \frac{5}{\sqrt{2}}$$

C(t)=1.546

$$y = \sqrt{\left(\frac{5}{\sqrt{2}} - 1.546\right)^2 + \left(\frac{5}{\sqrt{2}} - 1.546\right)^2}$$

$$y = 2.81$$

Where:

C(t) = The corrosion rate

x= is the Length of the weld before Corrosion takes place

y= is the Length of the weld after Corrosion takes place

Meshing - Boundary condition- Loading part

Geometry-Modelling part

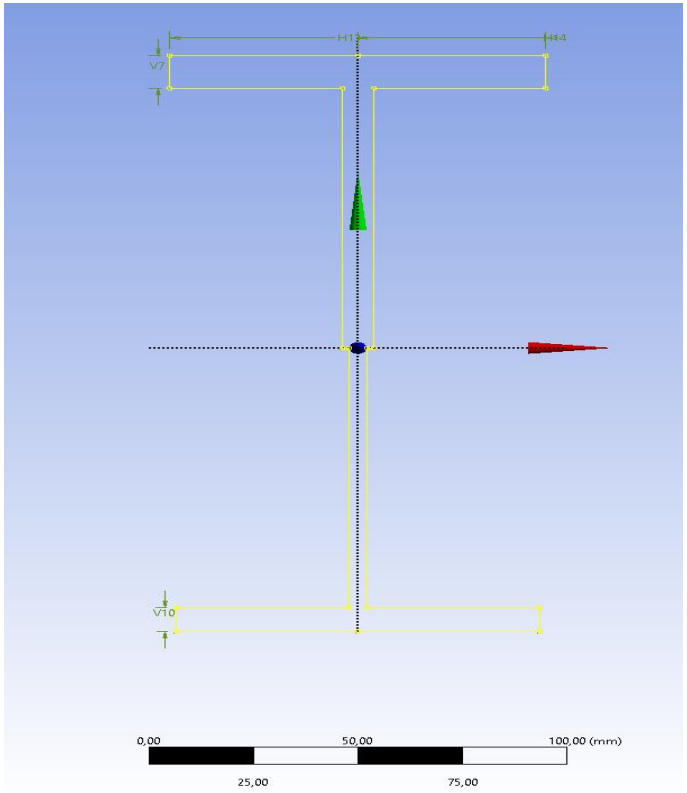

Figure 4.3.3-2: 2D View – Geometry -Modelling Part – Case Corrosion 2

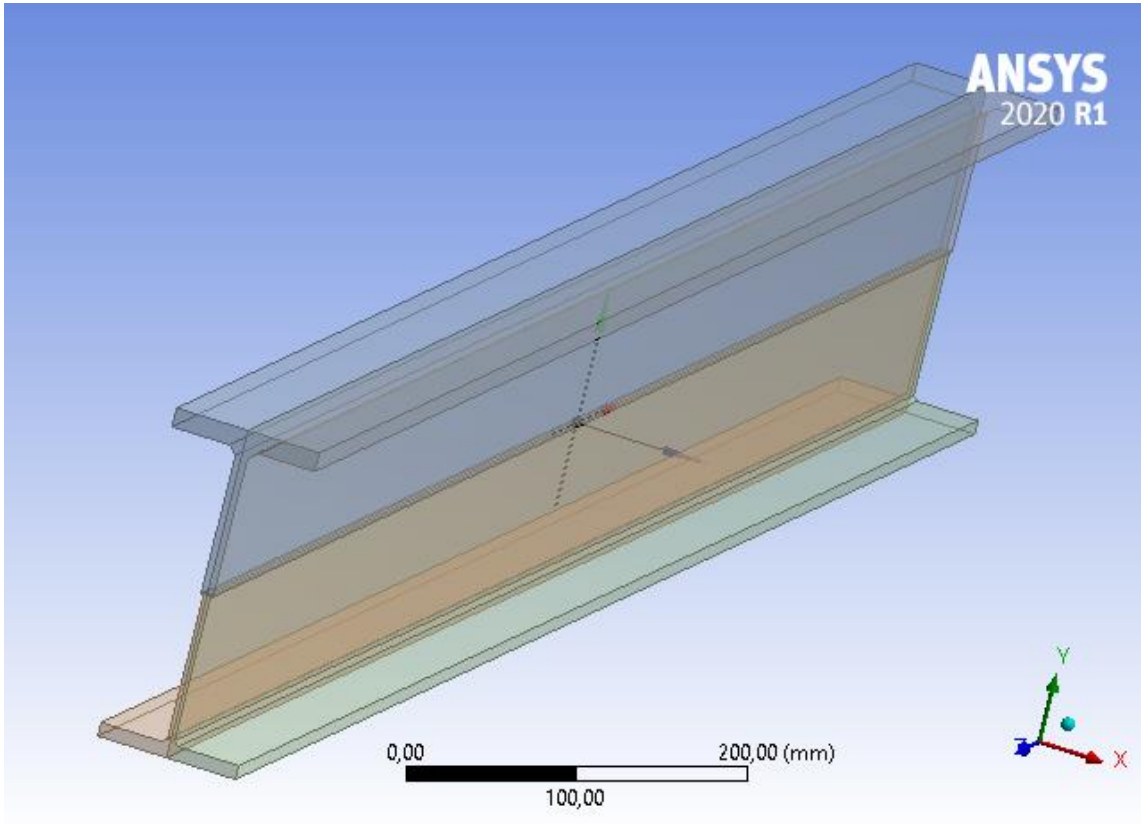

Figure 4.3.3-3: 3D – Geometry Part – Modelling Part – Case Corrosion 2

Meshing

Table 16: Meshing performers-Case Corrosion

Mesh performers	Program controlled
Mesh density	5mm

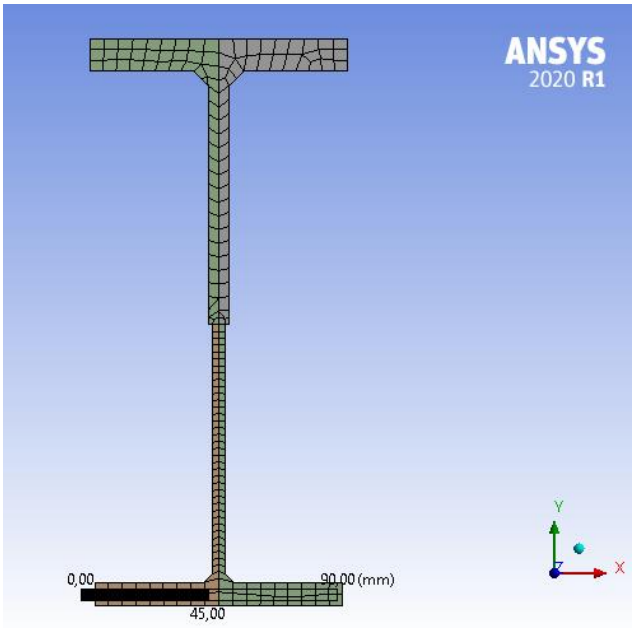

Figure 4.3.3-4 :2D Meshing View – Case Corrosion 2

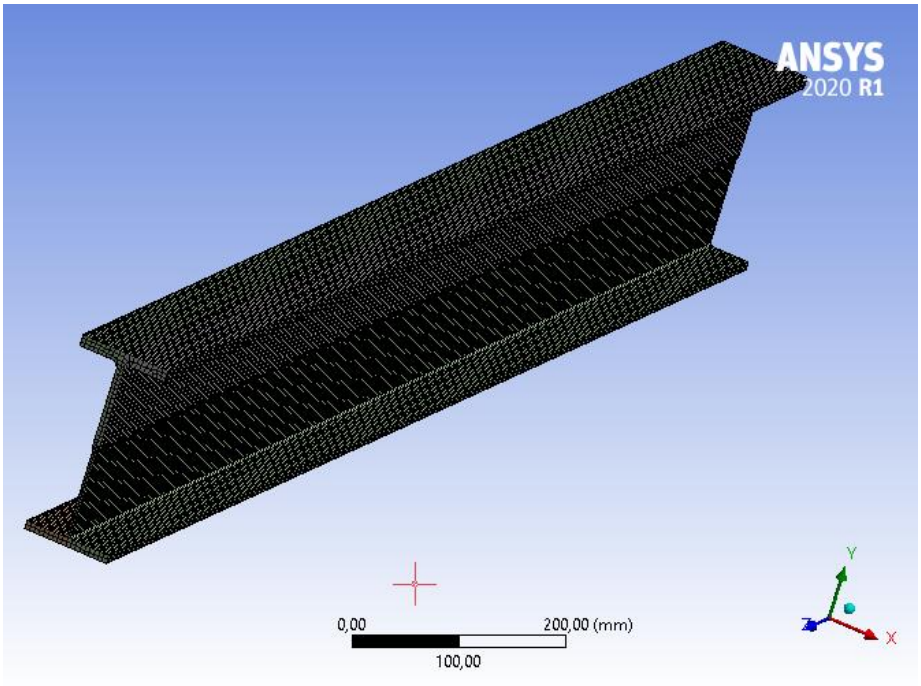

Figure 4.3.3-5: 3D Meshing View – Case Corrosion 2

Boundary conditions and loading

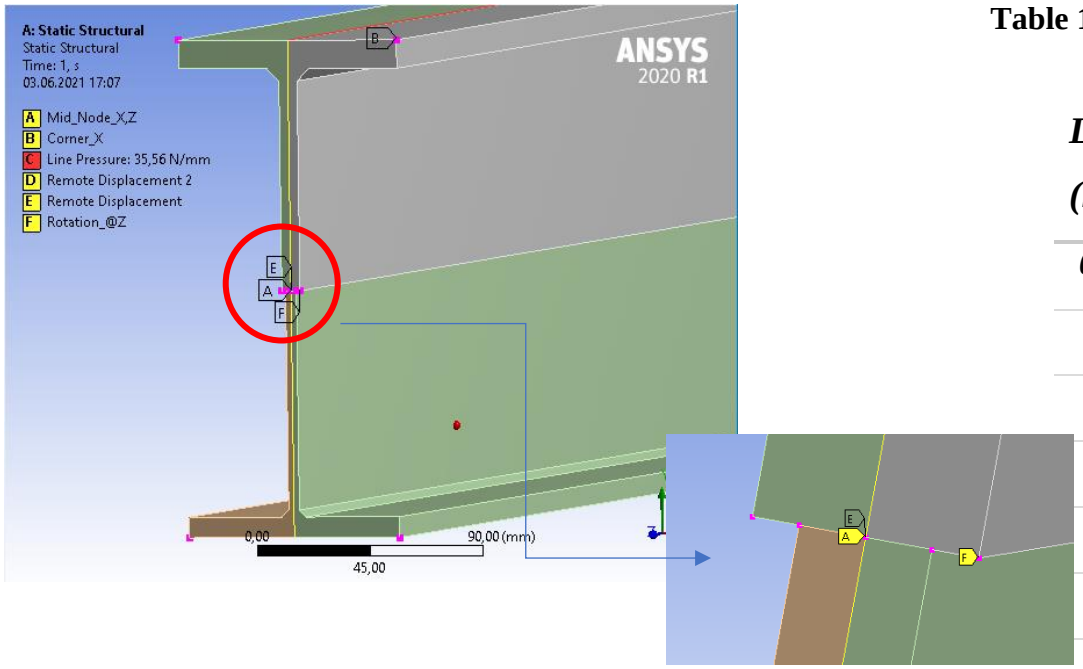

Figure 4.3.3-6: The 3D View – The Boundary Condition – Case Corrosion 2

AM-SLA Applied M - Static Analyses

AW-SL-LP Applied W - Static Linear – Line Pressure

AM-NLA Applied M – Non-Static Analyses

AW-NL-LP Applied W – Nonlinear – Line Pressure

Table 17: Case Corrosion 2 - Applied Load for linear- and nonlinear Analyses

L (m)	*AM-SLA (KNm)*	*AW-SLA (N/mm)*	*AM-NLA (KNm)*	*AW-NL-LP (N/mm)*
0.55	*10*	*264.5*	*120*	*3174*
1	*10*	*80*	*110*	*880*
1.5	*10*	*35.6*	*100*	*356*
2	*10*	*20*	*70*	*140*
2.3	*10*	*15.1*	*65*	*98.3*
2.5	*10*	*12.8*	*60*	*76.8*
3	*10*	*8.9*	*40*	*35.6*
3.4	*10*	*6.9*	*40*	*27.7*
4	*10*	*5*	*40*	*20*
5	*10*	*3.2*	*30*	*9.6*
7	*10*	*1.6*	*15*	*2.45*
10	*10*	*0.8*	*15*	*1.2*

4.3.4 Case Corrosion 3-Model 1

Case corrosion 3-Model 1 contains corrosion at 1/3 of the length of the I-beam at the top flange, bottom flange, and web. In other words, the I-beam will be divided into three parts. The first - and the third parts are without corrosion while the middle part is with corrosion and the dimensions implemented in the finite element model are given on *Table 18*.

Table 18: The Dimensions for case corrosion 3 – Model 1

Hight: No-C-F-Th (mm)	200
Top Flange Width: No-C-F-Th (mm)	90
Bottom Flange Width: No-C-F-Th (mm)	90
Web Thickness: No-C-F-Th (mm)	7.5
Web hight: No-C-F-Th (mm)	177.4
Top Flange thickness: No-C-F-Th (mm)	11.3
Bottom Flange thickness: No-C-F-Th (mm)	11.3
Hypotenuse 1-NC (mm)	$\sqrt{5^2 + 5^2} = 5\sqrt{2}$
Hypotenuse 1-C (mm)	$\sqrt{2.81^2 + 2.81^2} = 3.974$
Hight: C-M (mm)	196.908
Top Flange Width: C-M (mm)	86.908
Bottom Flange Width: C-M (mm)	86.908
Web Thickness: C-M (mm)	4.408
Web hight: C-M (mm)	180.492
Top Flange thickness: C-M (mm)	8.208
Bottom Flange thickness: C-M (mm)	8.208

No-C-F-Th = No corrosion for the first and third part of the beam

C-M = Corrosion at the middle part of the beam

Meshing - Boundary condition- Loading part

Geometry-Modelling part

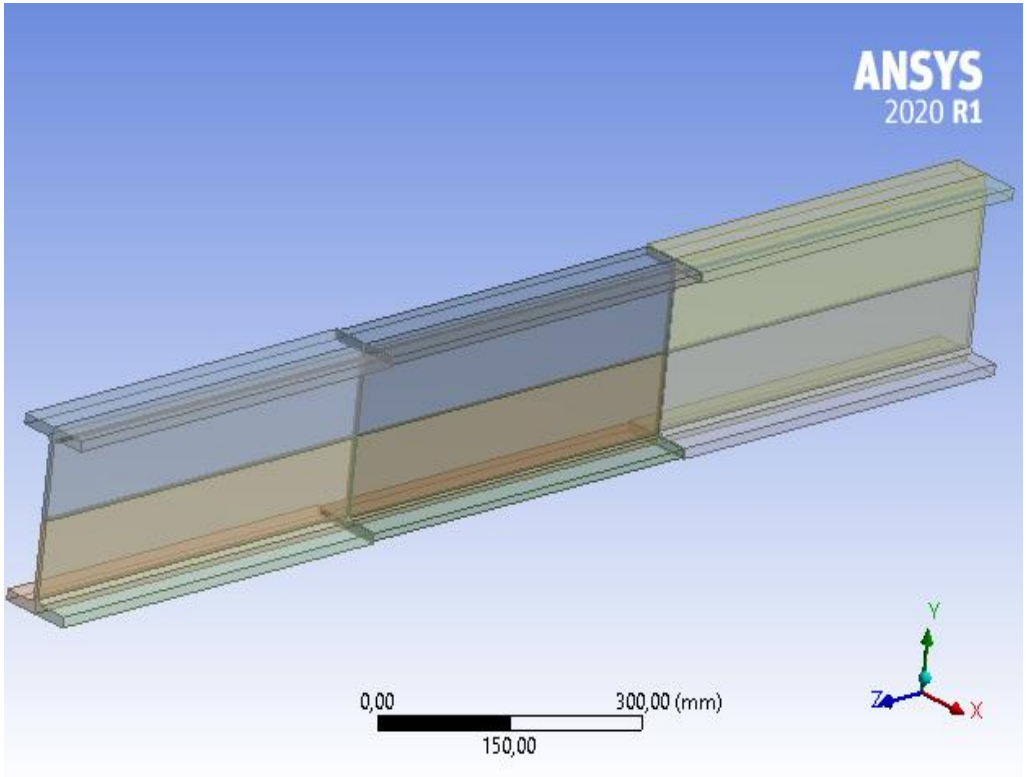

Figure 4.3.4-1: 2D View – Geometry – Modelling Part – Case corrosion 3- model 1

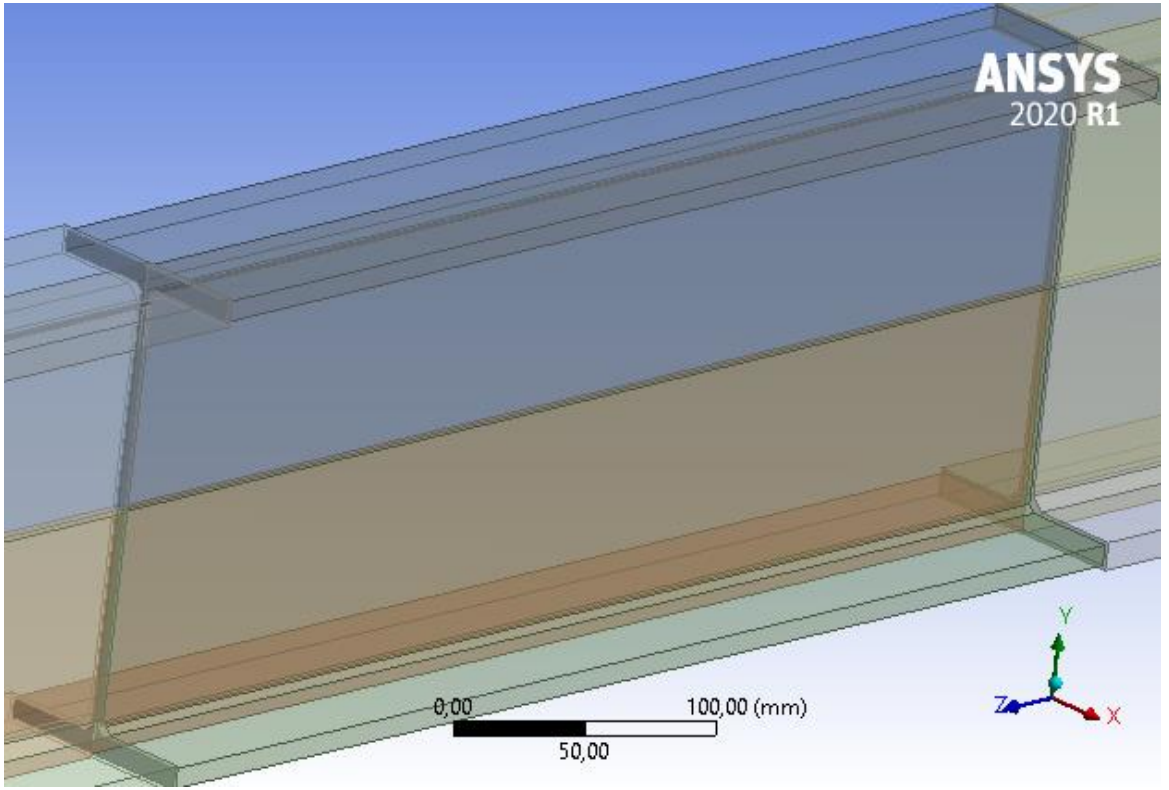

Figure 4.3.4-2: 3D View – A Zoom in – Modelling Part – Case Corrosion 3 – Model 1

Meshing

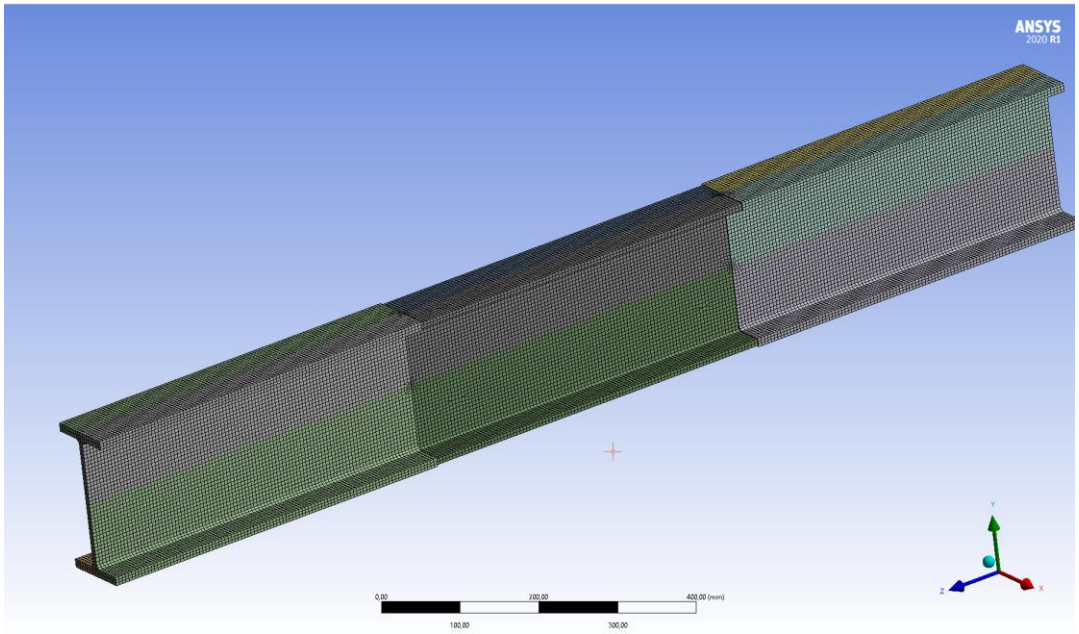

Figure 4.3.4-3: 3D Meshing View – Case Corrosion 3 – Model 1

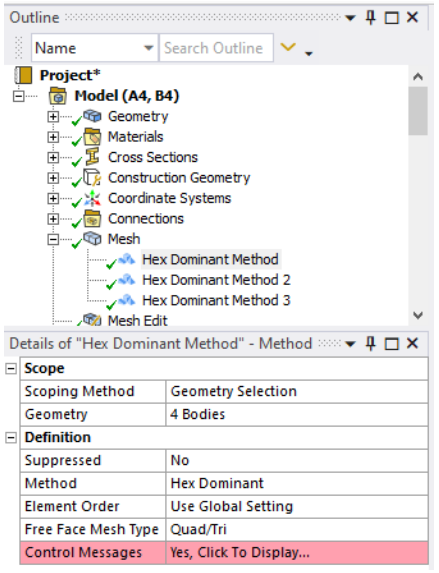

Figure 4.3.4-4: Ansys Meshing Overview-C-Case 3- Model 1

Table 19: Meshing Performers-Case Corrosion 3-Model 1

	Mesh performers	**Mesh density**
Part 1-No-C	Hex Dominant Method	5mm
Part 2-C	Hex Dominant Method 2	5mm
Part 3- No-C	Hex Dominant Method 3	5mm

Boundary conditions and loading

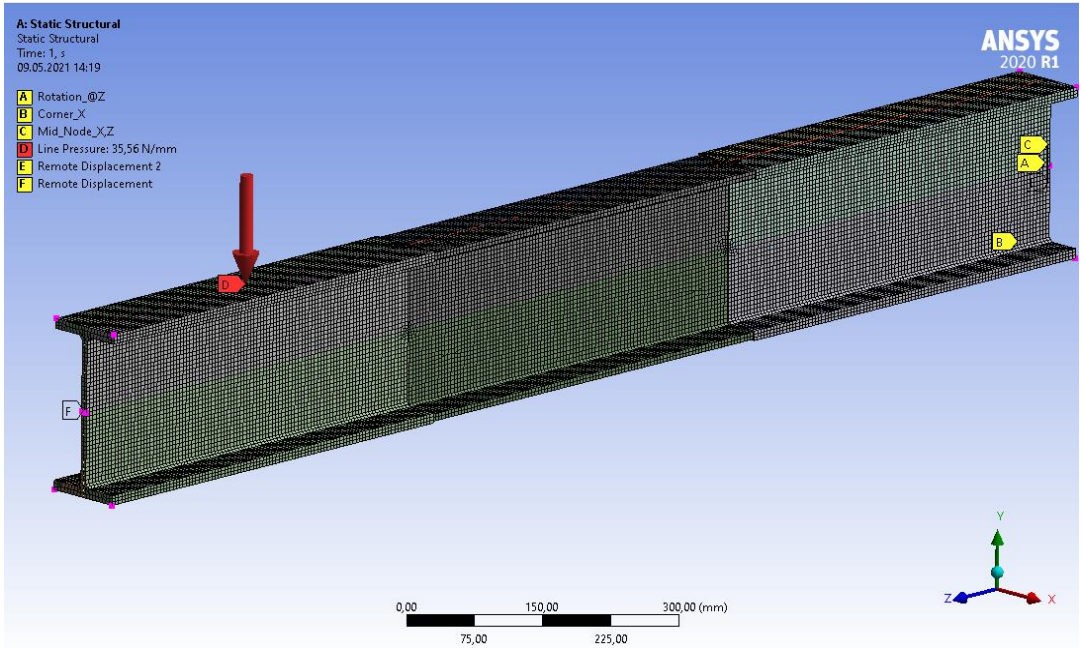

Figure 4.3.4-5: The 3D View – The boundary condition and Loading – Case Corrosion 3- Model 1

L	Length
AM-SLA	Applied M - Static Analyses
AW-SL-LP	Applied W - Static Linear – Line Pressure
AM-NLA	Applied M – Non-Static Analyses
AW-NL-LP	Applied W – Nonlinear – Line Pressure

Table 20: Applied Load for Linear- and Nonlinear-Corrosion 3 – Model 1

L (m)	*AM-SL-LP (KNm)*	*AW-SLA (N/mm)*	*AM-NLA (KNm)*	*AW-NL-LP (N/mm)*
0.55	*10*	*264.5*	*120*	*3174*
1	*10*	*80*	*110*	*880*
1.5	*10*	*35.6*	*90*	*320*
2	*10*	*20*	*87.5*	*175*
2.3	*10*	*15.1*	*65*	*98.3*
2.5	*10*	*12.8*	*60*	*76.8*
3	*10*	*8.9*	*40*	*35.6*
3.4	*10*	*6.9*	*40*	*27.7*
4	*10*	*5*	*40*	*20*
5	*10*	*3.2*	*30*	*9.6*
7	*10*	*1.6*	*15*	*2.45*
10	*10*	*0.8*	*15*	*1.2*

4.3.5 Case Corrosion 3- Model 2

Case corrosion 3-Model 2 contains corrosion at 1/3 of the length of the beam at the bottom flange and the bottom section of the web. In other words, the beam will be divided in three parts. The first and third parts are without corrosion while the middle part is with corrosion and the dimensions implemented in the model are given on *Table 21*.

Table 21: The Dimensions for case Corrosion 3-Model 2

Hight: No-C-F-Th (mm)	200
Top Flange Width: No-C-F-Th (mm)	90
Bottom Flange Width: No-C-F-Th (mm)	90
Top Web Thickness: No-C-F-Th (mm)	7.5
Web hight: No-C-F-Th (mm)	177.4
Top Flange thickness: No-C-F-Th (mm)	11.3
Bottom Flange thickness: No-C-F-Th (mm)	11.3
Hypotenuse 1-NC (mm)	$\sqrt{5^2 + 5^2} = 5\sqrt{2}$
Hypotenuse 1-C (mm)	$\sqrt{2.81^2 + 2.81^2} = 3.974$
Hight: C-M (mm)	198.454
Top Flange Width: C-M (mm)	90
Bottom Flange Width: C-M (mm)	86.908
Top Web Thickness: C-M (mm)	7.5
Bottom Web Thickness: C-M (mm)	4.408
Web hight: C-M (mm)	178.946
Top Flange thickness: C-M (mm)	11.3
Bottom Flange thickness: C-M (mm)	8.208

No-C-F-Th = No corrosion for the first and third part of the beam

C-M = Corrosion at the middle part of the beam

Meshing - Boundary condition- Loading part

Geometry-Modelling part

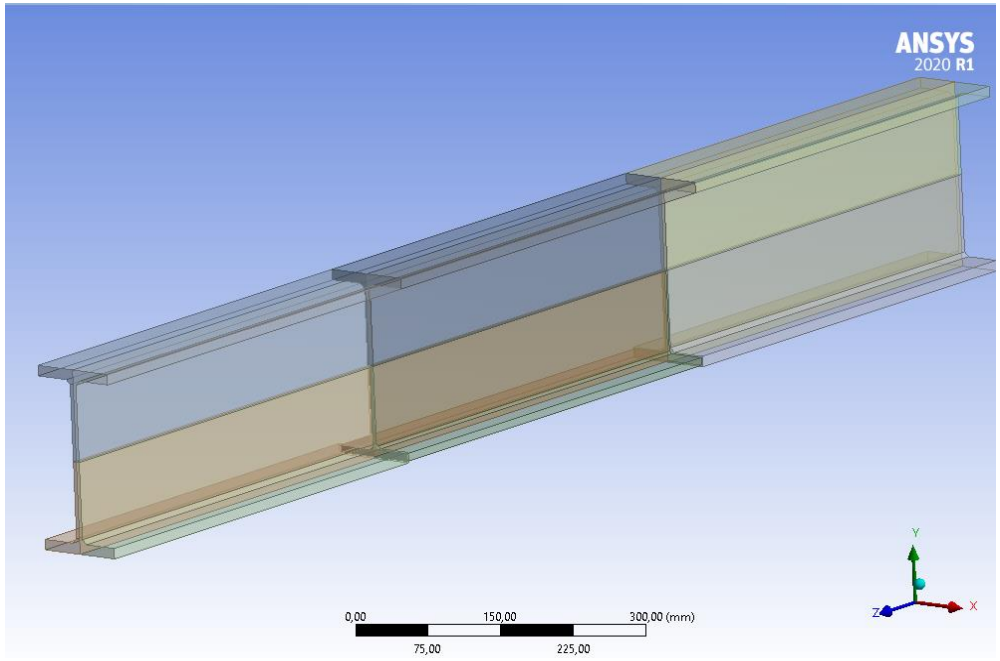

Figure 4.3.5-1: 2D View – Modelling Part – Case Corrosion 3 – Model 2

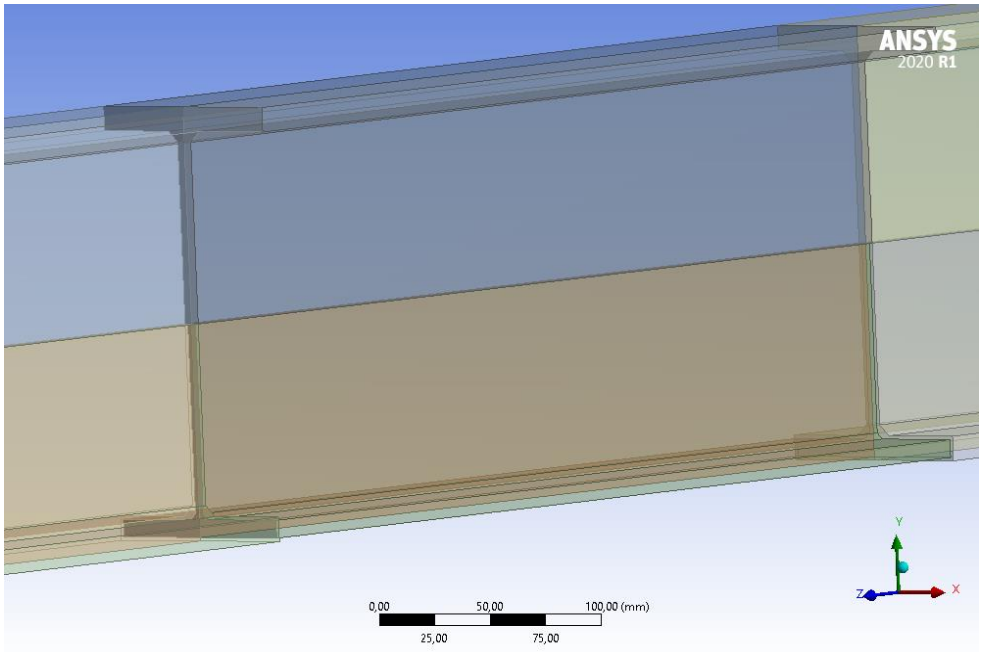

Figure 4.3.5-2: 2D View – A Zoon in – Modelling Part – Case Corrosion 3 – Model 2

Meshing

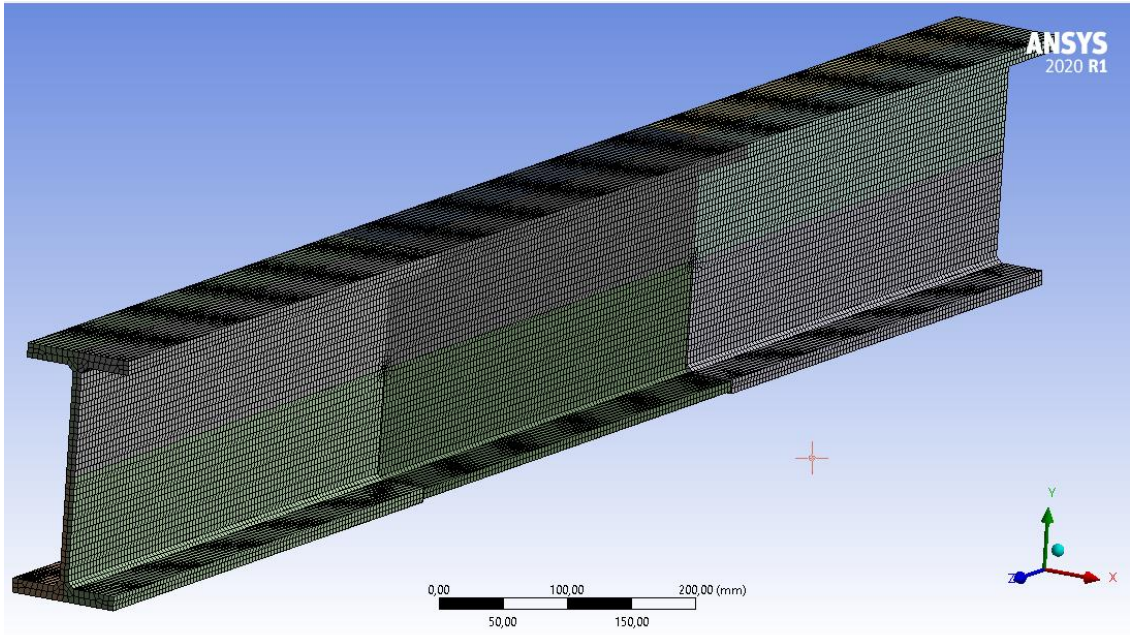

Figure 4.3.5-3: Meshing View – Case Corrosion 3 - Model 2

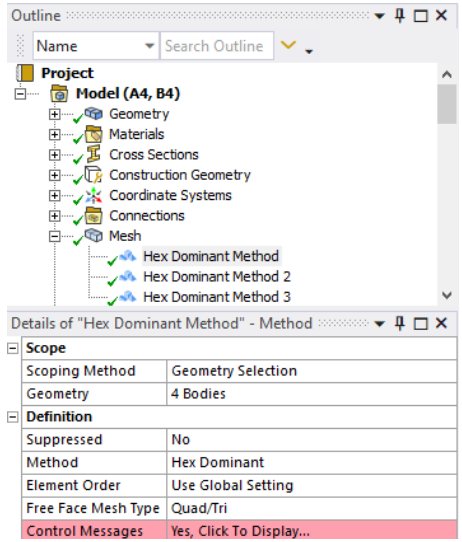

Figure 4.3.5-4: Ansys Meshing Overview- C-Case 3-Model 2

Table 22: Meshing performers- Case Corrosion 3- Model 2

	Mesh performers	Mesh density
Part 1-No-C	**Hex Dominant Method**	**5mm**
Part 2-C	**Hex Dominant Method 2**	**5mm**
Part 3- No-C	**Hex Dominant Method 3**	**5mm**

Boundary conditions and loading

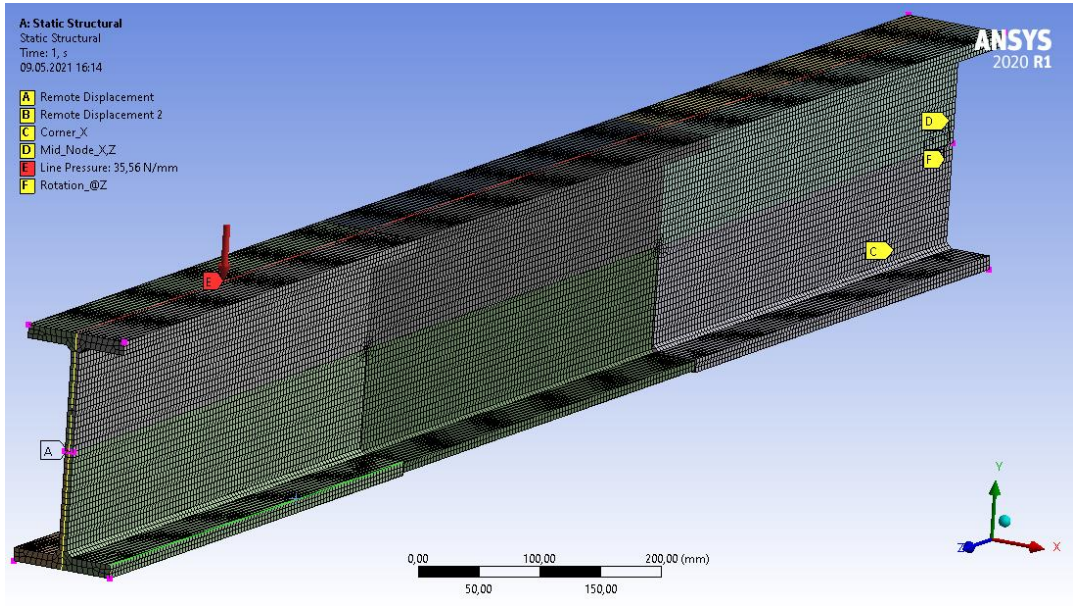

Figure 4.3.5-5: The 3D View – The boundary condition and loading – Case Corrosion 3 – Model 2

L	Length
AM-SLA	Applied M - Static Analyses
AW-SL-LP	Applied W - Static Linear – Line Pressure
AM-NLA	Applied M – Non-Static Analyses
AW-NL-LP	Applied W – Nonlinear – Line Pressure

Table 23: Applied Load for linear- and Nonlinear Analyses – Corrosion 3 – Model 2

L (m)	*AM-SL-LP (KNm)*	*AW-SLA (N/mm)*	*AM-NLA (KNm)*	*AW-NL-LP (N/mm)*
0.55	*10*	*264.5*	*120*	*3174*
1	*10*	*80*	*110*	*880*
1.5	*10*	*35.6*	*100*	*356*
2	*10*	*20*	*60*	*120*
2.3	*10*	*15.1*	*65*	*98.3*
2.5	*10*	*12.8*	*60*	*76.8*
3	*10*	*8.9*	*45*	*40*
3.4	*10*	*6.9*	*45*	*31.14*
4	*10*	*5*	*40*	*20*
5	*10*	*3.2*	*25*	*8*
7	*10*	*1.6*	*15*	*2.45*
10	*10*	*0.8*	*15*	*1.2*

4.3.6 The Static Linear Check - Maximum Displacement and Maximum Stress

The maximum displacement and the maximum stress is used in order to check the static linear analysis.

The Maximum Displacement

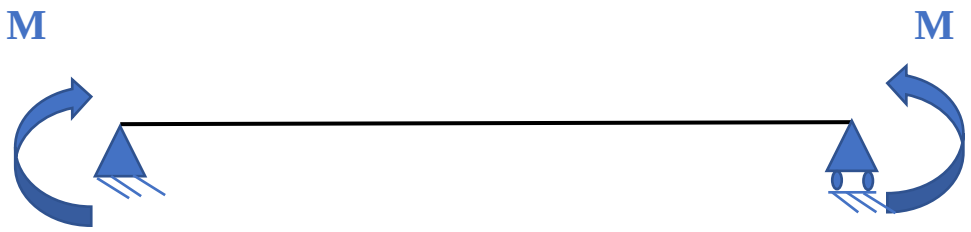

Figure 4.3.6-1: A simple support with end moments

$$\frac{dy}{dx}^2 = -\frac{M}{EI_y} \qquad \text{Eq. 36}$$

The Slope

$$\frac{dy}{dx} = -\frac{M}{EI_y}x + c_1 \qquad \text{Eq. 37}$$

The Displacement

$$y = \frac{M}{EI_y}\frac{x^2}{2} + c_1 x + c_2 \qquad \text{Eq. 38}$$

In order to find the unknown parameter c_1 and c_2 the following steps shown below are used:

Step 1

$$x = 0 \; and \; y = 0$$

$$0 = \frac{M}{EI_y}\frac{0^2}{2} + c_1 0 + c_2 \qquad \text{Eq. 39}$$

$$c_2 = 0$$

Step 2

The parameter x represents the length of the beam, which in this case is 1.5m and the parameter y represents the displacement of the beam. For each length the c_1 factor is changing.

$$x = 1.5 \; and \; y = 0$$

$$y = \frac{M}{EI_y}\frac{1.5^2}{2} + c_1 1.5 + 0 \qquad \text{Eq. 40}$$

$$c_1 = \frac{\frac{M}{EI_y} * \frac{(1.5)^2}{2}}{1.5} \qquad \text{Eq. 41}$$

The Maximum stress

For the static linear analysis, the applied moment (M) is the same for no corrosion case, case corrosion 1 and case corrosion 2. The parameters such as moment of inertia about y-y axis and the distance from the horizontal axis to the farthest point are changing with the different cases.

$$\sigma_{Max} = \frac{My}{Iyy} \qquad \text{Eq. 42}$$

Where:

M = Applied Moment

y = The distance from the horizontal axis to the farthest point

Iyy= Moment of inertia

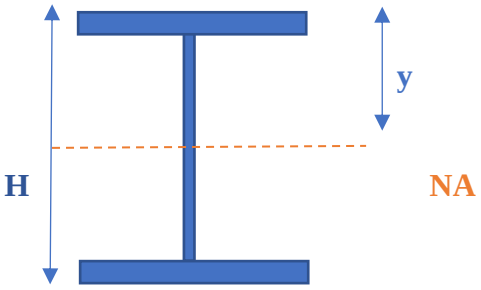

Figure 4.3.6-2: I-beam cross section

4.4 Parametric study: Results

In this section the parametric study results are illustrated with tables and figures for the considered corrosion cases.

4.4.1 Results – No corrosion Case

This section includes the results such as “The static linear analyses”, “The linear buckling analyses” and “The non-linear buckling analyses” for the non-corrosion case which are illustrated in Tables 24, 25 and 26.

Table 24: Static Linear Analyses – No Corrosion Results

L (m)	**0.55**	**1**	**1.5**	**2**	**2.3**	**2.5**	**3**	**3.4**	**4**	**5**	**7**	**10**
MSM (N/mm^2)	46.3	46.3	46.3	46.3	46.3	46.3	46.3	46.3	46.3	46.3	46.3	46.3
MSWA (N/mm^2)	44.2	45.1	45.3	45.4	45.4	45.4	45.4	45.4	45.5	45.5	45.4	45.5
MDM (mm)	0.083	0.28	0.62	1.1	1.46	1.72	2.48	3.18	4.41	6.9	13.5	27.5
MDWA (mm)	0.163	0.31	0.59	0.98	1.28	1.49	2.12	2.695	3.69	5.72	11.12	22.64

L=Length (m)

MSM=Max stress MATLAB

MSWA=Max stress Workbench Ansys

MDM= Max displacement MATLAB

MDWA=Max displacement Workbench Ansys

Table 25: Linear Buckling Analyses - No Corrosion Results

L (m)	0.55	1	1.5	2	2.3	2.5	3	3.4	4	5	7	10
MS	-	6	4	5	5	5	5	5	5	5	5	2
EB	-	19.041	11.15	7.62	6.37	5.74	4.57	3.91	3.19	2.38	1.46	0.76
AM (KNm)	10	10	10	10	10	10	10	10	10	10	10	10
Mcr-A (KNm)	-	190.41	111.5	76.2	63.7	57.4	45.7	39.1	31.9	23.8	14.6	7.6
Mcr-C (KNm)	936.2	313.3	160.5	104.7	86.3	77.3	61.3	52.6	43.5	33.9	23.6	16.3

L=Length

MS=Mode shape

EB=Eigenvalue Buckling

AM= Applied Moment

Mcr-A=Critical Moment Ansys

Mcr-C=Critical Moment Code

Table 26: Non-Linear Buckling Analyses – No Corrosion Results

L (m)	0.55	1	1.5	2	2.3	2.5	3	3.4	4	5	7	10
Mbrd-C (KNm)	93.5	83.9	72	60.5	54.5	50.9	43.5	38.9	33.5	27.2	19.8	14.2
Mbrd2 (KNm)	-	60	67.3	53.4	47	41	36	33	20	18	9	-
Mbrd3 (KNm)	-	65.3	70.7	59.5	54	50.6	44.3	40	36	30	17	-

Mbrd-C=Design buckling resistance moment-By the code

Mbrd2= Design buckling resistance moment- No more load-ULS design

Mbrd3= Design buckling resistance moment- ALS/Seismic design

ULS= Ultimate Limit State Design

ALS=Accidental Limit State Design

4.4.2 Results - Case Corrosion 1

This section includes the results such as “The static linear analyses”, “The linear buckling analyses” and “The non-linear buckling analyses” for the case corrosion 1 which are illustrated in Tables 27, 28 and 29.

Table 27: Static Linear Analyses – Case Corrosion 1 Results

L (m)	**0.55**	**1**	**1.5**	**2**	**2.3**	**2.5**	**3**	**3.4**	**4**	**5**	**7**	**10**
MSM (N/mm^2)	66.2	66.2	66.2	66.2	66.2	66.2	66.2	66.2	66.2	66.2	66.2	66.2
MSWA (N/mm^2)	62.3	63.8	64.1	64.2	64.2	64.3	64.3	64.24	64.24	64.21	64.1	64.1
MDM (mm)	0.12	0.40	0.90	1.60	2.12	2.50	3.60	4.63	6.41	10.01	19.6	40
MDWA (mm)	0.26	0.47	0.88	1.45	1.87	2.18	3.07	3.90	5.35	8.3	16.0	32.6

L=Length (m)

MSM=Max stress Matlap

MSWA=Max stress Workbench Ansys

MDM= Max displacement Matlap

MDWA=Max displacement Workbench Ansys

Table 28: Linear Buckling Analyses – Case Corrosion 1 Results

L (m)	0.55	1	1.5	2	2.3	2.5	3	3.4	4	5	7	10
MS	-	6	2	3	3	4	3	3	5	5	5	2
EB	-	9.063	5.524	3.475	2.750	2.387	1.738	1.385	1.009	0.606	0.169	-0.154
AM (KNm)	-	10	10	10	10	10	10	10	10	10	10	10
Mcr-A (KNm)	-	90.63	55.24	34.75	27.50	23.87	17.38	13.85	10.09	6.06	1.69	-1.54
Mcr-C (KNm)	598.9	191.7	93	57.9	46.7	41.2	31.8	26.8	21.8	16.6	11.3	7.7

L=Length

MS=Mode shape

AM= Applied Moment

EB= Eigenvalue Buckling

Mcr-C= Critical Moment-By the code

Mcr-A=Critical Moment-By Ansys

Table 29: Non-Linear Buckling Analyses – Case Corrosion 1 Results

L (m)	0.55	1	1.5	2	2.3	2.5	3	3.4	4	5	7	10
Mbrd-C (KNm)	63.3	56.1	46.3	36.7	32	29.4	24.1	21	17.6	13.9	9.8	6.9
Mbrd2 (KNm)	-	40	38	27	24	22.133	18	16	10	7	3.5	6.6
Mbrd3 (KNm)	-	46.1	45.4	35.6	31	28.7	24	21.5	18.8	13	7	6.6

Mbrd-C=Design buckling resistance moment-By the code

Mbrd2= Design buckling resistance moment- No more load-ULS design

Mbrd3= Design buckling resistance moment- ALS/Seismic design

ULS= Ultimate Limit State Design

ALS=Accidental Limit State Design

4.4.3 Results - Case Corrosion 2

This section includes the results such as “The static linear analyses”, “The linear buckling analyses” and “The non-linear buckling analyses” for the case corrosion 2 which are illustrated in Tables 30, 31 and 32.

Table 30: Static Linear Analyses – Case Corrosion 2 Results

L (m)	**0.55**	**1**	**1.5**	**2**	**2.3**	**2.5**	**3**	**3.4**	**4**	**5**	**7**	**10**
MSMC (N/mm^2)	48.5	48.5	48.5	48.5	48.5	48.5	48.5	48.5	48.5	48.5	48.5	48.5
MSWAC (N/mm^2)	45.1	43.2	43.2	43.2	43.2	43.2	43.2	43.2	43.2	43.2	43.2	43.2
MSMT (N/mm^2)	63.9	63.9	63.9	63.9	63.9	63.9	63.9	63.9	63.9	63.9	63.9	63.9
MSWAT (N/mm^2)	62.8	62.5	62.5	62.5	62.5	62.5	62.5	62.5	62.5	62.5	62.5	62.5
MDM (mm)	0.10	0.34	0.757	1.35	1.77	2.1	3.02	3.89	5.38	8.41	16.5	33.6
MDWA (mm)	0.21	0.396	0.739	1.22	1.58	1.84	2.6	3.31	4.54	7.02	13.6	27.7

L=Length (m)

MSMC=Max stress MATLAB-Compression

MSMT=Max stress MATLAB-Tension

MSWAC=Max stress Workbench Ansys- Compression

MSWAT=Max stress Workbench Ansys- Tension

MDM= Max displacement Matlap

MDWA=Max displacement Workbench Ansys

Table 31: Linear Buckling Analyses- Case Corrosion 2 Results

L (m)	0.55	1	1.5	2	2.3	2.5	3	3.4	4	5	7	10
MS	-	5	5	7	4	7	6	6	6	6	5	5
AM (KNm)	10	10	10	10	10	10	10	10	10	10	10	10
EB	-	15.7	9.36	6.16	5.02	4.44	3.39	2.81	2.18	1.495	0.742	0.211
Mcr-A (KNm)	-	157.12	93.6	61.6	50.2	44.4	33.9	28.1	21.8	14.95	7.42	2.11
Mcr-C (KNm)	749.8	248	124.8	80.4	66	59	46.3	39.6	32.6	25.3	17.5	12

L=Length

MS=Mode shape

EB=Eigenvalue Buckling

AM=Applied Moment

Mcr-A=Critical Moment - Ansys

Mcr-C= Critical Moment - Code

Table 32: Non-Linear Analyses – Case Corrosion 2 Results

L (m)	0.55	1	1.5	2	2.3	2.5	3	3.4	4	5	7	10
Mbrd-C (KNm)	74.5	66.8	56.95	47.3	42.3	39.4	33.4	29.7	25.4	20.5	14.8	10.6
Mbrd2 (KNm)	-	45.2	55.5	44.4	34	33	27	24	16	12.5	6.5	-
Mbrd3 (KNm)	-	53.1	59.5	49.1	44	41.2	34.4	32.4	28	23	13.5	-

Mbrd-C=Design buckling resistance moment-By the code

Mbrd2= Design buckling resistance moment- No more load-ULS design

Mbrd3= Design buckling resistance moment- ALS/Seismic design

ULS= Ultimate Limit State Design

ALS=Accidental Limit State Design

4.4.4 Results - Case Corrosion 3-model 1

This section includes the results such as “The static linear analyses”, “The linear buckling analyses” and “The non-linear buckling analyses” for the case corrosion 3- model 1 which are illustrated in Tables 33, 34 and 35.

Table 33: Static Linear Analyses – Case Corrosion 3 – Model 1 Results

L (m)	**0.55**	**1**	**1.5**	**2**	**2.3**	**2.5**	**3**	**3.4**	**4**	**5**	**7**	**10**
MSM (N/mm^2)	-	-	-	-	-	-	-	-	-	-	-	-
MSWA (N/mm^2)	64.7	65.1	65.4	65.5	65.6	65.6	65.6	65.6	65.6	65.7	65.7	65.7
MDM (mm)	-	-	-	-	-	-	-	-	-	-	-	-
MDWA (mm)	0.196	0.389	0.754	1.267	1.646	1.927	2.735	3.486	4.79	7.43	14.5	29.5

L=Length (m)

MSM=Max stress Matlap

MSWA=Max stress Workbench Ansys

MDM= Max displacement Matlap

MDWA=Max displacement Workbench Ansys

Table 34: Linear Buckling Analyses – Case Corrosion 3 – Model 1 Results

L (m)	**0.55**	**1**	**1.5**	**2**	**2.3**	**2.5**	**3**	**3.4**	**4**	**5**	**7**	**10**
MS	-	4	3	3	3	3	4	4	5	3	3	3
EB	-	14.64	8.64	5.93	4.96	4.46	3.54	3.0	2.42	1.75	0.99	0.433
AM (KNm)	10	10	10	10	10	10	10	10	10	10	10	10
Mcr-A (KNm)	-	146.4	86.4	59.3	49.6	44.6	35.4	30	24.2	17.5	9.9	4.33

L=Length

MS=Mode shape

EB=Eigenvalue Buckling

AM=Applied Moment

Mcr-A=Critical Moment - Ansys

Table 35: Non-Linear Buckling Analyses – Case Corrosion 3 – Model 1 Results

L (m)	**0.55**	**1**	**1.5**	**2**	**2.3**	**2.5**	**3**	**3.4**	**4**	**5**	**7**	**10**
Mbrd-C (KNm)	-	-	-	-	-	-	-	-	-	-	-	-
Mbrd2 (KNm)	-	53.3	50	43	38	36	31.5	28.1	22	20	12	-
Mbrd3 (KNm)	-	57.6	54	48.3	45	42.4	37.5	34	26.7	25.92	17	-

Mbrd-C=Design buckling resistance moment-By the Code

Mbrd2= Design buckling resistance moment- No more load-ULS design

Mbrd3= Design buckling resistance moment- ALS/Seismic design

ULS= Ultimate Limit State Design

ALS=Accidental Limit State Design

4.4.5 Results - Case Corrosion 3- Model 2

This section includes the results such as “The static linear analyses”, “The linear buckling analyses” and “The non-linear buckling analyses” for the case corrosion 3- model 1 which are illustrated in Tables 36, 37 and 38.

Table 36: Static Linear Analyses – Case Corrosion 3 – Model 2 Results

L (m)	**0.55**	**1**	**1.5**	**2**	**2.3**	**2.5**	**3**	**3.4**	**4**	**5**	**7**	**10**
MSM (N/mm^2)	-	-	-	-	-	-	-	-	-	-	-	-
MSWA (N/mm^2)	47.4	48.3	48.5	48.5	48.8	48.5	48.6	48.3	48.3	48.3	47.7	48.6
MDM (mm)	-	-	-	-	-	-	-	-	-	-	-	-
MDWA (mm)	0.18	0.35	0.67	1.123	1.649	1.704	2.414	3.08	4.23	6.55	12.78	25.91

L=Length (m)

MSM=Max stress Matlap

MSWA=Max stress Workbench Ansys

MDM= Max displacement MATLAB

MDWA=Max displacement Workbench Ansys

Table 37: Linear Buckling Analyses – Case Corrosion 3 – Model 2 Results

L (m)	**0.55**	**1**	**1.5**	**2**	**2.3**	**2.5**	**3**	**3.4**	**4**	**5**	**7**	**10**
MS	-	6	5	3	5	3	3	2	3	3	2	2
EB	-	18.14	10.76	7.32	7.73	5.45	4.28	3.65	2.91	2.097	1.33	0.483
AM (KNm)	10	10	10	10	10	10	10	10	10	10	10	10
Mcr (KNm)	-	181.4	107.6	73.2	77.3	54.5	42.8	36.5	29.1	20.97	13.33	4.83

L=Length

MS=Mode shape

EB=Eigenvalue Buckling

AM=Applied Moment

Mcr=Critical Moment

Table 38: Non-Linear Buckling Analyses - Case Corrosion 3 – Model 2 Results

L (m)	**0.55**	**1**	**1.5**	**2**	**2.3**	**2.5**	**3**	**3.4**	**4**	**5**	**7**	**10**
Mbrd1 (KNm)	-	-	-	-	-	-	-	-	-	-	-	-
Mbrd2 (KNm)	-	55	63	54	45	42	33	27	24.1	20	8.7	-
Mbrd3 (KNm)	-	64	68.6	58	52.4	48.9	43.12	32.5	29.5	25	16	-

Mbrd1=Design buckling resistance moment-Very conservative value

Mbrd2= Design buckling resistance moment- No more load-ULS design

Mbrd3= Design buckling resistance moment- ALS/Seismic design

ULS= Ultimate Limit State Design

ALS=Accidental Limit State Design

4.4.6 Consistent FEM Analyses Results Vs Not Consistent FEM Analyses Results

In this section the difference between the same load condition assumption, which provides consistent results from the FEMS, and not same load condition assumption, which provides non-consistent results from the FEMS, for the non-corrosion case with a beam length of 1.5m and with imperfection scale factors of 2 (Figure 4.4.6-1) and 1.5 (Figure 4.4.6-2) are shown.

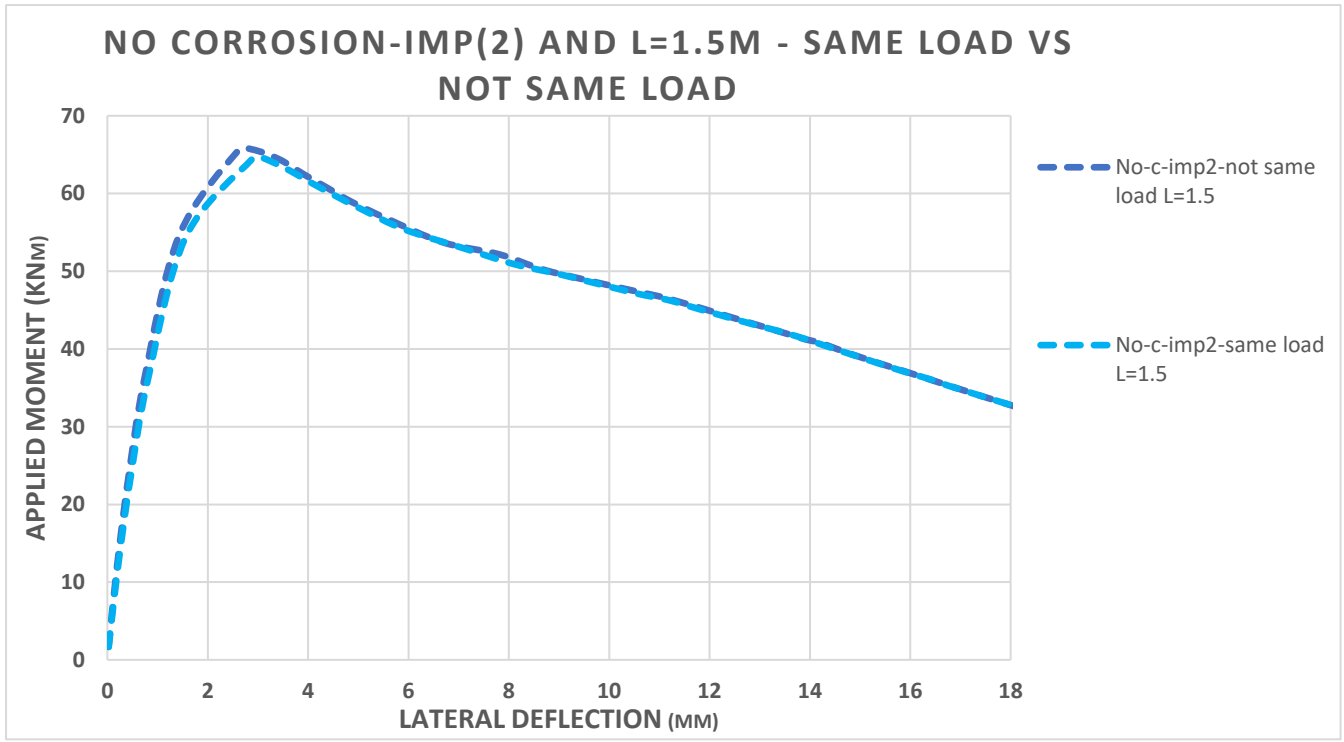

Figure 4.4.6-1: No Corrosion L=1.5m and Imperfection scale factor 2, Same Load Condition Vs Not Same Load Condition

Table 39: The applied Loading types and there elastic moment value given by workbench for L=1.5 and imp=2

Load condition	Applied Moment (KNm)
Same load condition	64.7
Not same load condition	65.4

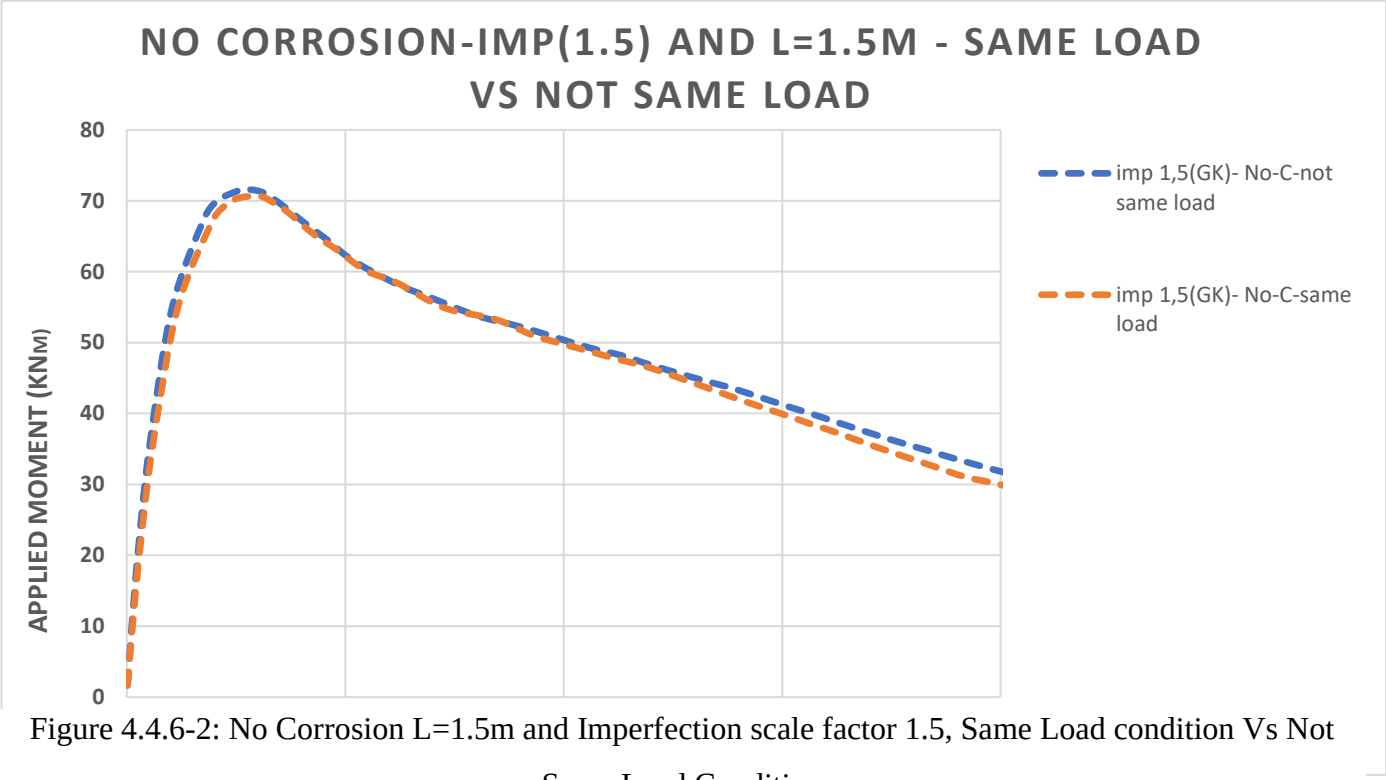

Figure 4.4.6-2: No Corrosion L=1.5m and Imperfection scale factor 1.5, Same Load condition Vs Not Same Load Condition

Table 40: The applied Loading types and there elastic moment value given by workbench for L=1.5 and imp=1.5

Load condition	Applied Moment (KNm)
Same load condition	70.7
Not same load condition	71.5

4.4.7 Comparing the FEM Results with the Eurocode 3 by maimpulating the imperfection scale factor

The comparation for the LTB moment capacity between the FEM results and Eurocode 3 are performed in this section by manipulating the imperfection scale factor for the case non corrosion with a beam length of 1.5m (Figure 4.4.7-1) and for the case non corrosion with a beam length of 2m (Figure 4.4.7-2).

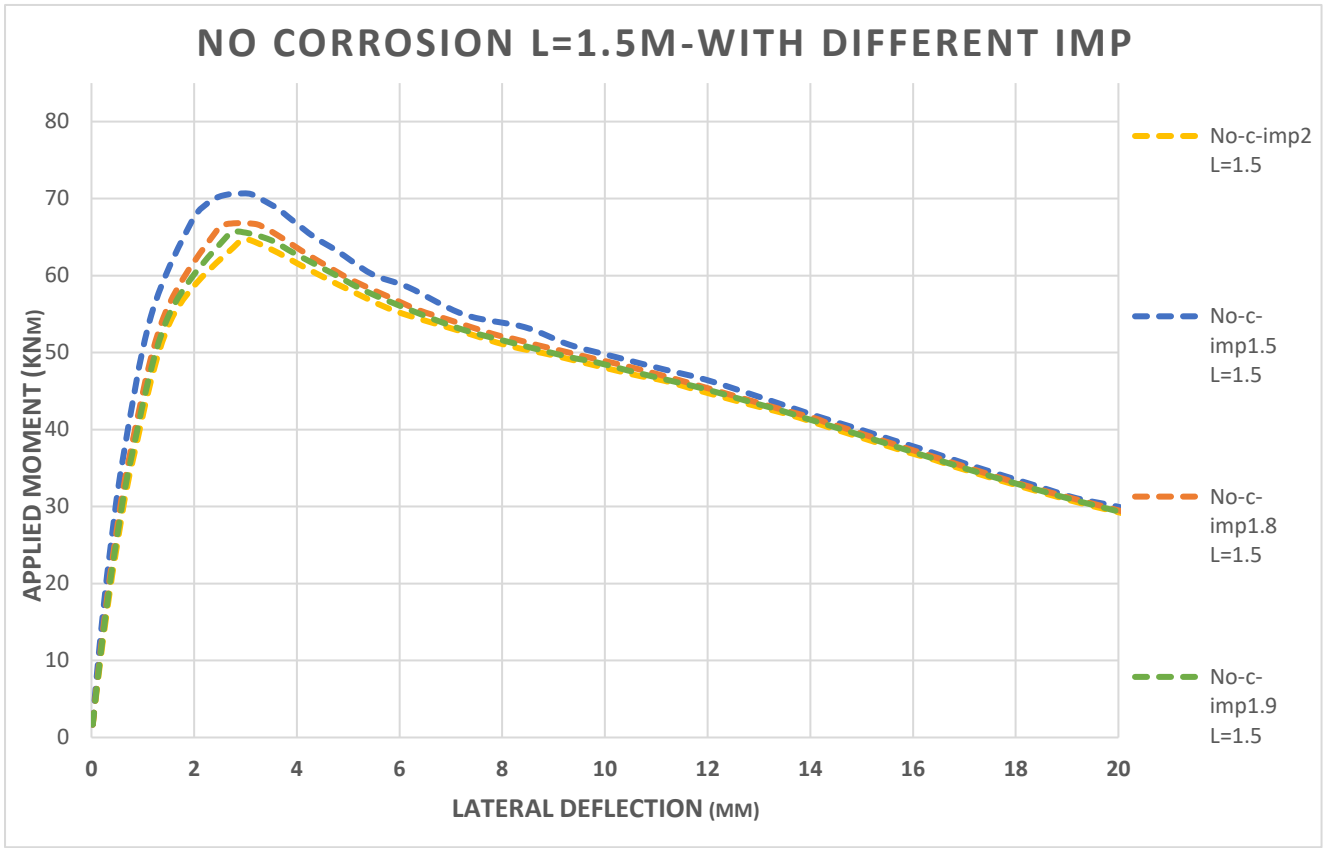

Figure 4.4.7-1: No Corrosion, L=1.5m with Different Imperfection Scale Factor Values

Table 41: No Corrosion, L=1.5m, Bending Moment and Imperfection scale factor

Imperfection Scale Factor	Maximum Bending Moment (Mpa)
1.5	71
1.8	67
1.9	66
2.0	65

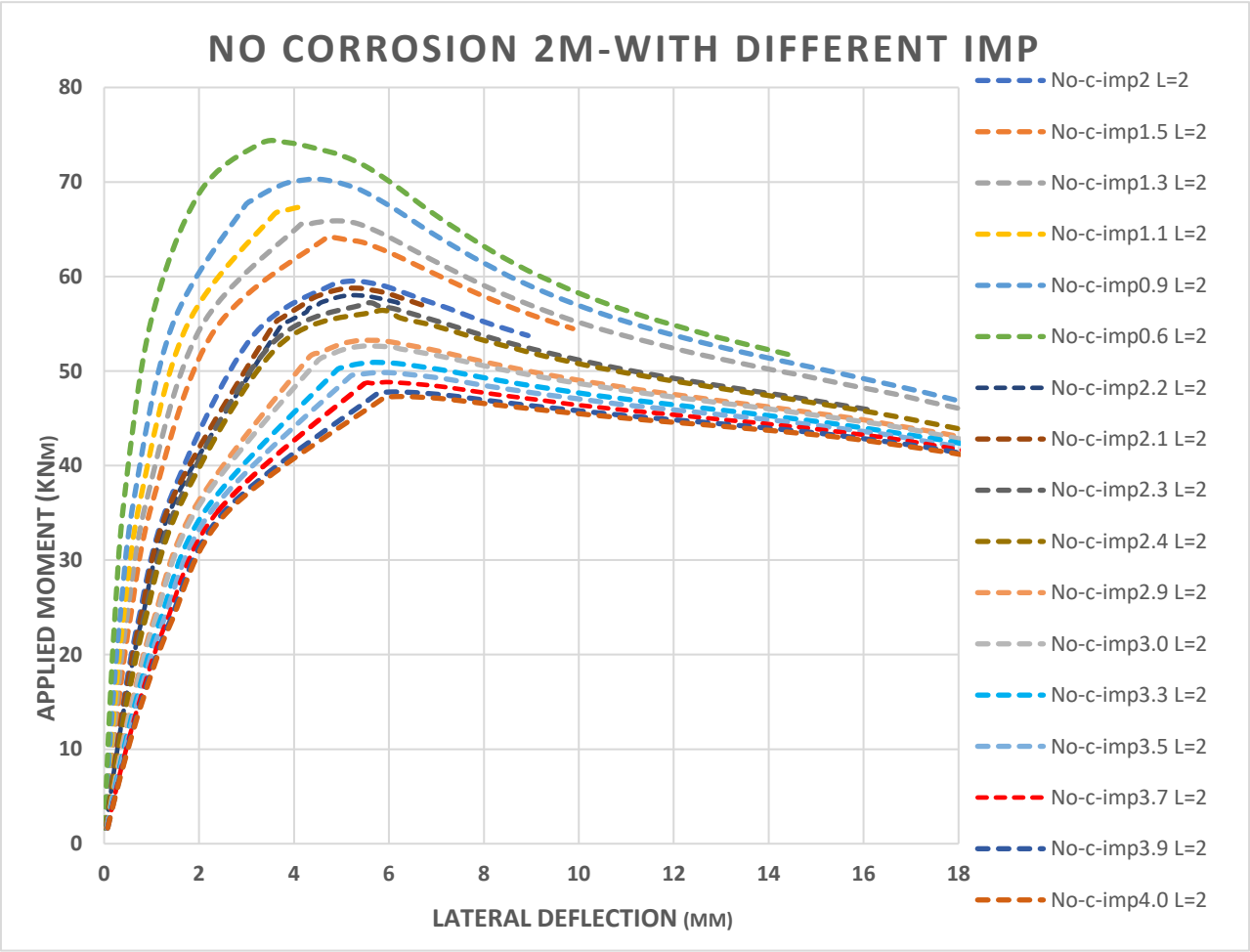

Figure 4.4.7-2: No Corrosion, L=2m with Different Imperfection Scale Factor Values

Table 42: No Corrosion, L=2m, Bending Moment and Imperfection scale factor

Imperfection scale factor	Maximum Bending Moment (Mpa)
0.6	74
0.9	70
1.1	67
1.3	66
1.5	64
2.0	60
2.1	59
2.2	58
2.3	57
2.4	56
2.9	53
3.0	52.5
3.3	51
3.5	50
3.7	49
3.9	48
4.0	47

4.4.8 Plots - Applied Moment vs Lateral deflection, five different cases for 12 lengths

In this section the results for the LTB moment capacity for the five corrosion cases of the non-linear buckling analyses are illustred in Figures 4.4.8-1to 4.4.8-11.

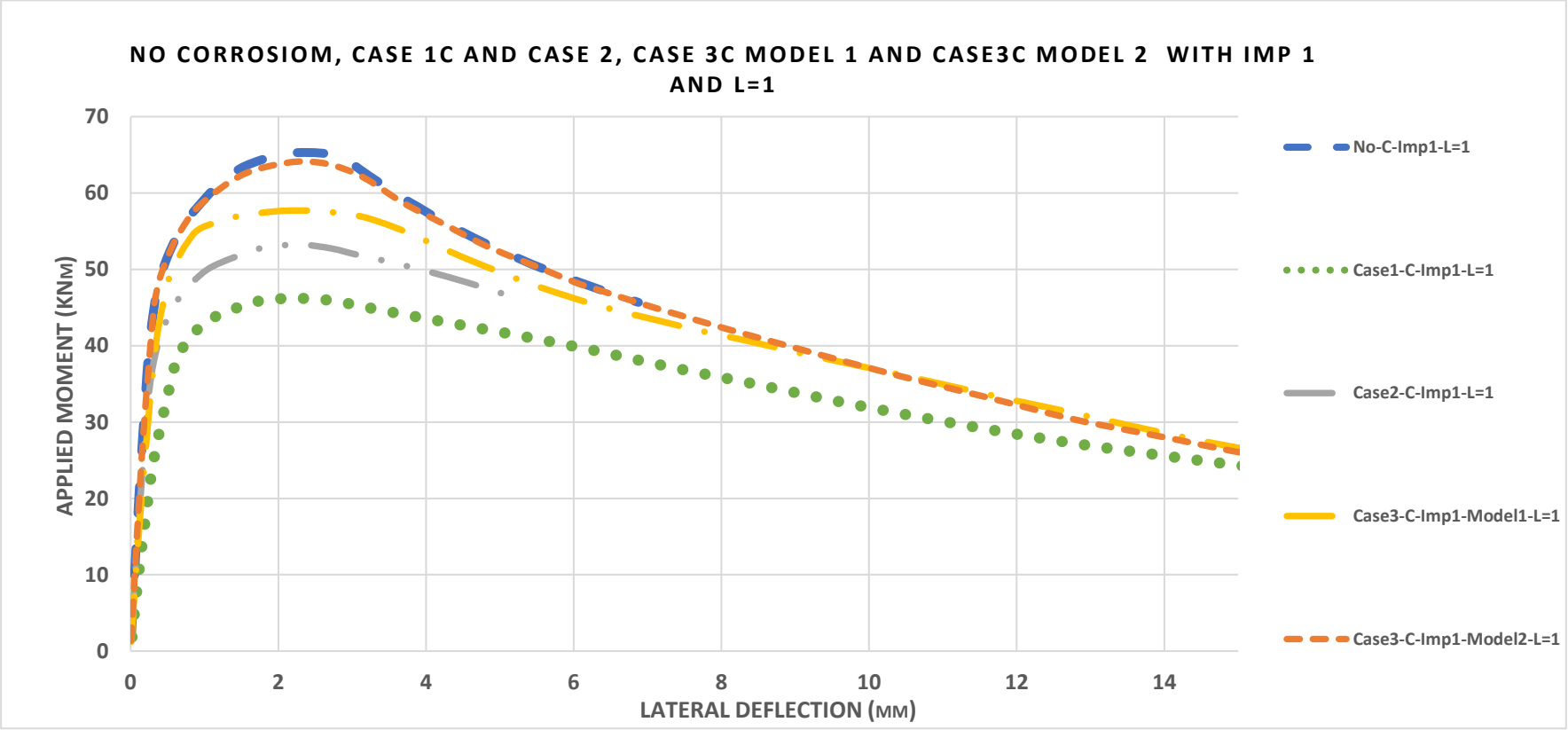

Figure 4.4.8-1: Applied Moment vs Lateral Deflection for L=1m, for five different cases

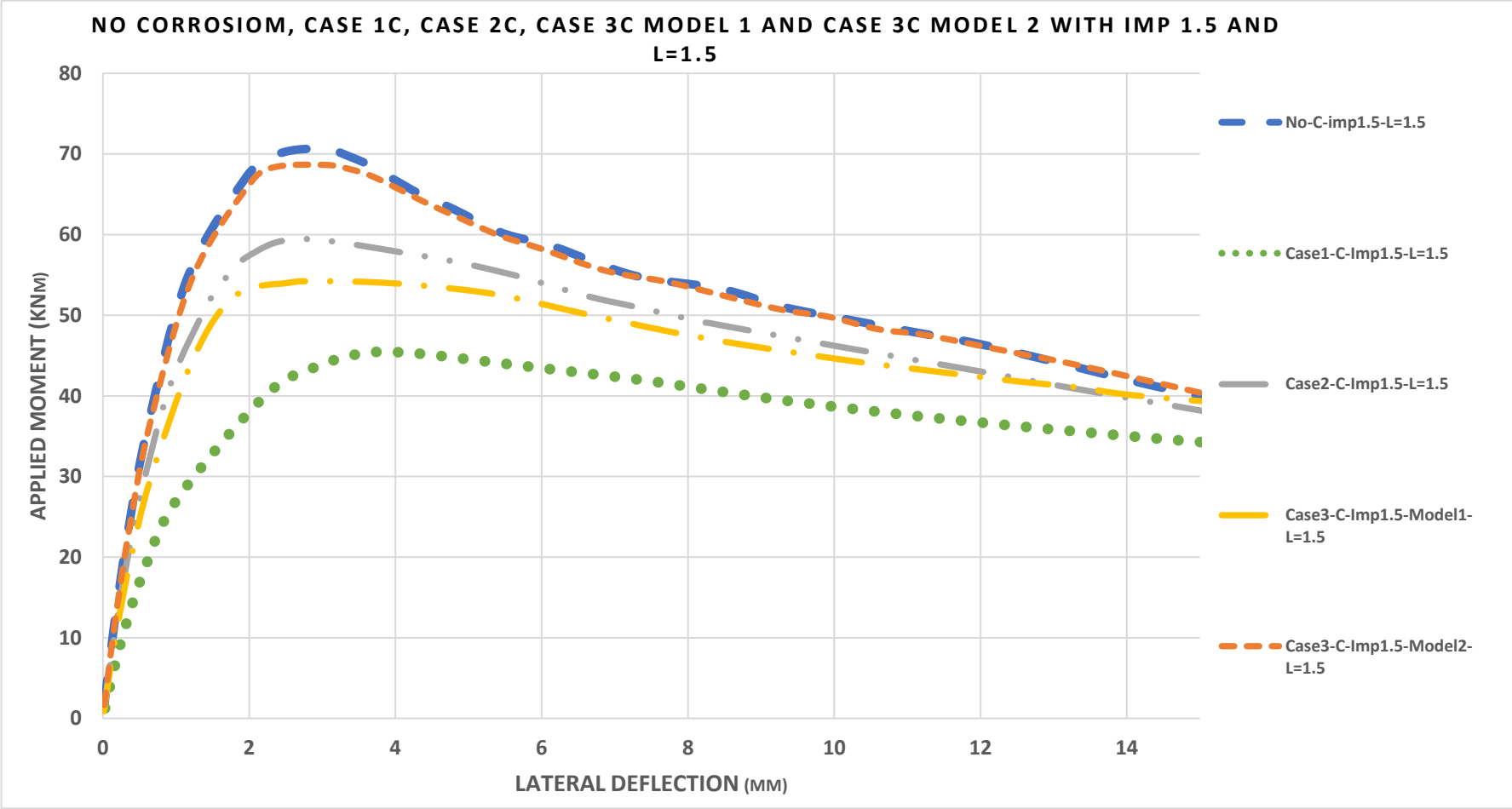

Figure 4.4.8-2: Applied Moment vs Lateral Deflection for L=1.5m, for five different cases

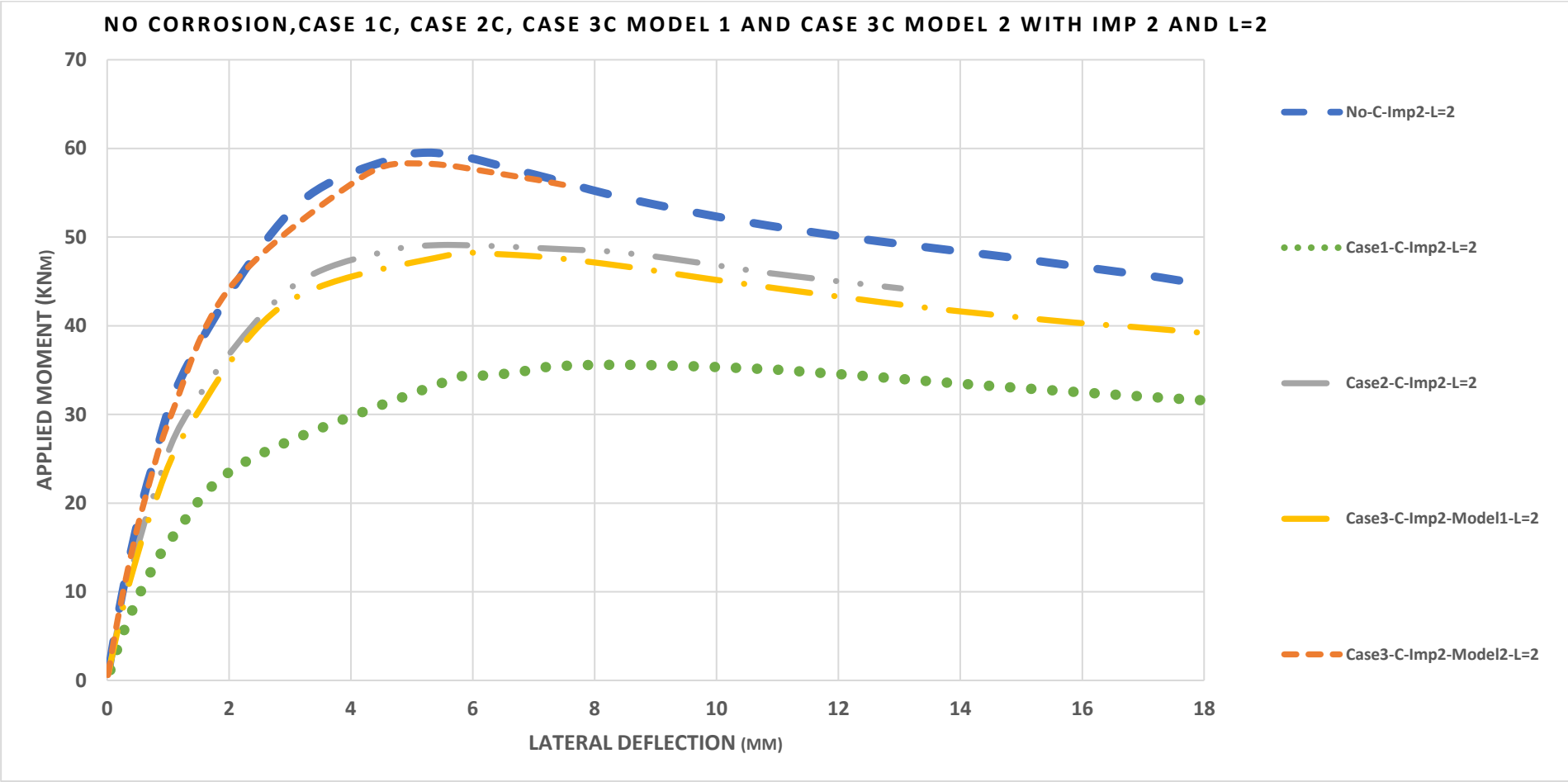

Figure 4.4.8-3: Applied Moment vs Lateral Deflection for L=2m, for five different cases

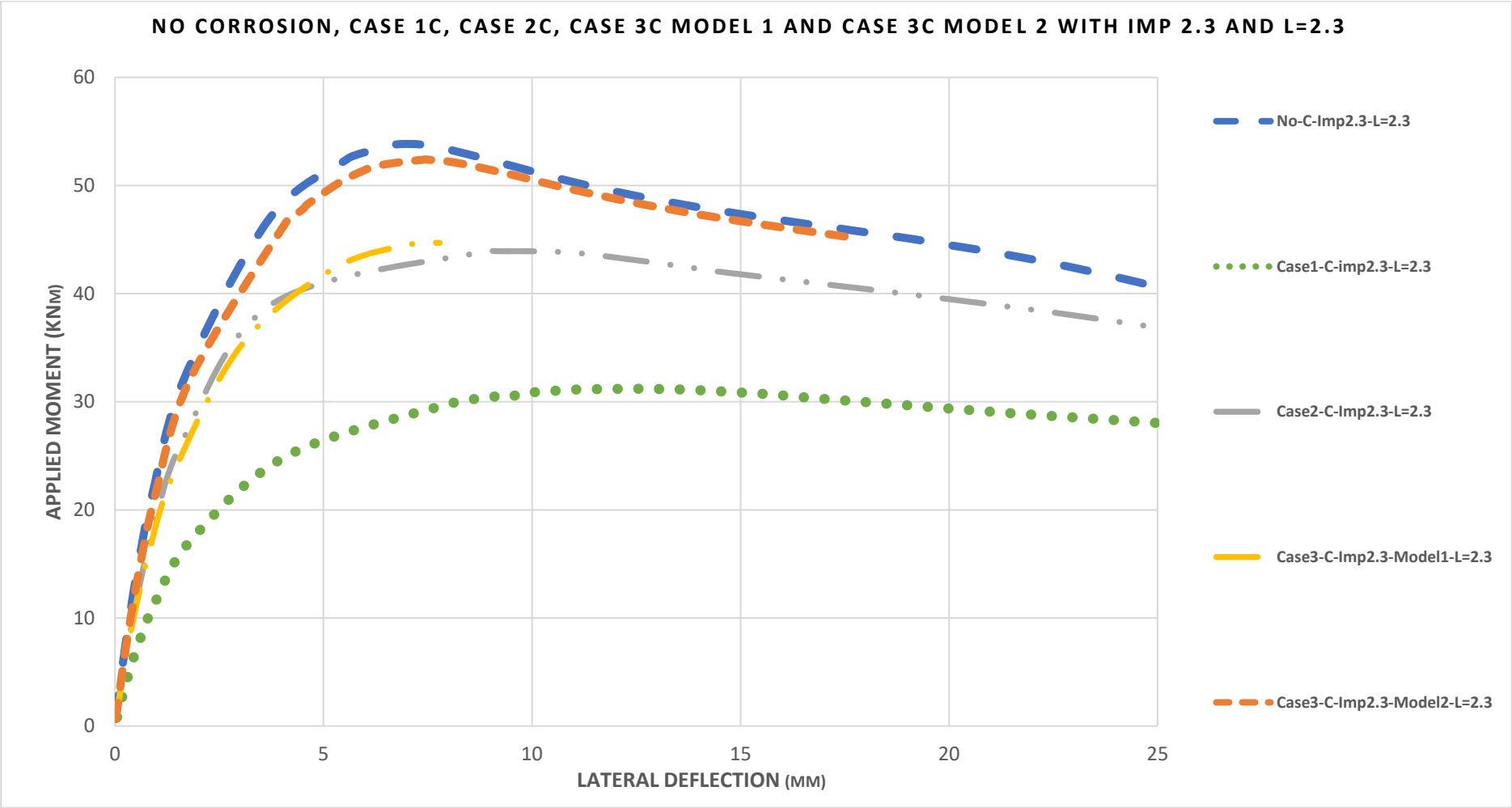

Figure 4.4.8-4: Applied Moment vs Lateral Deflection for L=2.3m, for five different cases

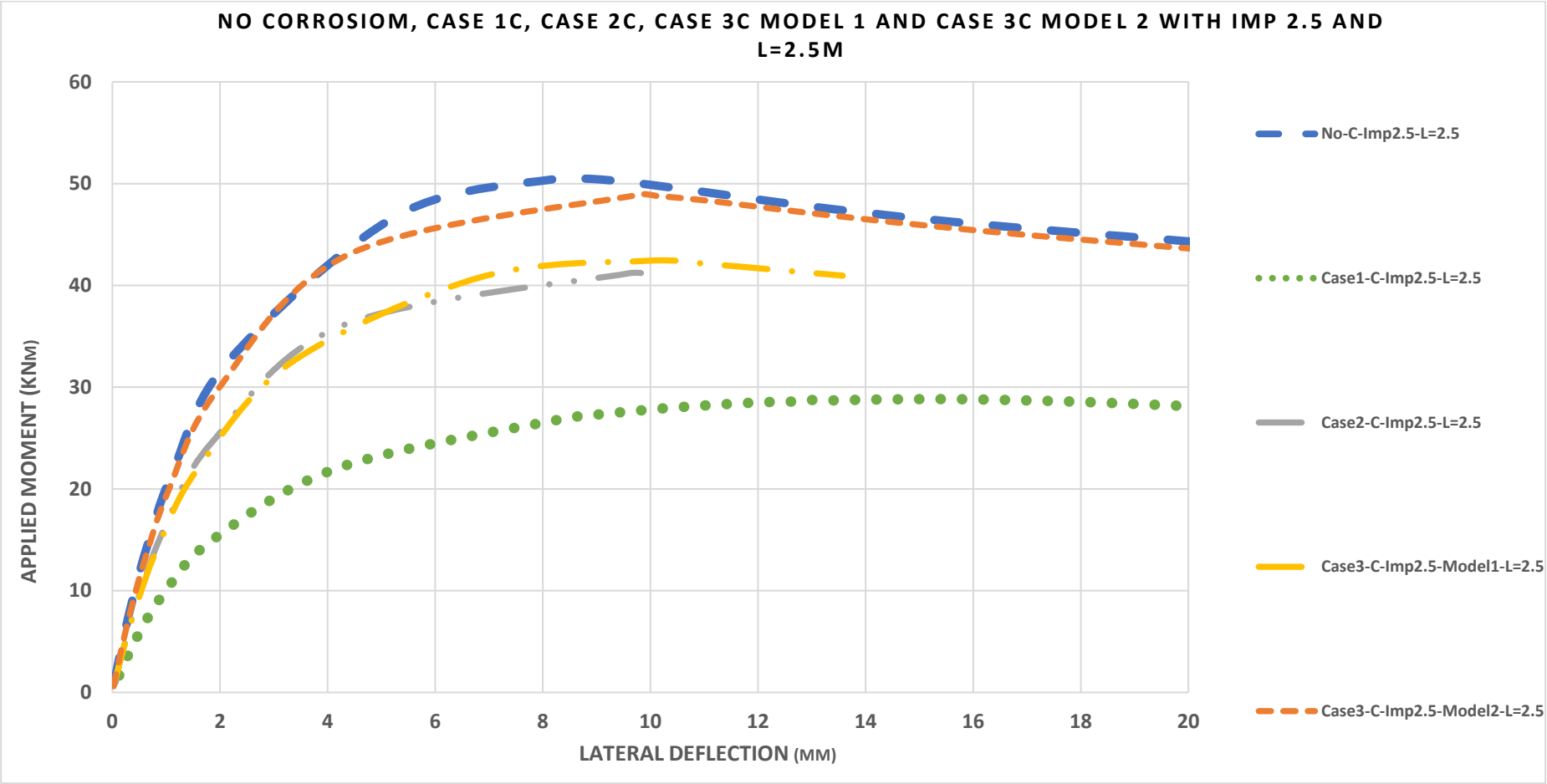

Figure 4.4.8-5: Applied Moment vs Lateral Deflection for L=2.5m, for five different cases

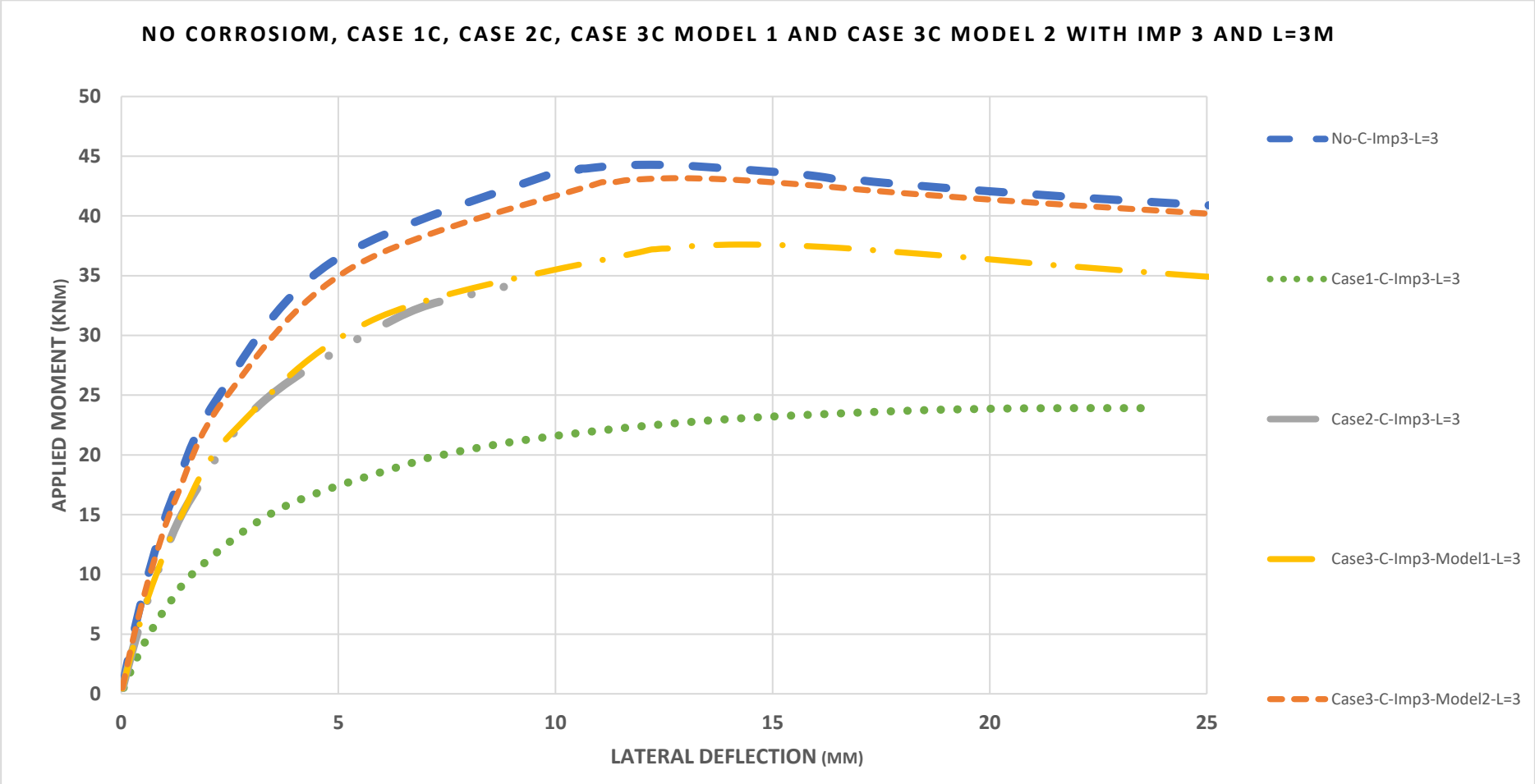

Figure 4.4.8-6: Applied Moment vs Lateral Deflection for L=3m, for five different cases

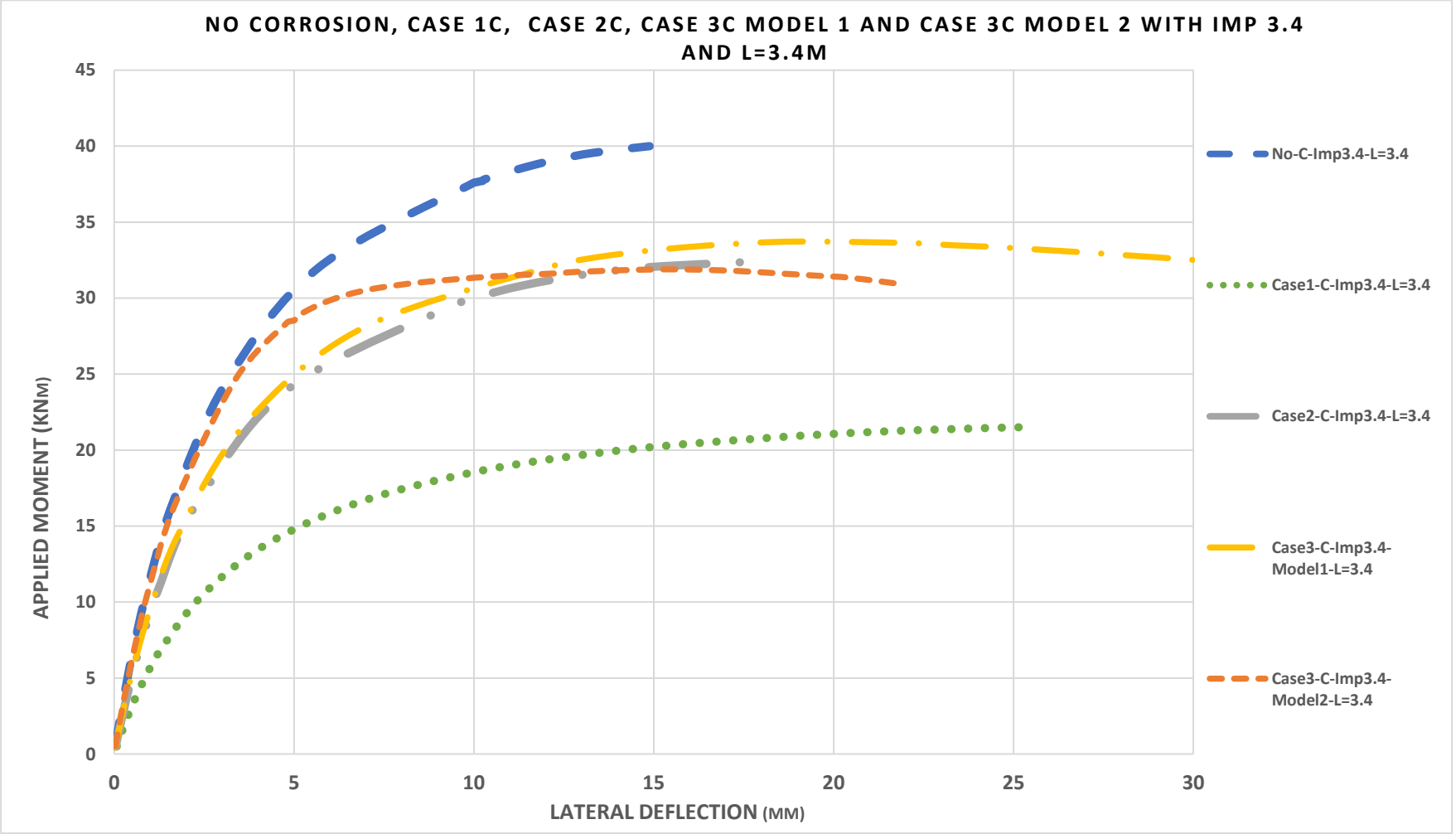

Figure 4.4.8-7: Applied Moment vs Lateral Deflection for L=3.4m, for five different cases

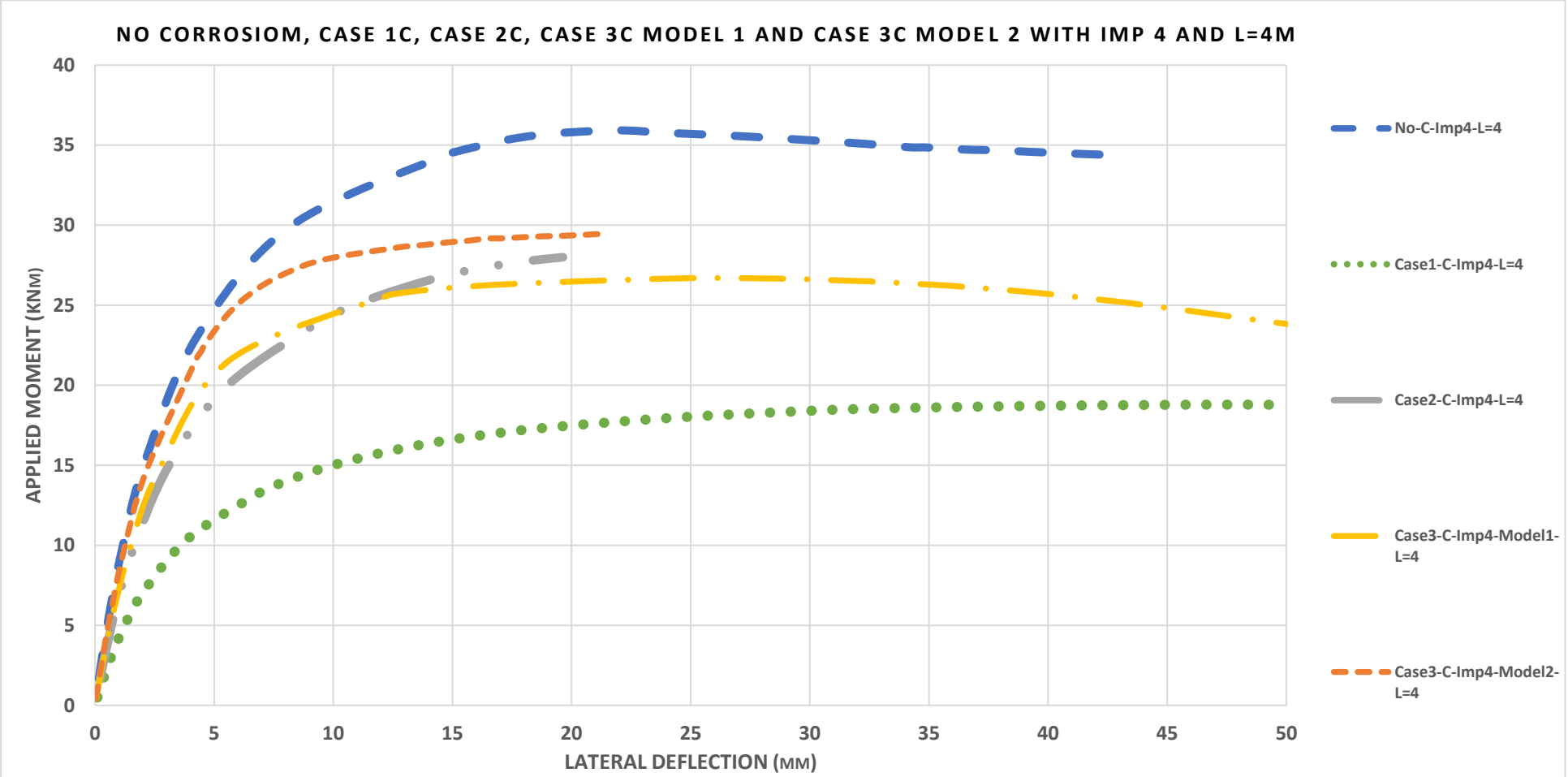

Figure 4.4.8-8: Applied Moment vs Lateral Deflection for L=4m, for five different cases

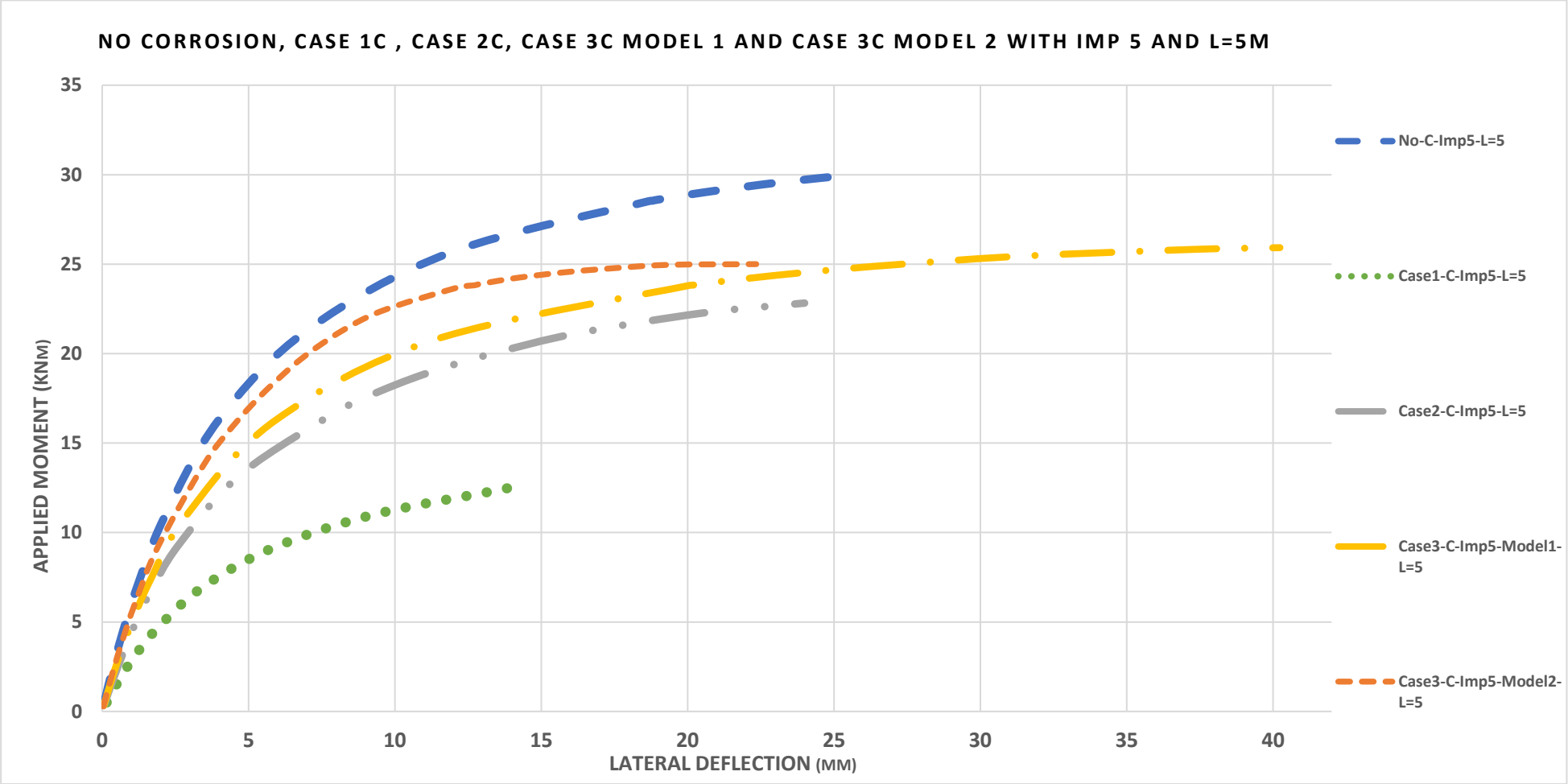

Figure 4.4.8-9: Applied Moment vs Lateral Deflection for L=5m, for five different cases

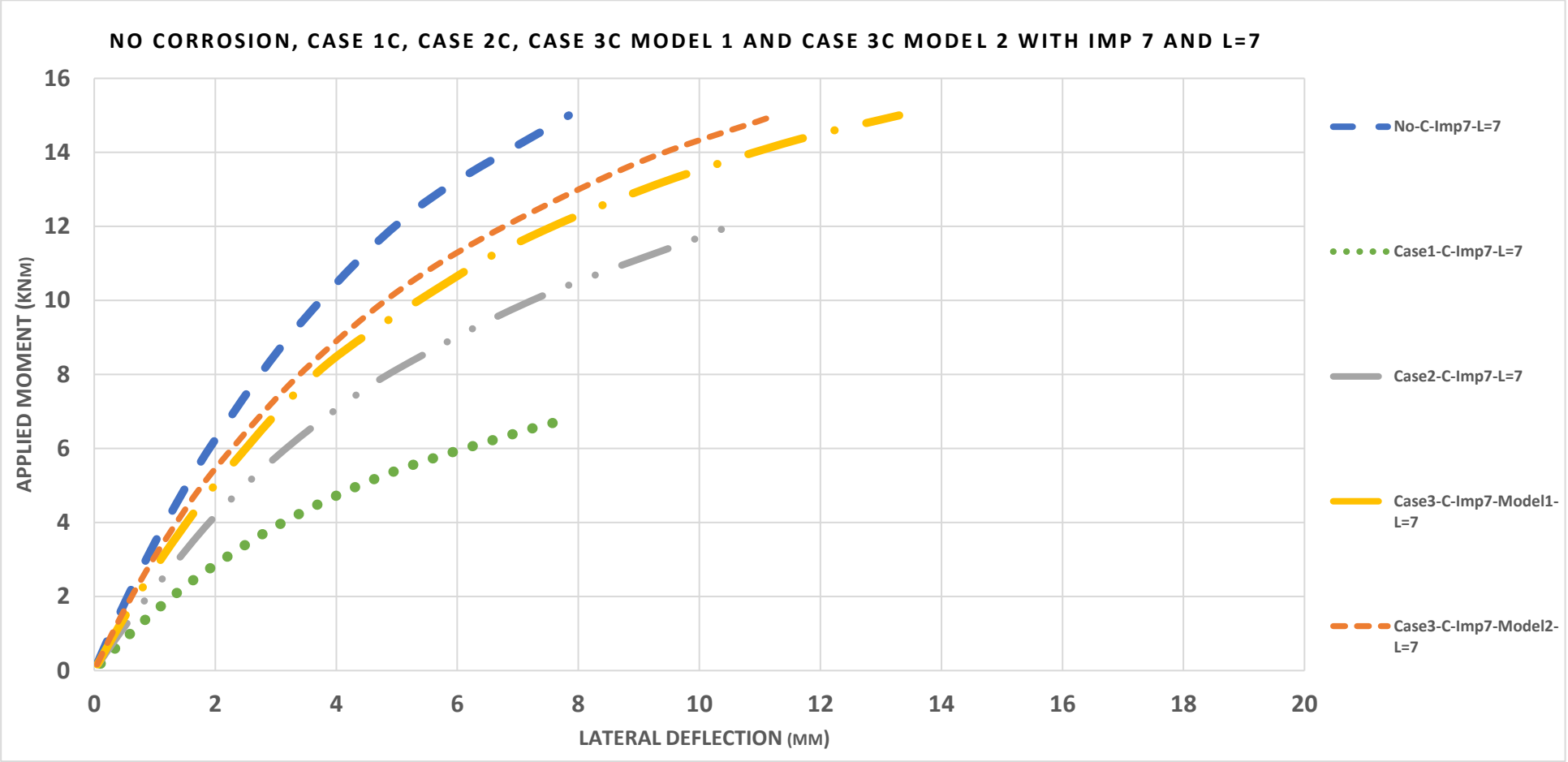

Figure 4.4.8-10: Applied Moment vs Lateral Deflection for L=7m, for five different cases

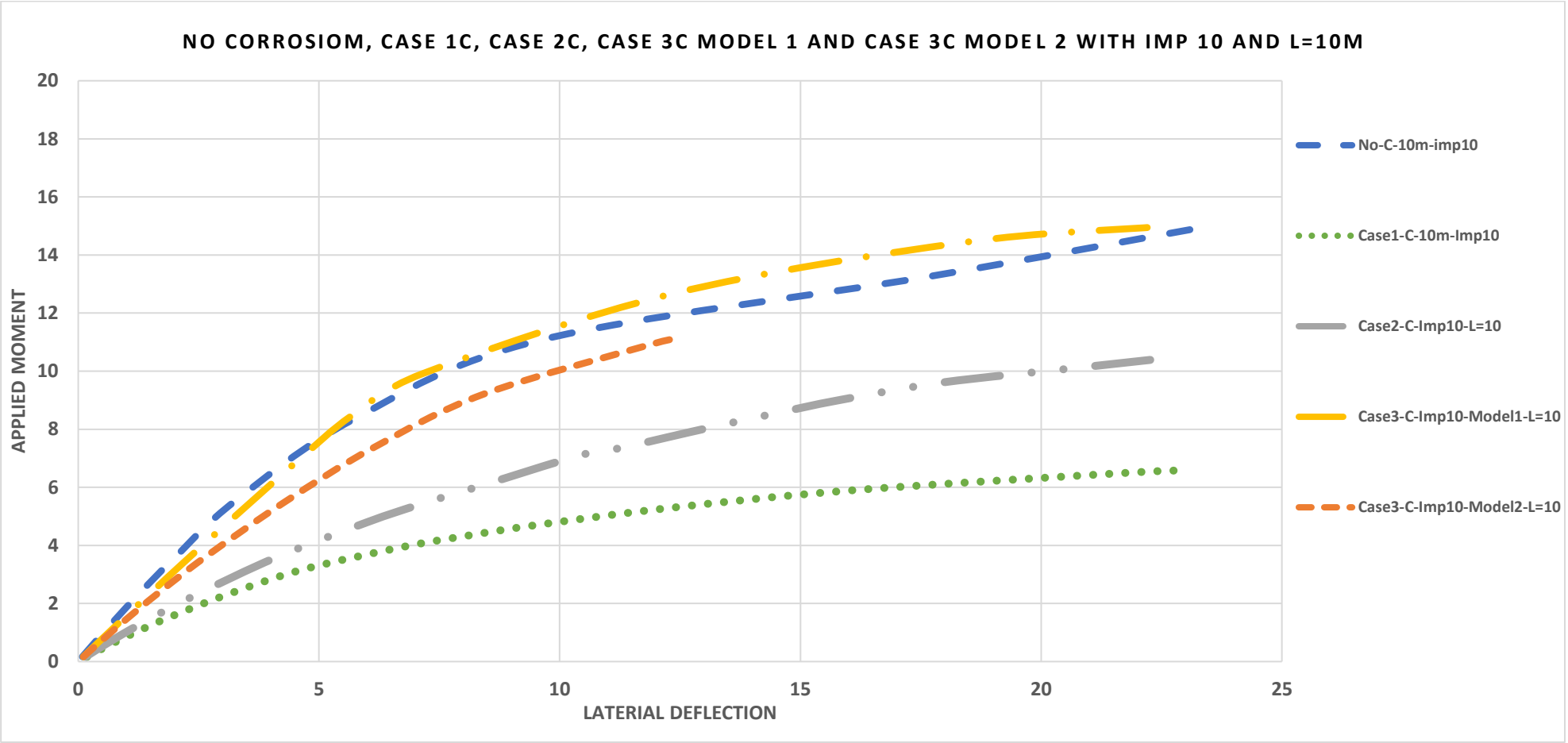

Figure 4.4.8-11: Applied Moment vs Lateral Deflection for L=10m, for five different cases

4.4.9 Lateral torsion buckling curves

In this section, the variation of the bucking reduction factor and the buckling moment capacity with the non-dimensional slenderness ratios is discussed in detail. This is very important to understand and quantitatively predict the variation of the effect of the various corrosion cases for the LTB moment capacity reduction. Figure 4.4.9-1 to Figure 4.4.9-6 show the plots.

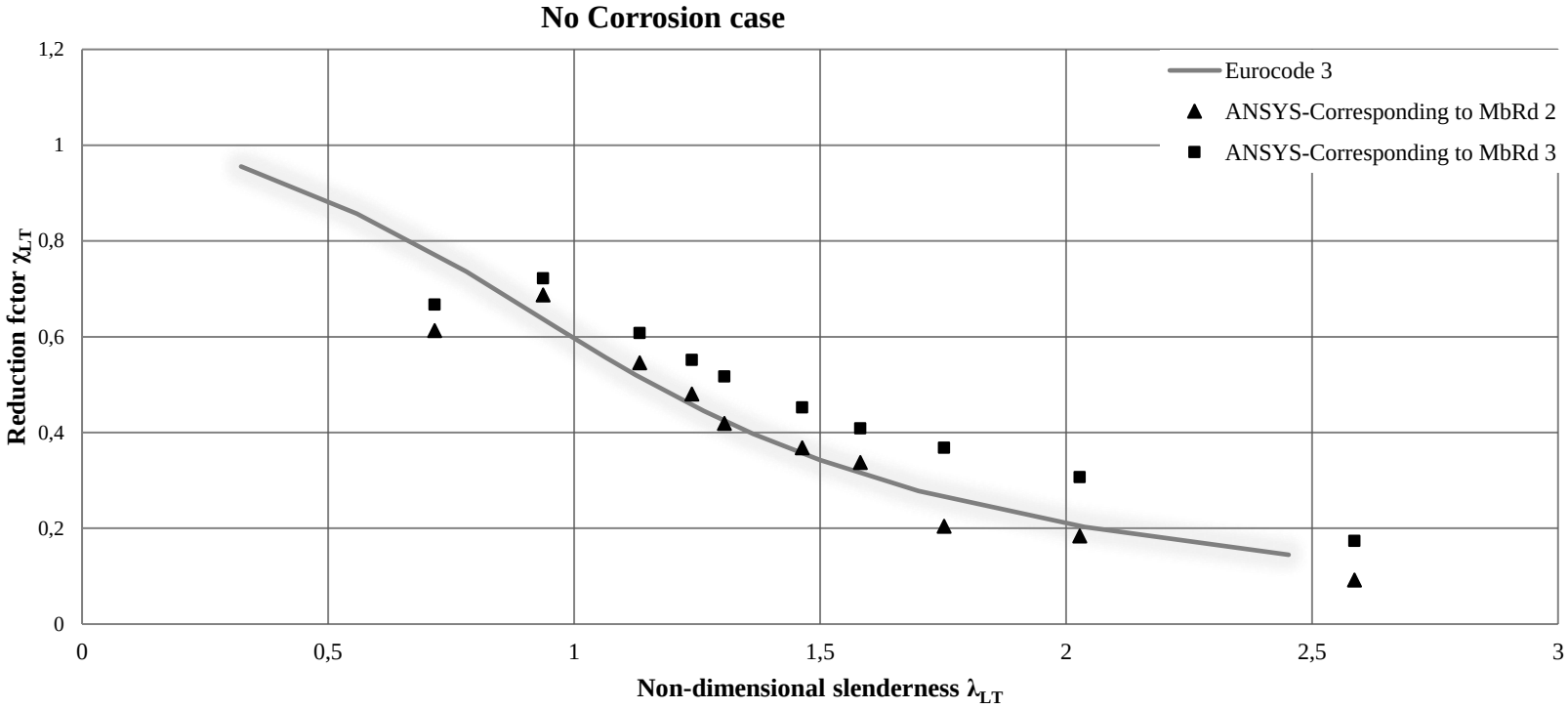

Figure 4.4.9-1: Reduction factor vs Non-dimensional – No Corrosion

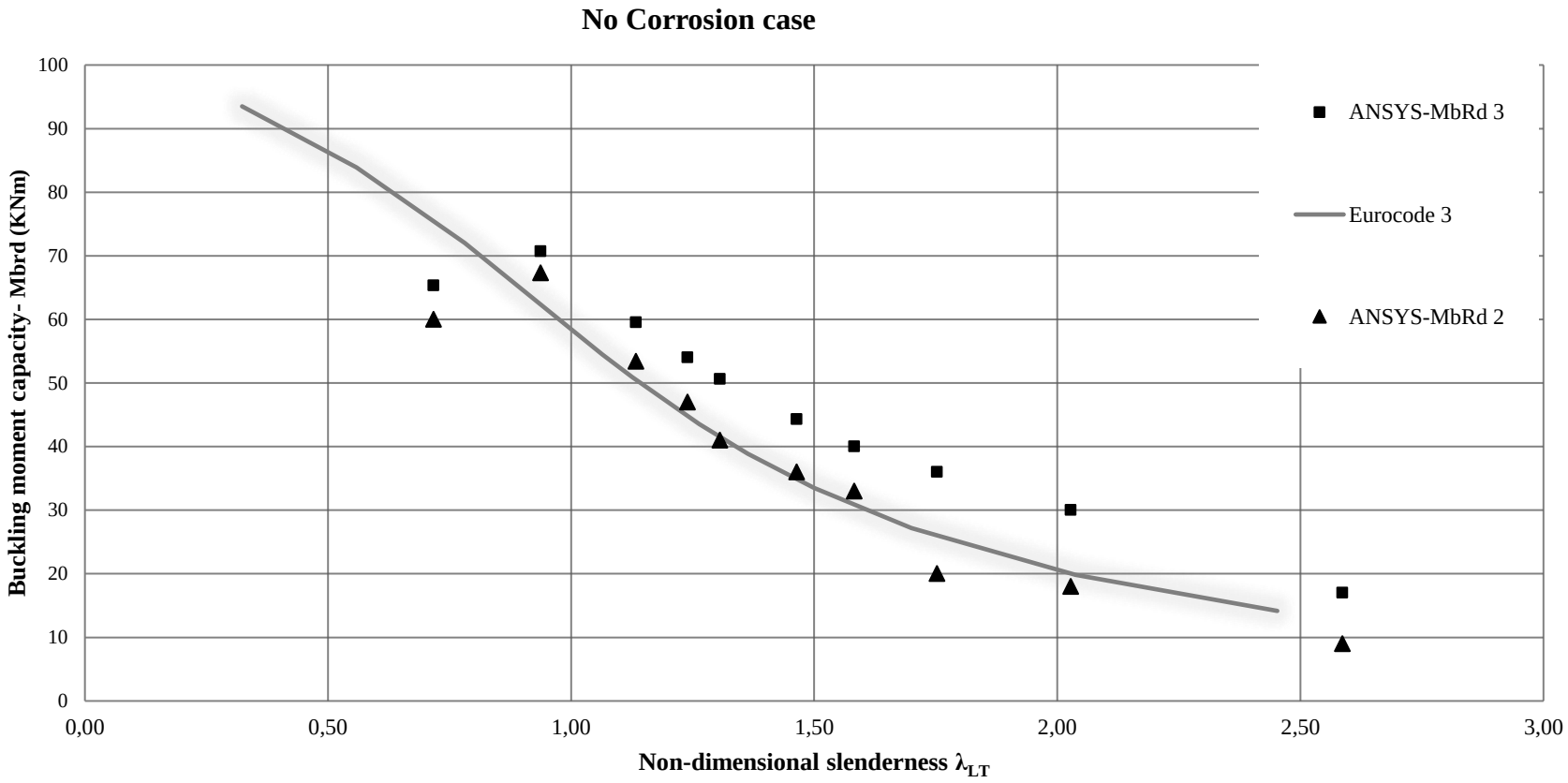

Figure 4.4.9-2: Buckling moment capacity vs Non-dimensional slenderness- No corrosion

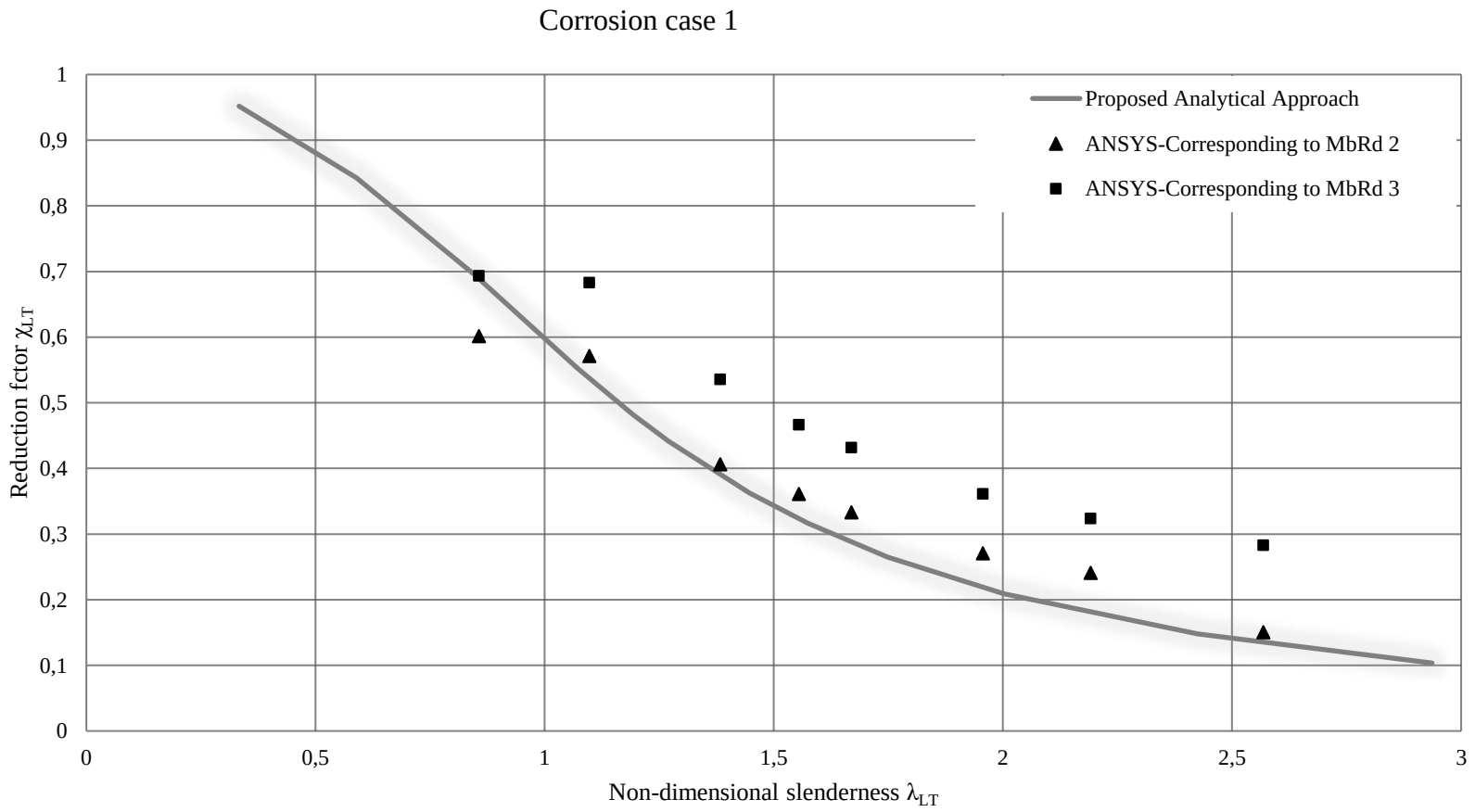

Figure 4.4.9-3: Reduction factor vs Non-dimensional – Case

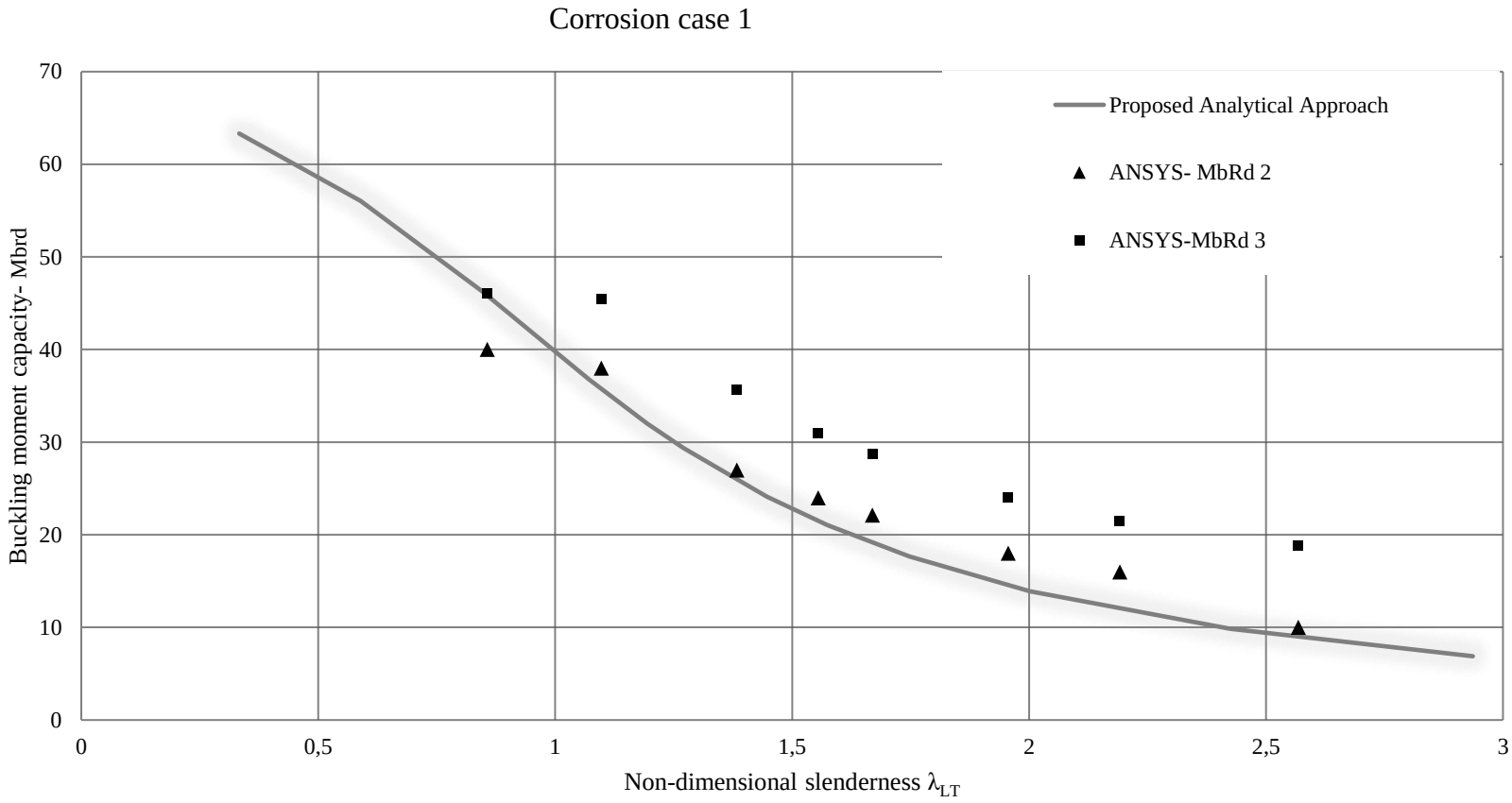

Figure 4.4.9-4: Buckling moment capacity vs Non-dimensional slenderness- Case Corrosion 1

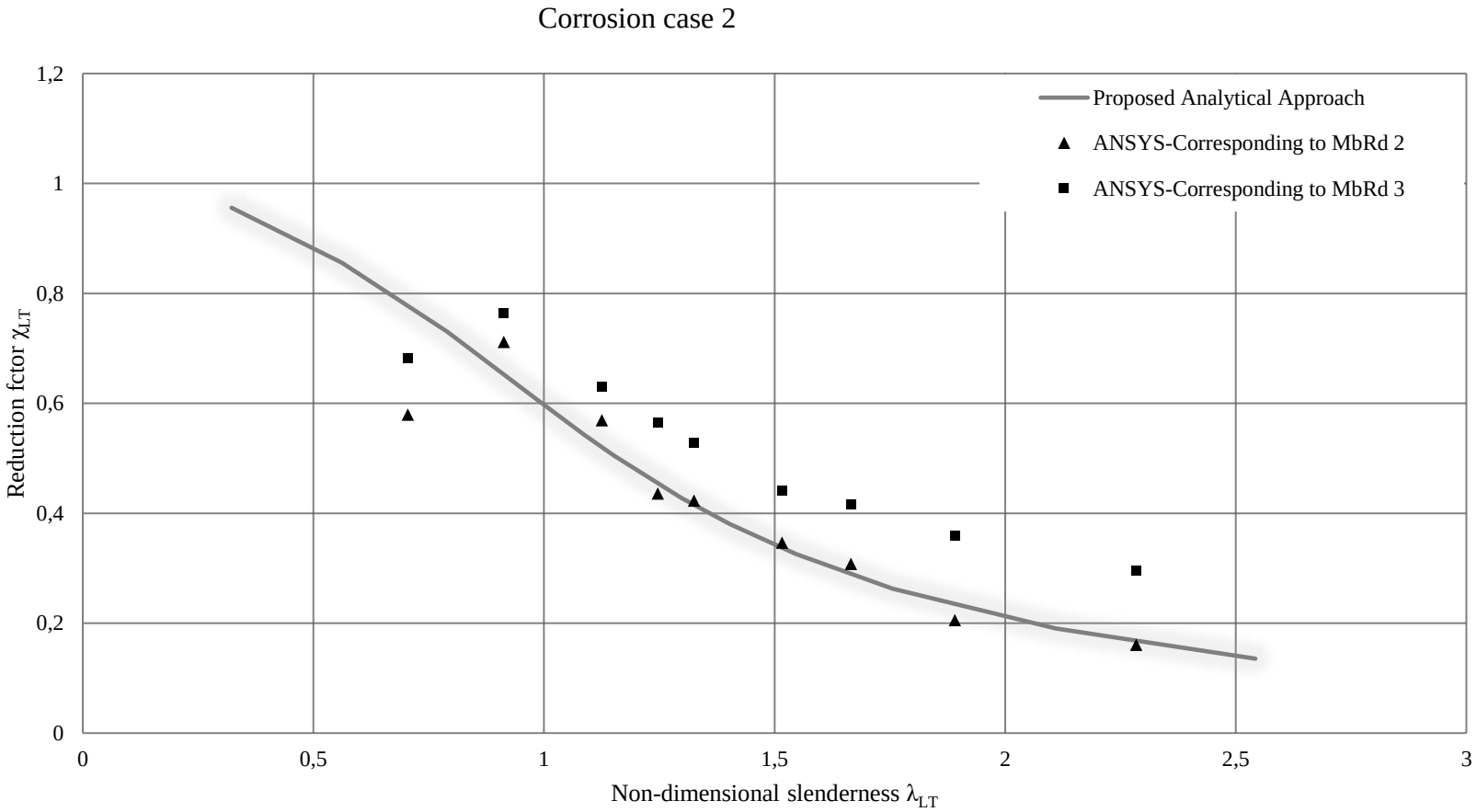

Figure 4.4.9-5: Reduction factor vs Non-dimensional – Case Corrosion 2

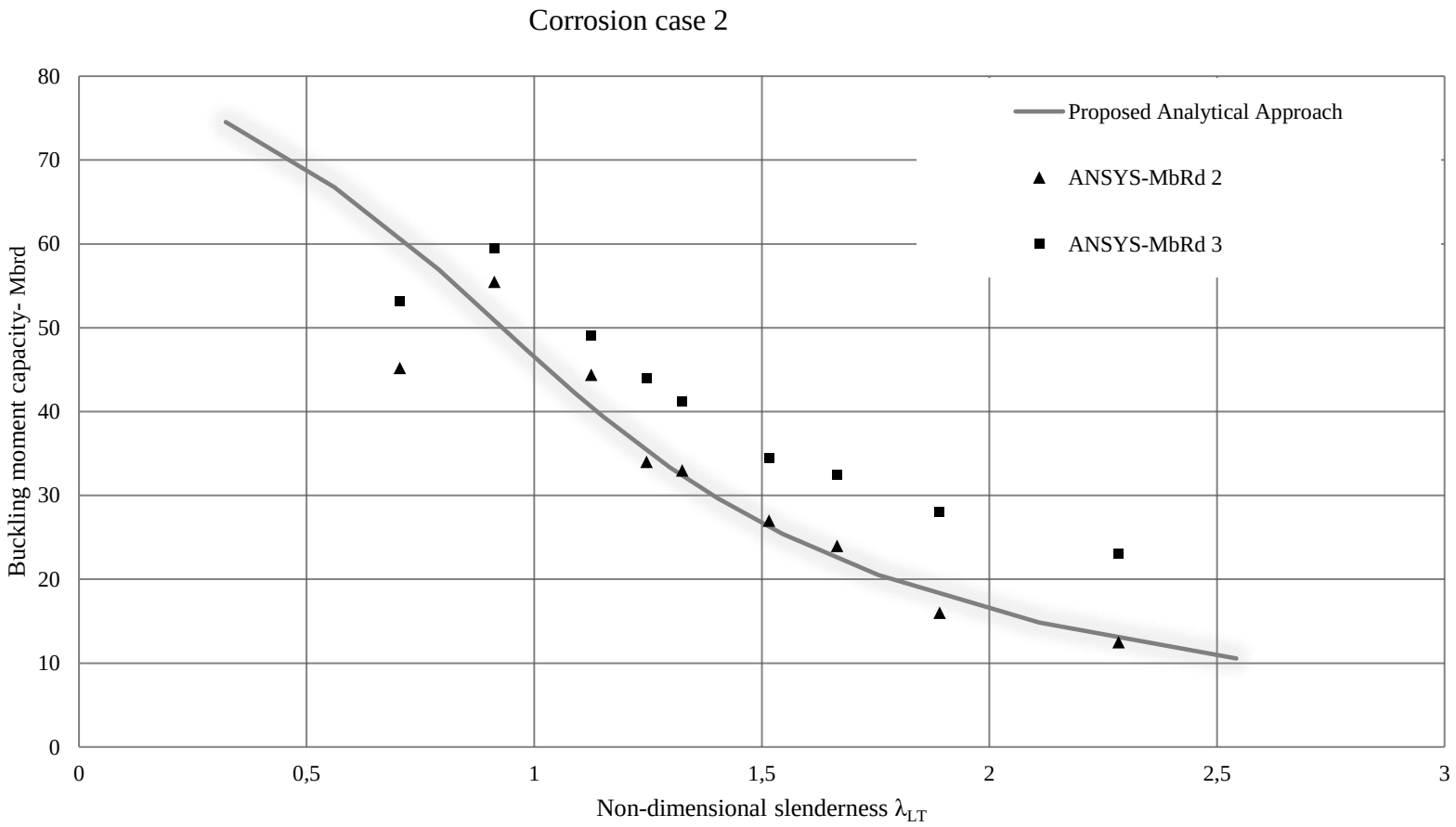

Figure 4.4.9-6: Buckling moment capacity vs Non-dimensional slenderness- Case Corrosion

5 Comparison of results and Discussions

5.1 The Accuracy of the FEM Results

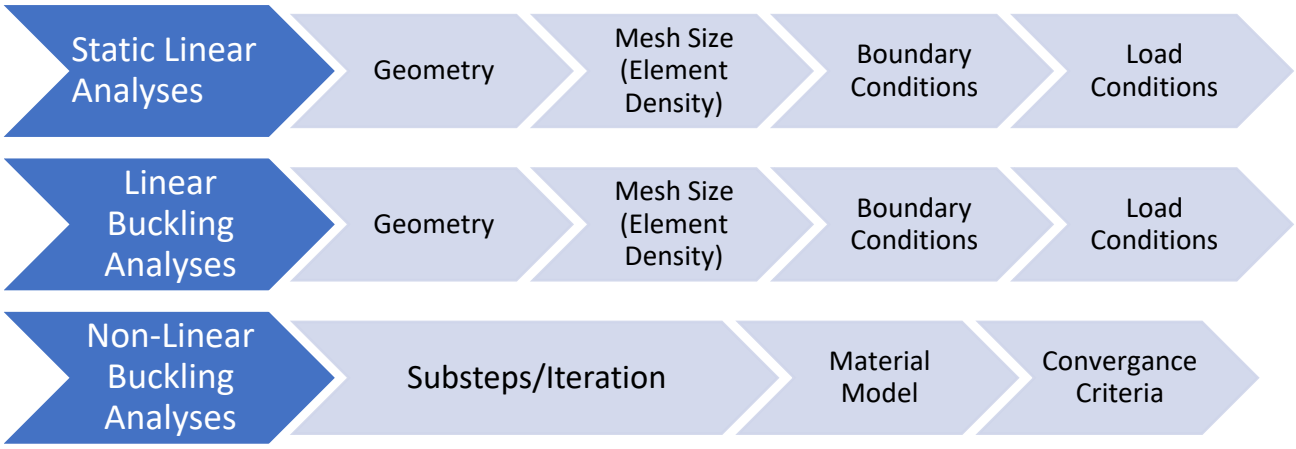

Figure 5.1-1: The Accuracy of the FEM results

Geometry:

To change the geometry is optional in order to investigate the accuracy of the FEM results. In this thesis the geometry part of the I-beam was not changed in order to investigate the accuracy of the FEM results.

Mesh Size (Element Density):

When increasing the mesh density, a certain density may be reached where the results do not vary significantly as illustrated in Figure 5.1-2. Therefore, a denser mesh than 5mm is not necessary in order to get more accurate FEM results. A denser mesh needs more computational time, while a coarse mesh needs less computational time. In this thesis a denser mesh than 5mm is not necessary. All the FE models are performed with a mesh density equal to 5mm.

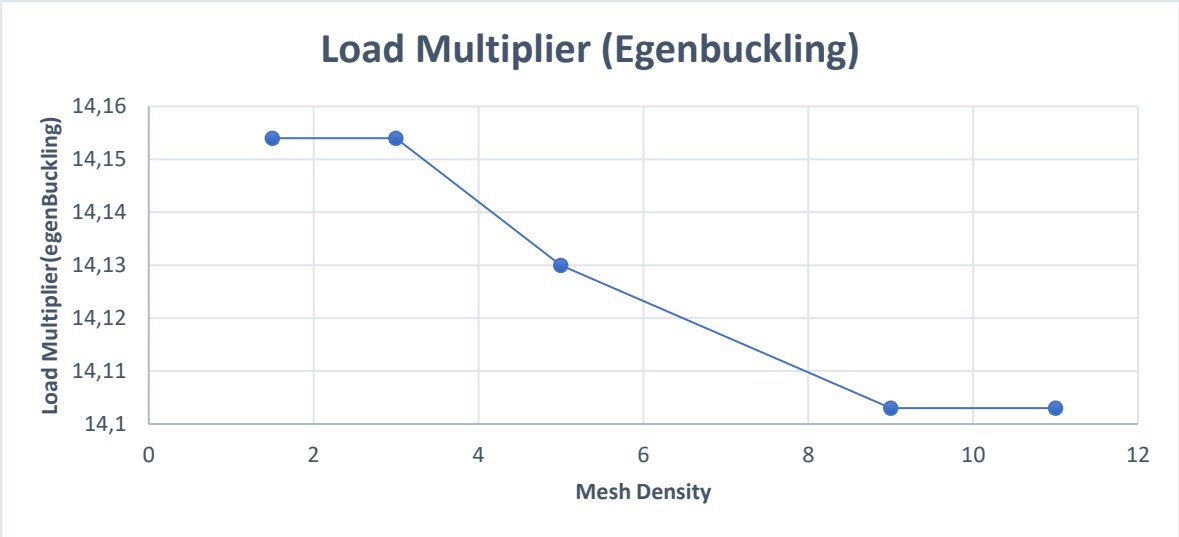

Figure 5.1-2: The Load Multiplier vs Mesh Density

Boundary Conditions:

The first boundary condition assumption, which is illustrated in figure 4.2-2, creates an unreasonable local deformation when running the static linear analysis in Ansys Workbench on all the finite element models included in this thesis. The second boundary condition, which is illustrated in figure 4.2-3, creates less or almost non unreasonable local deformation when running the static linear analysis in Ansys Workbench on all the finite element models included in this thesis.

Convergence Criteria:

To manipulate the FEM results we use the convergence criteria, but the accuracy of the FEM results will decrease. The optional convergence criterions which are available in Ansys Workbench are: Force Convergence, Moment Convergence, Displacement Convergence, Rotation Convergence and Newton-Raphson option. Instead of modifying the convergence criteria, the other conditions can be enhanced such as, refining the mesh density, selecting the proper load type, using the same load condition for linear and nonlinear buckling analyses, increasing the iterations and increasing the step size(sub-step) in the nonlinear buckling analyses.

Sub steps /Iteration:

By increasing the sub steps in the non-linear buckling analyses, the curves for the different cases may get more pronounced in the figures on the section ***"4.4.8 Plots – Applied Moment vs Lateral deflection, five different cases for 12 lengths".***

Arc-length method for nonlinear buckling:

The primary method to solve the non-linear buckling analysis is called the force-controlled method. This method doesn't work for curved plots, but it works for linear plots. The reason is demonstrated in Figure 5.1-3 shown below, where a chosen applied moment gives two values for the displacement axis. The displacement-controlled method and the arc-length method can be used in order to solve the non-linear buckling analysis for curved plots. The displacement-controlled method is accepted for the non-linear buckling analysis for curved plots, where a chosen displacement gives one value for the applied moment as illustrated in Figure 5.1-3.

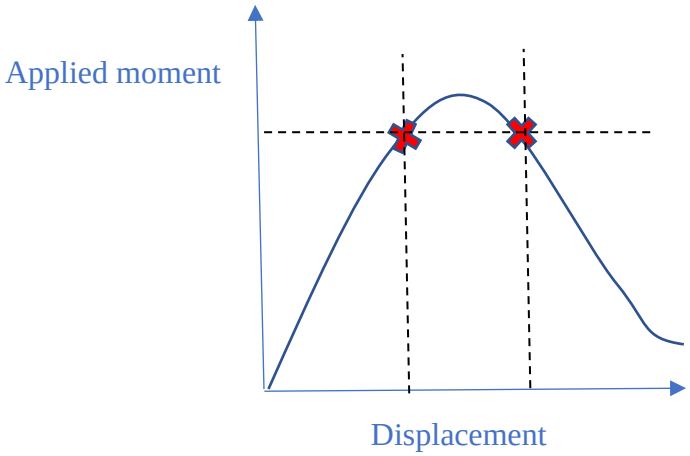

Figure 5.1-3: Applied moment Vs. Displacement

The Arc-length method was used in this thesis in order to perform the non-linear buckling analysis for curved plots, with the command shown below:

[ARCLEN, Key, MAXARC, MINARC]

Where:

Key=Arc-length Key (On or No)

MAXARC= The maximum multiplier of the reference arc-length radius (default=25)

MINARC= The minimum multiplier of the reference arc-length radius (default=1/1000)

The numerical tangent method:

The numerical tangent method is illustrated in Figure 5.1-4 and can be used in order to find the accurate values for the LTB moment capacities MbRd 2 and MbRd 3.

For the purposes of this thesis the aforementioned values were picked from the plots in section "4.4.8 Plots – Applied Moment vs Lateral deflection, five different cases for 12 lengths" by finding the intersection between the respective corrosion case curve and the plot's "y" axis (Applied Moment (kNm).

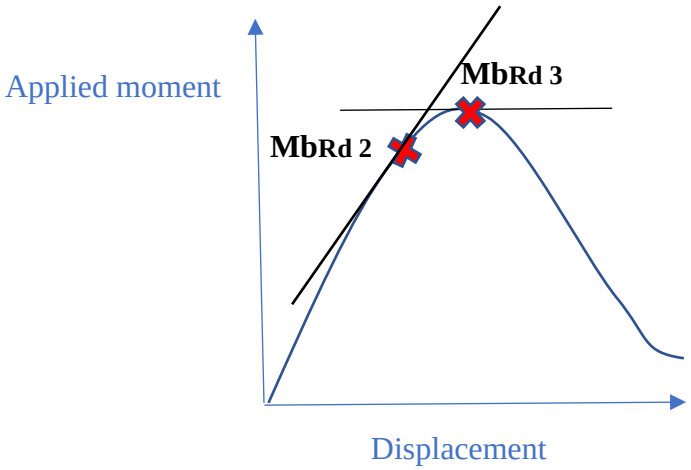

Figure 5.1-4: The Tangent Method-Mbrd 2 and Mbrd 3

Load Conditions:

Table 5 demonstrates the loading type: Ends moment at the end of the beam and uniform line pressure.

Table 6 demonstrates the loading type and its elastic critical moment value given by Ansys Workbench. The elastic critical moment is changing due to the load type. But why? Both the web and the flanges will get stressed by putting a line pressure which will cause that the Mcr decreases. The uniform line pressure load type gives a shear diagram and a moment diagram. If the load type increases the stress on the cross-section, this will lead to a decrease on the Mcr. By putting an end moment at the ends of the I-beam, only the flange is stressed while the web is not. Since only the flange is stressed the Mcr is higher.

An end moment at the ends of the I-beam gives a moment diagram, but not a shear diagram. When the load type decreases the stress on the cross-section, this leads to a increase on the Mcr.

Same load condition Vs Not same load condition

Same load condition: Using the same load type for the linear and nonlinear buckling analyses, such as line pressure.

Not same load condition: Not using the same load type for the linear and nonlinear buckling analyses, such as end moments at the end of the beam for the linear analyses and line pressure for the nonlinear analyses.

Figure 4.4.6-1 and Table 39 demonstrate the difference between the same load condition assumption and not same load condition assumption for the non-corrosion case with a beam length of 1.5m and with an imperfection scale factor of 2. The difference is calculated as percentage change value which is shown below.

$$\left(\frac{65.4 - 64.7}{65.4}\right) * 100\% = 1.07\%$$

Figure 4.4.6-2 and Table 40 demonstrate the difference between the same load condition assumption and not same load condition assumption for the non-corrosion case with a beam length of 1.5m and with an imperfection scale factor of 1.5. The difference is calculated as percentage change value which is shown below.

$$\left(\frac{71.5 - 70.7}{71.5}\right) * 100\% = 1.12\%$$

FEM results with different scale factor vs the Code

The first goal was to compare the buckling capacity of the FEM results with different scale factors versus the buckling capacity from the code, by assuming that the buckling moment capacity was only affected due to the imperfection scale factor, but that is not the case. The code does not only take into consideration the scale factor, there are other factors and assumptions.

Figure 4.4.7-1 and Tabell 41 demonstrates that the LTB moment capacity (applied moment) is decreasing when the imperfection scale factor is increasing for the non-corrosion case with a beam length equal to 1.5m. Four models were performed, where the beam length of 1.5m was constant, but the imperfection scale factor varies. The comparison of the non-corrosion case with beam length of 1.5m and different imperfection scale factors with the code was not completed do to the fact that the code does not only take into consideration the scale factor. Since the comparison which is mentioned above is not completed, the assumption is that the LTB moment capacity of the non-corrosion case with beam length of 1.5m and imperfection scale factor of 1.4 is comparable with the code.

Figure 4.4.7-2 and Tabell 42 demonstrate that the LTB moment capacity (applied moment) is decreasing when the imperfection scale factor is increasing for the non-corrosion case with beam length equal to 2m. The Tabell 42 demonstrates that the LTB moment capacity of the non-corrosion case with beam length of 2m and imperfection scale factor of 2 is comparable with the code.

5.2 Static Linear Analyses

The maximum displacement equations (from Eq. 36 to Eq. 41) and the maximum stress equation (Eq. 42) are used to check the accuracy of the static linear FEM analysis for the non-corrosion case, case corrosion 1 and case corrosion 2. In the Appendix D the MATLAB files for all the three cases mentioned above are included.

Table 24, Table 27 and Table 30 demonstrate that the difference between MDM (Max displacement MATLAB) and MDWA (Max displacement Workbench Ansys) for all the considered beam lengths is very low. In order to get the difference between MDM and MDWA even lower, the load type ends moment at the ends of the beam should be considered because the equation of max displacement applies to this load type. The difference between the MSM (Max stress MATLAB) and MSWA (Max stress workbench Ansys) for all the considered beam lengths is also low, but it can get lower by using the load type ends moment at the ends of the beam.

Table 33 and Table 36 do not demonstrate the difference between MDM (Max displacement MATLAB) and MDWA (Max displacement Workbench Ansys) for all the considered beam lengths, because there is no proposed analytical approach for case corrosion 3 -model 1 and for the case corrosion 3 -model 2

5.3 Linear Buckling Analyses

The LTB formulas mentioned in chapter 2 are used to calculate the elastic critical moment (Mcr) for case non-corrosion, case corrosion 1, and case corrosion 2. Refer to Appendix A for the MATLAB file code for the case non-corrosion, while for case corrosion 1 refer to Appendix B, and for case corrosion 2 refer to Appendix C.

Table 25, Table 28 and Table 31 document the difference between Mcr-A (Critical Moment-Ansys) and Mcr-C (Critical Moment-Code) for all the considered beam lengths except for beam length 0.55m. To perform an LTB behaviour on a cross-section with beam length equal to 0.55m in Ansys Workbench was not possible because a short I beam cross-section is not affected by the LTB behaviour. The difference is calculated as percentage change value which is shown below for case non-corrosion with length equal to 1.5m.

$$\left(\frac{160.5 - 111.5}{160.5}\right) * 100\% = 30.5\%$$

Table 6 demonstrates how the load type affects the elastic critical moment (Mcr), and the reason is explained in section 5.1 of this thesis. The percentage change difference for case non-corrosion with length equal to 1.5m and with load condition "moment at the end of the beam" is shown below:

$$\left(\frac{160.5 - 141.54}{160.5}\right) * 100\% = 11.8\%$$

Table 34 and Table 37 do not demonstrate the difference between Mcr-A (Critical Moment-Ansys) and Mcr-C (Critical Moment-Code) for all the considered beam lengths, because there is no proposed analytical approach for case corrosion 3 -model 1 and for case corrosion 3 -model 2.

5.4 Nonlinear Buckling Analyses

The LTB formulas mentioned in chapter 2 are used to calculate the M_{brd} for case non-corrosion, case corrosion 1, and case corrosion 2. Refer to Appendix A for the MATLAB file code for the case non-corrosion, while for case corrosion 1 refer to Appendix B, and for case corrosion 2 refer to the Appendix C.

Table 26, Table 29 and Table 32 demonstrate the difference between the Ansys FEM buckling capacity Mbrd2 and Mbrd 3 versus the buckling capacity moment by the code for all the documented beam lengths except for beam length 0.55m. The reason why it is not possible to perform LTB behaviour on a cross section with beam length equal to 0.55m is mentioned in section 5.3 “Linear Buckling Analysis”.

Table 26, Table 29, Table 32, Table 35 and Table 38 are created from the values selected from the figures on section ***“4.4.8 Plots – Applied Moment vs Lateral deflection, five different cases for 12 lengths”.***

Table 35 and Table 38 do not demonstrate the difference between the Ansys FEM buckling capacity Mbrd2 and Mbrd 3 versus the buckling capacity moment by the code for all the considered beam lengths, because there is no proposed analytical approach for case corrosion 3 -model 1 and for case corrosion 3 -model 2.

5.5 The Results from the Nonlinear buckling Analyses

Table 43 :The order of the resulting curves from Figure 4.4.8-1

The Order	Case	Length	Imperfection scale factor
1.	No Corrosion	1000mm	$\frac{L}{1000} = 1$
5.	Case Corrosion 1	1000mm	$\frac{L}{1000} = 1$
4.	Case Corrosion 2	1000mm	$\frac{L}{1000} = 1$
3.	Case Corrosion 3- Model 1	1000mm	$\frac{L}{1000} = 1$
2.	Case Corrosion 3-Model 2	1000mm	$\frac{L}{1000} = 1$

The curve for the non-corrosion case observed in Figure 4.4.8-1 and Table 43 show that the non-corrosion case has higher LTB moment capacity, while the curve for the case corrosion 1 show a lower LTB moment capacity. The curve for the case corrosion 3-model 2 show that the LTB moment capacity of the corroded I-beam does not get significantly affected by corrosion, where corrosion takes place at 1/3 of the length of the beam at the bottom flange, and the bottom section of the web. The curve for the case corrosion 3- model 1 is higher than the curve for case corrosion 2, which demonstrates that the corroded I-beam, where corrosion takes place at 1/3 of the length of the beam at the top flange, bottom flange, and the web, has higher LTB moment capacity than the case corrosion 2.

Table 44: The order of the resulting curves from Figure 4.4.8-2

The Order	Case	Length	Imperfection scale factor
1.	No Corrosion	1500mm	$\frac{L}{1000} = 1.5$
5.	Case Corrosion 1	1500mm	$\frac{L}{1000} = 1.5$
3.	Case Corrosion 2	1500mm	$\frac{L}{1000} = 1.5$
4.	Case Corrosion 3- Model 1	1500mm	$\frac{L}{1000} = 1.5$
2.	Case Corrosion 3- Model 2	1500mm	$\frac{L}{1000} = 1.5$

The curve for the non-corrosion case observed in Figure 4.4.8-2 and Table 44 show that the non-corrosion case has higher LTB moment capacity, while the curve for the case corrosion 1 show that the case corrosion 1 has lower LTB moment capacity. The curve for the case corrosion 3- model 2 show that the LTB moment capacity of the corroded I-beam does not get significantly affected by corrosion, where corrosion takes place at 1/3 of the length of the beam at the bottom flange, and the bottom section of the web. The curve for case corrosion 2 is higher than the curve for case corrosion 3- model 1, which demonstrates that the corroded I-beam, where corrosion takes place at 1/3 of the length of the beam at the top flange, bottom flange, and the web has lower LTB moment capacity than the case corrosion 2.

Table 45: The order of the resulting curves from Figure 4.4.8-3

The Order	Case	Length	Imperfection scale factor
1.	No Corrosion	2000mm	$\frac{L}{1000} = 2$
5.	Case Corrosion 1	2000mm	$\frac{L}{1000} = 2$
3.	Case Corrosion 2	2000mm	$\frac{L}{1000} = 2$
4.	Case Corrosion 3- Model 1	2000mm	$\frac{L}{1000} = 2$
2.	Case Corrosion 3-Model 2	2000mm	$\frac{L}{1000} = 2$

The curve for the non-corrosion case observed in Figure 4.4.8-3 and Table 45 show that the non-corrosion case has higher LTB moment capacity, while the curve for the case corrosion 1 show that the case corrosion 1 has lower LTB moment capacity. The curve for the case corrosion 3- model 2 show that the LTB moment capacity of the corroded I-beam does not get significantly affected by corrosion, where corrosion takes place at 1/3 of the length at the bottom flange, and the bottom section of the web. The other observation in Figure 4.4.8-3 is that the curve for case corrosion -model 2 is not fully curved at some positions, which in this case is approximately from 3mm to 5mm. The curve for case corrosion 2 is higher than the curve for case corrosion 3- model 1, which demonstrates that the corroded I-beam, where corrosion takes place at 1/3 of the length of the beam at the top flange, bottom flange, and the web has lower LTB moment capacity than the case corrosion 2.

Table 46: The order of the resulting curves from Figure 4.4.8-4

The Order	Case	Length	Imperfection scale factor
1.	No Corrosion	2300mm	$\frac{L}{1000} = 2.3$
5.	Case Corrosion 1	2300mm	$\frac{L}{1000} = 2.3$
4.	Case Corrosion 2	2300mm	$\frac{L}{1000} = 2.3$
3.	Case Corrosion 3- Model 1	2300mm	$\frac{L}{1000} = 2.3$
2.	Case Corrosion 3-Model 2	2300mm	$\frac{L}{1000} = 2.3$

The curve for the non-corrosion case observed in Figure 4.4.8-4 and Table 46 show that the non-corrosion case has higher LTB moment capacity, while the curve for the case corrosion 1 show that the case corrosion 1 has lower LTB moment capacity. The curve for the case corrosion 3- model 2 show that the LTB moment capacity for the corroded I-beam does not get significantly affected by corrosion, where corrosion takes place at 1/3 of the length of the beam at the bottom flange, and the bottom section of the web. The curve for the case corrosion 3- model 2 is higher than the curve for case corrosion 2, which demonstrates that the corroded I-beam, where corrosion takes place at 1/3 of the length of the beam at the top flange, bottom flange, and the web has higher LTB moment capacity than the case corrosion 2.

Table 47: The order of the resulting curves from Figure 4.4.8-5

The Order	Case	Length	Imperfection scale factor
1.	No Corrosion	2500mm	$\frac{L}{1000} = 2.5$
5.	Case Corrosion 1	2500mm	$\frac{L}{1000} = 2.5$
4.	Case Corrosion 2	2500mm	$\frac{L}{1000} = 2.5$
3.	Case Corrosion 3- Model 1	2500mm	$\frac{L}{1000} = 2.5$
2.	Case Corrosion 3-Model 2	2500mm	$\frac{L}{1000} = 2.5$

The curve for the non-corrosion case observed in Figure 4.4.8-5 and Table 47 show that the non-corrosion case has higher LTB moment capacity, while the curve for the case corrosion 1 show that the case corrosion 1 has lower LTB moment capacity. The curve for the case corrosion 3- model 2 show that the LTB moment capacity of the corroded I-beam starts to get affected by corrosion, where corrosion takes place at 1/3 of the length of the beam at the bottom flange, and the bottom section of the web. The other observation in Figure 4.4.8-5 is that the curve for the case corrosion 3 -model 2 is not fully curved at some positions, which in this case is approximately from 4.2mm to 5mm. The curve for the case corrosion 3- model 1 is higher than the curve for case corrosion 2, which demonstrates that the corroded I-beam, where corrosion takes place at 1/3 of the length of the beam at the top flange, bottom flange, and the web has higher LTB moment capacity than the case corrosion 2.

Table 48: The order of the resulting curves from Figure 4.4.8-6

The Order	Case	Length	Imperfection scale factor
1.	No Corrosion	3000mm	$\frac{L}{1000} = 3$
5.	Case Corrosion 1	3000mm	$\frac{L}{1000} = 3$
4.	Case Corrosion 2	3000mm	$\frac{L}{1000} = 3$
3.	Case Corrosion 3- Model 1	3000mm	$\frac{L}{1000} = 3$
2.	Case Corrosion 3-Model 2	3000mm	$\frac{L}{1000} = 3$

The curve for the non-corrosion case observed in Figure 4.4.8-6 and Table 48 show that the non-corrosion case has higher LTB moment capacity, while the curve for the case corrosion 1 show that the case corrosion 1 has lower LTB moment capacity. The curve for the case corrosion 3- model 2 show that the LTB moment capacity of the corroded I-beam has started to get affected by corrosion, where corrosion takes place at 1/3 of the length of the beam at the bottom flange and the bottom section of the web. The curve for the case corrosion 3- model 2 is higher than the curve for case corrosion 2, which demonstrates that the corroded I-beam, where corrosion takes place at 1/3 of the length of the beam at the top flange, bottom flange, and the web has higher LTB moment capacity than the case corrosion 2.

Table 49: The order of the resulting curves from Figure 4.4.8-7

The Order	Case	Length	Imperfection scale factor
1.	No Corrosion	3400mm	$\frac{L}{1000} = 3.4$
5.	Case Corrosion 1	3400mm	$\frac{L}{1000} = 3.4$
3.	Case Corrosion 2	3400mm	$\frac{L}{1000} = 3.4$
2.	Case Corrosion 3- Model 1	3400mm	$\frac{L}{1000} = 3.4$
4.	Case Corrosion 3-Model 2	3400mm	$\frac{L}{1000} = 3.4$

The curve for the non-corrosion case observed in Figure 4.4.8-7 and Table 49 show that the non-corrosion case has higher LTB moment capacity, while the curve for the case corrosion 1 show that the case corrosion 1 has lower LTB moment capacity. The LTB stiffness of the curve for case corrosion 3 -model 2 is decreasing drastically after the lateral deflection is approximately equal to 5mm due to local stress concentration and its effect to the nonlinear behaviour. The local stress concentration arises due to the transition of the geometry, such as the transition from the non-corroded part to the corroded part. The curve for the case corrosion 3- model 2 is higher than the curve for case corrosion 2, which demonstrates that the corroded I-beam, where corrosion takes place at 1/3 of the length of the beam at the top flange, bottom flange, and the web has higher LTB moment capacity than the case corrosion 2.

Table 50: The order of the resulting curves from Figure 4.4.8-8

The Order	Case	Length	Imperfection scale factor
1.	No Corrosion	4000mm	$\frac{L}{1000} = 4$
5.	Case Corrosion 1	4000mm	$\frac{L}{1000} = 4$
3.	Case Corrosion 2	4000mm	$\frac{L}{1000} = 4$
4.	Case Corrosion 3- Model 1	4000mm	$\frac{L}{1000} = 4$
2.	Case Corrosion 3-Model 2	4000mm	$\frac{L}{1000} = 4$

The curve for the non-corrosion case observed in Figure 4.4.8-8 and Table 50 show that the non-corrosion case has higher LTB moment capacity, while the curve for the case corrosion 1 show that the case corrosion 1 has lower LTB moment capacity. The LTB stiffness of the curve for case corrosion 3 -model 2 is decreasing drastically after the lateral deflection is approximately equal to 6mm due to local stress concentration and its effect to the nonlinear behaviour. The local stress concentration arises due to the transition of the geometry, such as the transition from the non-corroded part to the corroded part. The curve for case corrosion 2 is higher than the curve for case corrosion 3- model 2, which demonstrates that the corroded I-beam, where corrosion takes place at 1/3 of the length of the beam at the top flange, bottom flange, and the web has lower LTB moment capacity than the case corrosion 2.

Table 51: The order of the resulting curves from Figure 4.4.8-9

The Order	Case	Length	Imperfection scale factor
1.	No Corrosion	5000mm	$\frac{L}{1000} = 5$
5.	Case Corrosion 1	5000mm	$\frac{L}{1000} = 5$
4.	Case Corrosion 2	5000mm	$\frac{L}{1000} = 5$
3.	Case Corrosion 3- Model 1	5000mm	$\frac{L}{1000} = 5$
2.	Case Corrosion 3-Model 2	5000mm	$\frac{L}{1000} = 5$

The curve for the non-corrosion case observed in Figure 4.4.8-9 and Table 51 show that the non-corrosion case has higher LTB moment capacity, while the curve for the case corrosion 1 show that the case corrosion 1 has lower LTB moment capacity. The LTB stiffness of the curve for case corrosion 3 -model 2 is decreasing drastically after the lateral deflection is approximately equal to 10mm due to local stress concentration and its effect to the nonlinear behaviour. The local stress concentration arises due to the transition of the geometry, such as the transition from the non-corroded part to the corroded part. The curve for the case corrosion 3- model 2 is higher than the curve for case corrosion 2, which demonstrates that the corroded I-beam, where corrosion takes place at 1/3 of the length of the beam at the top flange, bottom flange, and the web has higher LTB moment capacity than the case corrosion 2.

Table 52: The order of the resulting curves from Figure 4.4.8-10

The Order	Case	Length	Imperfection scale factor
1.	No Corrosion	7000mm	$\frac{L}{1000} = 7$
5.	Case Corrosion 1	7000mm	$\frac{L}{1000} = 7$
4.	Case Corrosion 2	7000mm	$\frac{L}{1000} = 7$
3.	Case Corrosion 3- Model 1	7000mm	$\frac{L}{1000} = 7$
2.	Case Corrosion 3-Model 2	7000mm	$\frac{L}{1000} = 7$

The curve for the non-corrosion case observed in Figure 4.4.8-10 and Table 52 show that the non-corrosion case has higher LTB moment capacity, while the curve for the case corrosion 1 show that the case corrosion 1 has lower LTB moment capacity. The curve for the case corrosion 3- model 2 show that the LTB moment capacity of the corroded I-beam has been affected by corrosion, where corrosion takes place at 1/3 of the length of the beam at the bottom flange and at the bottom section of the web. The curve for the case corrosion 3- model 2 is higher than the curve for case corrosion 2, which demonstrates that the corroded I-beam, where corrosion takes place at 1/3 of the length of the beam at the top flange, bottom flange, and the web has higher LTB moment capacity than the case corrosion 2. It is observed that none of the curves for the implemented corrosion cases achieved conversion in Figure 4.4.8-10.

Table 53: The order of the resulting curves from Figure 4.4.8-11

The Order	Case	Length	Imperfection scale factor
1.	No Corrosion	10000mm	$\frac{L}{1000} = 10$
5.	Case Corrosion 1	10000mm	$\frac{L}{1000} = 10$
4.	Case Corrosion 2	10000mm	$\frac{L}{1000} = 10$
3.	Case Corrosion 3- Model 1	10000mm	$\frac{L}{1000} = 10$
2.	Case Corrosion 3-Model 2	10000mm	$\frac{L}{1000} = 10$

The curve for the case corrosion 1 observed in Figure 4.4.8-11 and Table 53 show that case corrosion 1 has a lower LTB moment capacity. The curve for the non-corrosion case is increasing at the start but, after some time, it decreases and then increases without converging. The curve for the case corrosion 3 -model 1 is behaving the way it should at the start, but after some time it increases and then it converges at the end. The curve for the case corrosion 3 -model 1 is higher than the curve for case corrosion 3 -model 2, which, conflictingly, shows that the corroded I beam with less cross-sectional area has higher LTB moment capacity than the corroded I-beam with higher cross-sectional area.

Two the five curves which are observed in Figure 4.4.8-11 are behaving accordingly while the three remaining curves do not. The curves for the case corrosion 1 and case corrosion 2 behaved as expected while the curves for case non-corrosion, case corrosion 3 -model 1 and especially case corrosion 3 -model 2 show results that do not comply with the rules of physics.

There are uncertainties with regards to the resulting curves observed in Figure 4.4.8-11.

5.6 The Results from Reduction factor Vs Non-dimensional

The following observations from Figure 4.4.9-1 and Figure 4.4.9-2 for the non-corrosion case are mentioned below:

- The buckling capacities Mbrd2 and Mbrd 3 from the Ansys FEMs matched with those obtained from the Eurocode 3 except for when the "non-dimensional slenderness" parameter (λ_{LT}) is equal to 0.7 and where the values for Mbrd2 and Mbrd 3 deviate from the value obtained from the Eurocode 3.

The following observations from Figure 4.4.9-3 and Figure 4.4.9-4 for the case corrosion 1 are mentioned below:

- The buckling capacities Mbrd2 and Mbrd 3 from the Ansys FEMs matched with those obtained from the proposed analytical approach.

The following observations from Figure 4.4.9-5 and Figure 4.4.9-6 for the case corrosion 2 are mentioned below:

- The buckling capacities Mbrd2 and Mbrd 3 from the Ansys FEMs matched with those obtained from the proposed analytical approach except for when the "non-dimensional slenderness" parameter (λ_{LT}) is equal to 0.7 and where the values for Mbrd2 and Mbrd 3 deviate from the value obtained from the proposed analytical approach.

6 Conclusions

6.1 Summary of the study

In this thesis, the LTB moment capacity of corroded I-beams is studied in detail, where five different cases are considered. One of the cases is without corrosion, while the rest of the considered cases consist of corrosion on various locations throughout the I beam cross-section. The considered corrosion cases are,

I. **Case non-corrosion:** The non-corrosion case doesn't contain any form or type of corrosion.
II. **Case corrosion 1:** Case corrosion 1 represents the situation that everywhere of the I beam is subjected to uniform corrison and therefore uniform thickness reduction is applied throughout the I-beam cross section.
III. **Case corrosion 2**: Case corrosion 2 represents the situation that bottom flange and the lower half of the web are subjected to uniform corrosion and therefore uniform thickness reduction is applied throughout the bottom flange and the lower half of the web of the I-beam cross section.
IV. **Case corrosion 3 -model 1:** Case corrosion 3-Model 1 represents the situation that 1/3 of mid-span length of the I-beam at the top flange, bottom flange, and web are subjected to uniform corrosion and therefore uniform thickness reduction is applied over 1/3 of the length of the I-beam at the top flange, bottom flange, and web.
V. **Case corrosion 3 -model 2:** Case corrosion 3-Model 2 represents the situation that 1/3 of mid-span length of the I-beam at the at the bottom flange and the lower half of the web are subjected to uniform corrosion and therefore uniform thickness reduction is is applied over 1/3 of the length of the I-beam at the bottom flange and the lower half of the web.

In order to analyse in debt the effect of the various corrosion cases on the LTB moment capacity (Mbrd) of the I-beam, 12 different beam lengths were defined and each of the previously explained corrosion cases were applied to the I beam cross-section for each of the defined beam lengths. The beam lengths employed in the finite element analysis are as follows:

Table 54: The Employed beam length in the FEM analysis -2

L1=0.55m	**L2=1.00m**	**L3=1.50m**	**L4=2.00m**	**L5=2.30m**	**L6=2.50m**
L7=3.00m	**L8=3.40m**	**L9=4.00m**	**L10=5.00m**	**L11=7.00m**	**L12=10.00m**

The Linear buckling analysis and the nonlinear buckling analysis were performed on the finite element models for each of the considered corrosion cases which, additionally, included each of the defined beam lengths, creating 5x12 finite element models.
In order to analyse the various results obtained from the 60 finite element models, 12 plots were created for each of the defined beam lengths which included the results for each of the 5 corrosion cases, see Figures 4.4.8-1 to 4.4.8-11.

Additionally, in order to obtained a comparison between the LTB moment capacities obtained from the finite element models and the LTB moment capacity (Mbrd) obtained from Eurocode 3, the observed LTB moment capacities Mbrd 2 and Mbrd 3 for the corrosion case "Case non-corrosion", were plotted for the "non-dimensional slenderness" parameter (λ_{LT}) against the "reduction factor" (χ_{LT}) parameter and for the "non-dimensional slenderness" parameter (λ_{LT}) against the "LTB moment capacity" (Mbrd), see Figure 4.4.9-1 and Figure 4.4.9-2.

Furthermore, in order to obtained a comparison between the LTB moment capacities obtained from the finite element models and the LTB moment capacity (Mbrd) obtained from the analytical approach, the observed LTB moment capacities Mbrd 2 and Mbrd 3 for the corrosion cases "Case corrosion 1" and "Case corrosion 2", were plotted for the "non-dimensional slenderness" parameter (λ_{LT}) against the "reduction factor" (χ_{LT}) parameter and for the "non-dimensional slenderness" parameter (λ_{LT}) against the "LTB moment capacity" (Mbrd), see Figures 4.4.9-3 to 4.4.9-6.
Moreover, the corrosion cases "Case corrosion 3 -model 1" and "Case corrosion 3 -model 2" can not be plotted since, at present, there are no analytical approaches to compute these LTB moment capacities (Mbrd).
Hence following conclusions are made:

6.2 Concluding remarks

This thesis illustrates how corrosion on various locations throughout the I beam cross-section reduces the LTB capacity drastically by using the finite element method in ANSYS Workbench. Corrosion causes cross-sectional area reductions on the I-beam cross section which will lead to a reduction of the LTB moment capacity.

The following conclusions are made based on the observations from Figures 4.4.8-1 to 4.4.8-10:

- Case corrosion 1 has the lowest LTB moment capacity (Mbrd). This conclusion is valid since, in this corrosion case, the I beam is most affected by corrosion.

- The curve for the case corrosion 3- model 2 observed from the figures mentioned in section 4.4.8 “Plots – Applied Moment vs Lateral deflection, five different cases for 12 lengths” illustrate that the LTB moment capacity (Mbrd) reduces approximately up to 48.8% due to corrosion when the length of the I-beam increases.

- The LTB stiffness of the curve for the case corrosion 3 -model 2 decreases drastically after the lateral deflection is approximately equal to 7 mm, especially for beam lengths 3.4 m and 4m, due to local stress concentration and its effect to the nonlinear behaviour. The local stress concentration arises due to the transition of the geometry, such as the transition from the non-corroded part to the corroded part.

The following conclusions are made from the observations from Figure 4.4.8-11:

- There are doubts about the resulting curves as shown in Figure 4.4.8-11, where the LTB behaviours for the 5 corrosion cases are shown for the 10m beam length case, since only the corrosion cases “Case corrosion 1” and “Case corrosion 2” are behaving as expected while the corrosion cases “Case non-corrosion”, “Case corrosion 3-model 1” and specially “Case corrosion 3-model 2” are not behaving as expected. The reason for this phenomenon is related to the ratio between the beam’s depth and the beam’s length which, in the case of the 10m beam length, is found to be very small and it is this ratio which affects specially the resulting curves from the previously mentioned non-behaving corrosion cases.

The following conclusions for the non-corrosion case are made from the observations from Figure 4.4.9-1 and Figure 4.4.9-2:

- The results for the buckling capacities Mbrd2 and Mbrd 3 from the Ansys FEMs matched with those obtained from the Eurocode 3, except for when the “non-dimensional slenderness” parameter (λ_{LT}) is equal to 0.7 and where the values for Mbrd2 and Mbrd 3 deviate from the value obtained from Eurocode 3. The reason for this discrepancy in the values stems from the fact that short columns are more prone to be exposed to local buckling than global LTB buckling.

The following conclusions are made for case corrosion 1 from the observations from Figure 4.4.9-3 and Figure 4.4.9-4:

- The results for the buckling capacities Mbrd2 and Mbrd 3 from the Ansys FEMs matched with those obtained from the proposed analytical approach.

The following conclusions for case corrosion 2 are made from the observations from Figure 4.4.9-5 and Figure 4.4.9-6:

- The results for the buckling capacities Mbrd2 and Mbrd 3 from the Ansys FEMs matched with those obtained from the proposed analytical approach, except for when the "non-dimensional slenderness" parameter (λ_{LT}) is equal to 0.7 and where the values for Mbrd2 and Mbrd 3 deviate from the value obtained from Eurocode 3. The reason for this discrepancy in the values stems from the fact that short columns are more prone to be exposed to local buckling than global LTB buckling.

Furthermore, Table 54 shows the comparison method used to compare the obtained LTB moment capacities (MbRds) for the considered five corrosion cases.

Table 55: LTB moment capacity comparison method for the 5 corrosion cases

Corrosion case:	Analytical approach:	FEA:
Non-corrosion case	Eurocode 3	Ansys Workbench
Corrosion case 1	Eurocode 3	Ansys Workbench
Corrosion case 2	Proposed approach	Ansys Workbench
Corrosion case 3 -model 1	----------	Ansys Workbench
Corrosion case 3 -model 2	----------	Ansys Workbench

Since the corrosion cases Non-corrosion and Corrosion case 1 display a continuos uniform cross-section across the length of the I beam, it was possible to compare the LTB moment capacities (MbRds) obtained from the Ansys FEMs with those obtained from the equations as described in Eurocode 3.
Additionally, since the Corrosion case 2 displays a continuos irregular cross-section across the length of the I beam, it was possible to compare the LTB moment capacities (MbRds) obtained from the Ansys FEMs with those obtained from the proposed equations as described in "Remaining fatigue life estimation of corroded bridge members, 2014" [23].

Furthermore, since the corrosion cases Corrosion case 3 -model 1 and Corrosion case 3 -model 2 display a discontinuos irregular cross-section across the length of the I beam, and, since there are not any published proposed analytical approaches for these kind of scenarios, it was not possible to compare the LTB moment capacities (MbRds) obtained from the Ansys FEMs.

Table 55 shows the approximate percentage change in the values for the LTB moment capacity obtained from the FEMs. The percentage change is calculated for each beam length by comparing the results obtained from the FEMs for the case non-corrosion with the results obtained from the FEMs for the remaining four corrosion cases.

Table 56: FEMs LTB percentage change between case non-corrosion and the remaining corrosion cases

Beam lengths:	Corrosion case 1	Corrosion case 2	Corrosion case 3 -model 1	Corrosion case 3 -model 2
L 1m	29.2%	18.5%	10.8%	1.54%
L 1.5m	35.2%	16.9%	22.5%	2.8%
L 2m	41.7%	18.3%	23.3%	3.3%
L 2.3m	42.6%	18.5%	17%	3.7%
L 2.5m	44%	18%	14%	2%
L 3m	48.9%	22.7%	15.9%	4.5%
L 3.4m	45%	18.8%	15%	18.8%
L 4m	50%	24%	27.8%	19.4%
L 5m	58.3%	25%	13.3%	16.7%
L 7m	61.8%	20.6%	29.4%	48.8%

It can be observed on Table 55 that the reduction of the LTB moment capacity is not continuous as the beam lengths are increasing, as shown in red colour. This trend can be explained by taking into account the interaction effect of local buckling behaviour with both geometrical and material non-linear behaviours which affects the accuracy of the simulation.

Additionally, it can be observed on Table 55 that the effects from corrosion on the LTB moment capacity of the I beam can be neglected for corrosion case 3 -model 2 for beam lengths 1m to 3m, where the percentage change between the case non-corrosion and case corrosion 3 -model 2 is less than 5%.

Finally, it can be observed on Table 55 that, for all the corrosion cases, the LTB moment capacity reduces more drastically as the beam length increases, leading to the conclusion that the LTB moment capacity is not only affected by the effects of corrosion but is also affected by the length of the chosen I beam.

6.3 Recommendation for future studies

The first recommendation for future studies is an experimental comparison instead of a comparison made from software results. The second recommendation for future studies is to compare the experimental results with FEM results and with the analytical results.

A third recommendation would be to repeat the parametric study by changing the dimensions of the cross-section of the I-beam. For example, increasing the height of the cross-section compared to the length of the beam.

The most important recommendation for future studies is to perform the derivation of the analytical formula for case corrosion 3 -model 1 and case corrosion 3 -model 2 and for newly implemented corrosion cases in order to compare with the software results and experimental results.

7 Referanser

[1] Y. Sharifi og J. K. Paik, «Ultimate strength reliability analysis of corroded steel-box girder bridges,» *Thin-Walled struct.,49,* pp. 157-166, 2011.

[2] J. R. Kayser, «The effects of corrosion on the reliability of steel girder bridges,» *PhD thesis. Ann Arbor. Mich., USA. University of Michigan,* 1988.

[3] J. K. Paik, J. M. Lee og M. J. Ko, «Ultimate shear strength of plate elements with pit corrosion wastage,» *Thin-Walled Struct.,* p. 1161–1176., 2004.

[4] W. Glaser og L. G. Wright, «Mechanically assisted degradation,» *ASM handbooks. ASM internationals,* pp. 137-144, 1992.

[5] Z. X. Li og T. H. T. Chan, «Fatigue criteria for integrity assessment of long span steel bridge health monitoring,» *Theo App. Fract. Mech., 46,,* pp. 114-127, 2006.

[6] K. Lima, N. Robson, S. Oosterhof, S. Kanji, J. DiBattista og C. J. Montgomery, «Rehabilitation of a 100-year-old steel truss bridge,» *CSCE 2008 Annual Conference,* pp. 10-13, June 2008.

[7] S. Nakamura og K. Suzumurab, «Hydrogen embrittlement and corrosion fatigue of corroded bridge wires,» *J. Constr. Steel.Res 65,* p. 269–277, 2009.

[8] Y. Yukikazu og K. Makoto, «Maintenance of steel bridges on Honshu- Shikoku crossing,» *J. Constr. Steel. Res.,58,* pp. 131-150, 2002.

[9] N. S. Trahair, M. A. Bradford, D. A. Nethercot og L. Gardner, THE BEHAVIOUR AND DESIGN OF STEEL STRUCTURES TO EC3, London and New York: Taylor and Francis group, 2008.

[10] Y. Sharifi og R. Rahgozar, «Evaluation of the remaining lateral torsional buckling capacity in corroded steel members,» *Department of Civil Engineering, Kerman University, Kerman, Iran,* 2010.

[11] J. Vales , Z. Kala, J. Martinasek og A. Omishore, «FE nonlinear analysis of lateral-torsional buckling resistance,» *International Journal of mechanics,* p. 236, 2016.

[12] NS-EN 1993-1-1:2005+A1:2014+NA:2015, «Eurokode 3: Prosjektering av stålkonstruksjoner, Del 1-1: Allmenne regler og regler for bygninger».*Eurocode 3: Design of steel structures part 1-1: General rules and rules for buildings.*

[13] M. J. Gallon, «Managing structural Corrosion in Chemical Plant,» *ICI Engineering, New Steel Construction, UK,* 1993.

[14] A. A. Czarnecki og A. S. Nowak, «Time-variant reliability profiles for steel girder bridges,» *Structural Safety 30(1),* pp. 49-64, 2008.

[15] B. 5950, «Structural Use of Steel Work in building, Code of Practice Design in Simple and Continuous Construction,Hot Rolled Section.,» *British Standard Institution,* 1985.

[16] M. J. Gallon, V. Sarvesvaran og J. W. Smith, «Structural Assesment of Corrosion Damaged Steel Work,» *Proceeding of the Extensively the Life Span of Structures, IABSE Symposium, San Francisco,USA,* 1995.

[17] J. W. Smith, «Mechanical Properties of Samples of Structural Steel Affected by Corrosion,» *Report No. UBCE/JWS/93/01, Department of Civil Engineering,University of Bristol, UK,* 1993.

[18] R. Rahgozar, *Journal of Constructional Steel Research, 65(2),* pp. 299-307, 2009.

[19] R. Rahgozar, «Remaining capacity assessment of corro-sion damaged beams using minimum curves.,» *Journal of Constructional Steel Research 65(2),* pp. 299-307.

[20] D. A. Nethercot , Limit States Design of Structural Steelwork (3rd Ed.), London, UK. : Spon Press, 2001.

[21] A. K. Rathore og N. Kushwah, «A Review on Simulation Analysis in Lateral Torsional Buckling of Channel Section by using Ansys Software,» *International Journal of Trend in Scientific Research and Development (IJTSRD),* 2019.

[22] H. P. Hauksson og J. B. Vilhjalmsson, «Lateral-Torsional Buckling of Steel Beams with Open Cross Section,» *Elastic Critical Moment Study and Software Application,* 2014.

[23] N. D. Adasooriya og S. C. Siriwardane, «Remaing fatigue life estimation of corroded bridge members,» *Department of Structural and Mechanical Engineering and Material Science,* 2014.

[24] J. R. Kayser og A. S. Nowak, pp. 1525-1537, 1989.

[25] A. Rossi, D. H. Saito, C. H. Martins og A. S. C. De Souza, «The influence of structural imperfections on the LTB strength of I-beams,» *Structures 29 (2021) 1173-1186,* 2020.

Appendix A: No-Corrosion Case

To retrieve the results for the specified lengths as employed in this LTB analysis (0.55m, 1m, 1.5m, 2m, 2.3m, 2.5m, 3m, 3.4m, 5m, 7m and 10m), apply the corresponding value to the parameter "L" as specified in the following MATLAB code:

```
% I-Beam Without Corrosion
% Step 1: Finding the Izz, Iyy, It and Iw
%The dimensions of the no-corroded I-beam

H=200 %(mm)
B=90 %(mm)
tf=11.3 %(mm)
tw=7.5 %(mm)
Bw=H-2*tf
L=1500%(mm) The length of the beam
E=210*10^3  %(N/mm2)
G=80769   %(N/mm^2)
rareE=1

%Classification with corrosion:
%Flange-compression:
((B-tw)/2)/tf*rareE

%Web-Bending
(H-2*tf)/tw*rareE

% Moment of Inertia about z-axis (mm^4)-Equation 1.2
Izz= 2*(1/12*tf*B^3)+(1/12*(Bw*tw^3))

% Moment of Inertia about y-axis (mm^4)-Equation 2.2
Iyy=2*(B*tf^3)/12+2*(B*tf*(H/2-tf/2)^2)+(tw*(Bw)^3)/12

%Torsion Rigidity (mm^4)-Equation 3
It=2*(1/3*B*tf^3)+1/3*Bw*tw^3

%Torsion Warping (mm^6)-Equation 4
Iw= 1/24*B^3*(H-tf)^2*tf

% Step 2: Calculating the Mcr, Wply, ?LT, ?LT, XLT and Mbrd

% Critical Moment (Mcr)-Equation 5
Mcr1=sqrt(((pi^2*E*Izz)/L^2)*((G*It)+((pi^2*E*Iw)/L^2))) %Nmm

Mcr11=(sqrt(((pi^2*E*Izz)/L^2)*((G*It)+((pi^2*E*Iw)/L^2))))/10^6 % KNm

%The limits check-in order to choose the right buckling curve from
Table 2.2-1-Table 6.4
H/B %(h/b>2)

%The next step is to select the imperfection factor deltaLT=?LT from
Tabell 2.2 2 - Table 6.3
```

```
deltaLT=0.34 %(Buckling curve b)

%The plastic section modulus (Wply)-Equation 7

Wply=(B*tf*(H-tf)/2)*2+((H/2-tf)*tw*(H/2-tf)/2)*2 %(mm^3)
fy=390.02 %N/mm^2
ym1=1 %no safety factor in order to compare with Ansys workbench
results!

% rareLt=Non dimensional slenderness ratio (?LT)-Equation 6

rareLT=sqrt(Wply*fy/(Mcr11*10^6))

% Olt=?LT - Equation 8 part 1

Olt=0.5*(1+deltaLT*(rareLT-0.2)+(rareLT)^2)

% Reduction factor - Equation 8 part 2

XLT=1/(Olt+sqrt(Olt^2-rareLT^2))



%The buckling moment capacity-Equation 9

Mbrd1=XLT*Wply*(fy/ym1) %Nmm

Mbrd=Mbrd1/10^6   %KNm
```

Appendix B: Corrosion Case 1

To retrieve the results for the specified lengths as employed in this LTB analysis (0.55m, 1m, 1.5m, 2m, 2.3m, 2.5m, 3m, 3.4m, 5m, 7m and 10m), apply the corresponding value to the parameter "L" as specified in the following MATLAB code:

```
% I-Beam with Case Corrosion 1
% Step 1: Finding the Izzc, Iyyc, Itc and Iwc

A=0.0706 %(mm)-Model Parameter (The corrosion rate in the first year
of exposure)
B=0.789 % Model Parameter (The corrosion rate for representing the
long-term decrease
t=100 % years
t0=50 %years

% Corrosion wastage rate modelling
ctm=A*((t-t0)^B) %mm

%The dimensions of the uniformly corroded I-beam

Hc=200-2*ctm %(mm)
Bc=90-2*ctm %(mm)
tfc=11.3-2*ctm %(mm)
Hwc=Hc-2*tfc
twc=7.5-2*ctm %(mm)
L=1500 %(mm) The length of the beam
E=210*10^3 %(N/mm2)
G=80769 %(N/mm^2)
rareE=1

%Classification with corrosion:
%Flange-compression:
((Bc-twc)/2)/tfc*rareE

%Web-Bending
(Hc-2*tfc)/twc*rareE

%Corroded - Moment of Inertia about z-axis-(mm^4)-Equation 10

Izzc= 2*(1/12*tfc*Bc^3)+(1/12*(Hwc*tfc^3))

%Corroded - Moment of Inertia about y-axis-(mm^4)-Equation 11

Iyyc=2*(Bc*tfc^3)/12+2*(Bc*tfc*(Hc/2-tfc/2)^2)+(twc*(Hwc)^3)/12

%Corroded - Torsion Rigidity(mm^4)-Equation 12

Itc=2*(1/3*Bc*tfc^3)+1/3*(Hwc*twc^3)

%Corroded - Torsion Warping (mm^6)-Equation 13

Iwc= 1/24*(Bc^3*(Hc-tfc)^2*tfc)
```

```
% Step 2: Calculating the Mcr, Wply, ?LT, ?LT, XLT and Mbrd

%Corroded - Critical Moment (Mcr)-Equation 15

Mcr2=sqrt(((pi^2*E*Izzc)/L^2)*((G*Itc)+((pi^2*E*Iwc)/L^2))) %Nmm

Mcr22=(sqrt(((pi^2*E*Izzc)/L^2)*(G*Itc+(pi^2*E*Iwc)/L^2)))/10^6 % KNm

%The limits check-inorder to choose the right buckling curve from
Table 2.2-1-Table 6.4
Hc/Bc %(h/b>2)

%The next step is to select the imperfection factor deltaLT=?LT from
Tabell 2.2 2 - Table 6.3
deltaLT=0.34 %(Buckling curve b)

%Corroded - The plastic section modulus (Wply)-Equation 14

Wplyc=(Bc*tfc*(Hc-tfc)/2)*2+((Hc/2-tfc)*twc*(Hc/2-tfc)/2)*2 %(mm^3)
fy=390.20 %N/mm^2
ym1=1.0

% Corroded - rareLt=Non dimensional slenderness ratio (?LT)-Equation
16

rareLT=sqrt((Wplyc*fy)/(Mcr22*10^6))

% Corroded- Olt=?LT -Equation 17-part 1

Olt=0.5*(1+deltaLT*(rareLT-0.2)+(rareLT)^2)

% Corroded- Reduction factor--Equation 17-part 2

XLT=1/(Olt+sqrt(Olt^2-rareLT^2))

%The buckling moment capacity-Equation 18
Mbrdc1=XLT*Wplyc*(fy/ym1) %(Nmm)
Mbrdc=Mbrdc1/10^6   %KNm
```

Appendix C: Corrosion Case 2

To retrieve the results for the specified lengths as employed in this LTB analysis (0.55m, 1m, 1.5m, 2m, 2.3m, 2.5m, 3m, 3.4m, 5m, 7m and 10m), apply the corresponding value to the parameter “L” as specified in the following MATLAB code:

```
% I-Beam with Case Corrosion 2
% Step 1: Finding the Wplyeff
A=0.0706
B=0.789 %
t=100 % years
t0=50  %years
ctm=A*((t-t0)^B) %mm

B=90
H=200
tw=7.5
tf=11.3
Hc=H-1*ctm %(mm)
Bc=B-2*ctm %(mm)
tfc=tf-2*ctm %(mm)
twc=tw-2*ctm %(mm)
Hw=(Hc-tf-tfc)
 rareE=1

%Classification with corrosion:

%Flange-compression:

((Bc-twc)/2)/tfc*rareE

%Web-Bending

(Hc-2*tfc)/twc*rareE

%In order to find the plastic neutral axis
%T=C
%At*fy=AC*fy
%At=Ac
yp=((Hc*tw)-(tfc*tw)-(Hw/2*tw)+(Hw/2*twc)+(Bc*tfc)-
(B*tf)+(tf*tw))/(2*tw)

%In order to find the Plastic modulus Wply

%Tension Part
At1=B*tf
At2=(yp-tf)*tw
yt1=yp-(tf/2)
yt2=(yp-tf)/2

%Compression part
Ac1=Bc*tfc
Ac2=(Hw/2)*twc
Ac3=(Hc-yp-tfc-(Hw/2))*tw
```

```
yc1=Hc-yp-(tfc/2)
yc2=Hc-yp-tfc-(Hw/4)
yc3=(Hc-yp-tfc-(Hw/2))/2

Wplyeff=(At1*yt1)+(At2*yt2)+(Ac1*yc1)+(Ac2*yc2)+(Ac3*yc3)

%The main important parameters which effect LTB behaviour are taking
from
%Sap2000 and from Ansys Workbench


%The effective Moment of inertia in y-y axis-(mm^4)
Iyyeff=1.766*10^7

%The effective Moment of inertia in z-z axis-(mm^4)
Izzeff=1.139*10^6

%The effective Torsion constant-(mm^4)
Iteff=73827

%The effective Warping constant-(mm^6)
Iweff=9.643*10^9

E=210*10^3  %(N/mm2)
G=80769% (N/mm^2
L=10000%mm
Hc=198.454
B=90
Bc=90-2*ctm

% Step 2: Calculating the Mcr, Wply, ?LT, ?LT, XLT and Mbrd
%Corroded - Critical Moment (Mcr)-Equation 27

Mcr=sqrt(((pi^2*E*Izzeff)/L^2)*((G*Iteff)+((pi^2*E*Iweff)/L^2))) %Nmm

Mcrcor=(sqrt(((pi^2*E*Izzeff)/L^2)*((G*Iteff)+((pi^2*E*Iweff)/L^2))))/
10^6%KNm

%The limits check-in order to choose the right buckling curve from
Table 2.2-1-Table 6.4
Hc/B  %(h/b>2)
Hc/Bc %(h/b>2)

%The next step is to select the imperfection factor deltaLT=?LT from
Tabell 2.2 2 - Table 6.3
deltaLT=0.34 % (Buckling curve b)

fy=390.02 %N/mm^2
ym1=1 %no safety factor in order to compare with Ansys workbench
results!

% Corroded - rareLtcor=Non dimensional slenderness ratio (?LT)-
Equation 28

rareLTcor=sqrt(Wplyeff*fy/(Mcrcor*10^6))

% Corroded- Oltcor=?LT-Equation 29-part 1
```

```
Oltcor=0.5*(1+deltaLT*(rareLTcor-0.2)+(rareLTcor)^2)

% Corroded- Reduction factor--Equation 29-part 2

XLTcor=1/(Oltcor+sqrt(Oltcor^2-rareLTcor^2))

%The corroded buckling moment capacity-Equation 30

Mbrd1=XLTcor*(Wplyeff)*(fy/ym1) %Nmm

Mbrdcor=(Mbrd1/10^6) %Knm
```

Appendix D: Static Linear Analyses-No Corrosion, Case Corrosion 1 and Case Corrosion 2

No corrosion

```
% Check the Static structural stage--> No corrosion

%Displacement check
M=10*10^3   % Nm2
E=2.1*10^11  % N/m^2
Iyy=(2.1617*10^7)/10^12 % m^4
L=10 %(m)
x=L/2   %The displacement at the middle
c1=((M/(E*Iyy))*(L^2/2))/L

y=(-M/(E*Iyy))*(x^2/2)+c1*x   % Displacement
ymaximum=y*10^3

%Stress check
H=200  %The Hight of the beam
M1=10*10^6  %Nmm^2
ymax=H/2
Iyy1=2.1617*10^7 %mm^4

sigmamax=M1*ymax/Iyy1
```

Case Corrosion 1

```
% Check the Static structural stage->case corrosion 1

% Maximum Displacement Check
M=10*10^3   % Nm2
E=2.1*10^11  % N/m^2
Iyy=(1.4867*10^7 )/10^12 % m^4
L=1.5 %m
c1=((M/(E*Iyy))*(L^2/2))/L
```

```
x=L/2   %The displacement at the middle

y=(-M/(E*Iyy))*(x^2/2)+c1*x   % Maximum Displacement
ymaximum=y*10^3

% Maximum Stress Check
H=196.908 %The Hight of the beam for case corrosion 1
M1=10*10^6  %Nmm^2
ymax=H/2
Iyy1=1.4867*10^7 %mm^4

sigmamax=M1*ymax/Iyy1
```

Case Corrosion 2

```
% Check the Static structural stage->case corrosion 2

%Displacement check
M=10*10^3   % Nm2
E=2.1*10^11  % N/m^2
Iyy=(1.77*10^7 )/10^12 % m^4
L=10
c1=((M/(E*Iyy))*(L^2/2))/L
x=L/2   %The displacement at the middle

y=(-M/(E*Iyy))*(x^2/2)+c1*x   % Displacement
y1=y*10^3



%Maximum Stress check
H=198.454 %The hight of the beam for case corrosion 2
M1=10*10^6  %Nmm
yp=62.085 %The platic Neutral axis
ye=112.8368 % The elastic Neutral axis (tension part)
zmax=H-ye % The compression part
Iyy1=1.7664*10^7 %mm^4

%Maximun Stress in the compression part
```

```
sigmamaxC=M1*(zmax)/Iyy1

%Maximun stress in the tension part
sigmamaxT=M1*(ye)/Iyy1
```

Appendix E: The calculated corroded parameters for case corrosion 2 in Sap2000 and Ansys Workbench.

Sap2000:

Step 1

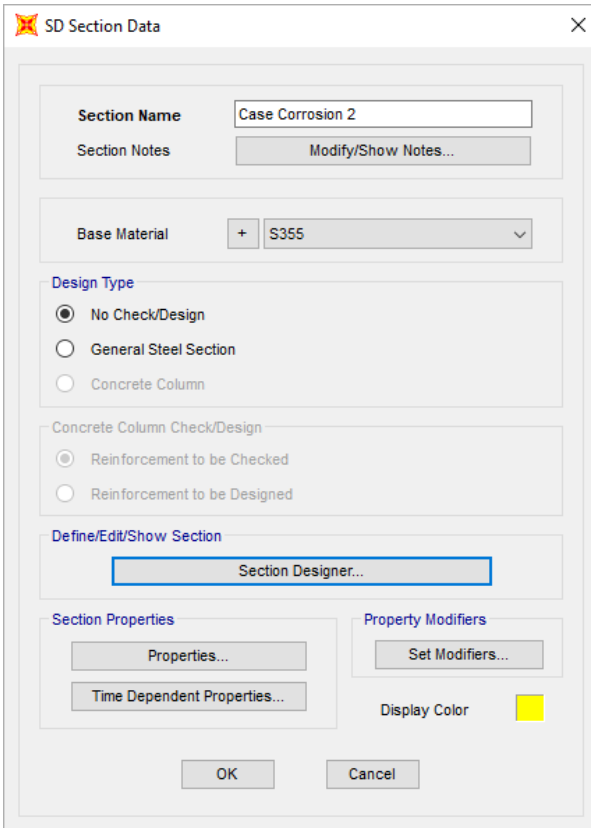

Step 2-The design model of case corrosion 2-Sap2000

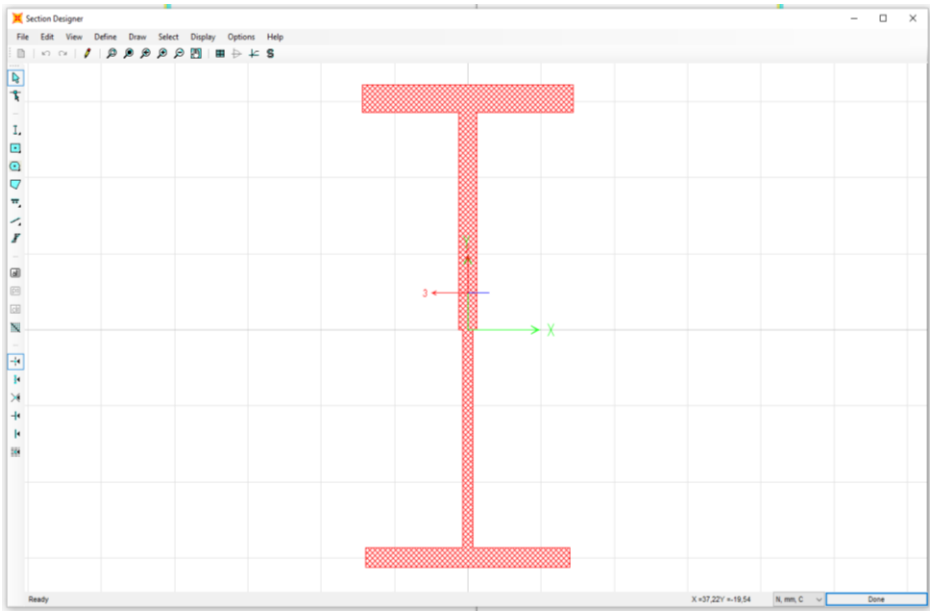

Step 3- the main corroded parameter for case corrosion 2-Sap2000

Property Data

Section Name	FSEC1		
Properties			
Cross-section (axial) area	2795,7853	Section modulus about 3 axis	156554,81
Moment of Inertia about 3 axis	17664685,	Section modulus about 2 axis	25316,618
Moment of Inertia about 2 axis	1139247,8	Plastic modulus about 3 axis	199931,34
Product of Inertia about 2-3	0,	Plastic modulus about 2 axis	40074,1
Shear area in 2 direction	1098,012	Radius of Gyration about 3 axis	79,4879
Shear area in 3 direction	1690,1759	Radius of Gyration about 2 axis	20,1863
Torsional constant	72584,82	Shear Center Eccentricity (x3)	0,

OK

Ansys Workbench:

Step 1- the design model of case corrosion 2-Ansys Workbench

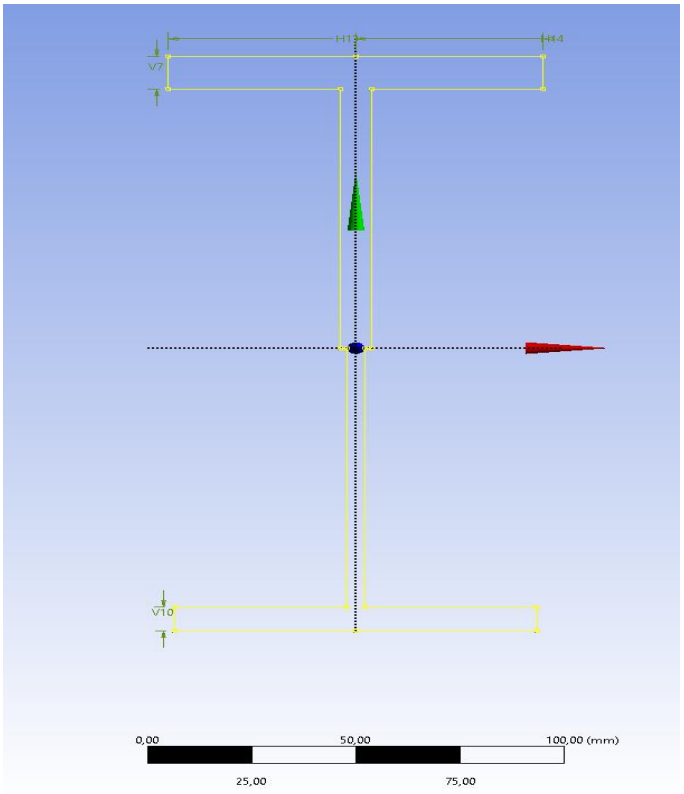

Step 2- the main corroded parameter for case corrosion 2 -Ansys Workbench

Physical Properties: 10	
A	2795,8 mm²
Ixx	1,7665e+07 mm^4
Ixy	6,8842e-10 mm^4
Iyy	1,1392e+06 mm^4
Iw	9,643e+09 mm^6
J	73827 mm^4
CGx	0 mm
CGy	15,153 mm
SHx	-1,7501e-12 mm
SHy	20,421 mm